2013-07-15

Morphogenetic Requirements for Embryo Patterning and the Generation of Stem Cell-derived Mice: A Dissertation

Yeonsoo Yoon
University of Massachusetts Medical School

Morphogenetic requirements for embryo patterning and the generation of stem cell-derived mice

A Dissertation Presented

By

YEONSOO YOON

Submitted to the Faculty of the
University of Massachusetts Graduate School of Biomedical Sciences, Worcester
In partial fulfillment of the requirements for the degree of

DOCTOR OF PHILOSOPHY

JULY 15, 2013

CELL AND DEVELOPMENTAL BIOLOGY

Morphogenetic requirements for embryo patterning and the generation of stem cell-derived mice

A Dissertation Presented
By

Yeonsoo Yoon

The signatures of the Dissertation Defense Committee signify completion and approval as to style and content of the Dissertation

---

Jaime A. Rivera-Perez, Thesis Advisor

Charles Sagerstrom, Member of Committee

Karl Simin, Member of Committee

Junhao Mao, Member of Committee

M. Isabel Dominguez, Member of Committee

The signature of the Chair of the Committee signifies that the written dissertation meets the requirements of the Dissertation Committee

---

Janet Stein, Chair of Committee

The signature of the Dean of the Graduate School of Biomedical Sciences signifies that the student has met all graduation requirements of the school.

Anthony Carruthers, Ph.D.,
Dean of the Graduate School of Biomedical Sciences

Cell Biology

July 15, 2013

DEDICATION

This dissertation is dedicated to my parents and brothers, who have been supporting me throughout my life. It is also dedicated to my wife Myoung, my partner for life.

ACKNOWLEDGEMENTS

First of all, I would like to thank my wife, Myoungsook Han, who always supports me and encourages me to do my work. I also wish to express my gratitude to my mother, father and my brothers, who made it possible for me to be here and continue to enjoy what I have been hoping to do.

I also would like to thank to my former and current lab mates, Giovane Tortelote and Tingting Huang, who went through all the paths together from the beginning of graduate school and lab life, Sakthi Balaji, who helped me to settle down in the lab and always supported me as a good assistant and good friend, Kristina Gonzalez, who spent her own time in discussing with me and sharing my feelings without hesitation, and Joy Riley, who directly helped me perform my chimera experiments and for sharing her thoughts.

I also thank the members of the UMass Transgenic core facility, Steve Jones, Judy Gallant, Marilyn Keeler and Zdenka Matijasevic, who help me extend my findings through their technological expertise.

I also would like to show the gratitude to my TRAC members, Drs. Janet Stein, Charles Sagerstrom, Karl Simin, Junhao Mao, and Isabel Dominguez for their superb scientific support and guidance.

Lastly, I would like to thank my advisor, Dr. Jaime Rivera, who mentored me the last 6 years, shared most of the accomplishments during that period and made me keep on track. I appreciate so much your personal kindness and scientific guidance.

ABSTRACT

Cell proliferation and differentiation are tightly regulated processes required for the proper development of multi-cellular organisms. To understand the effects of cell proliferation on embryo patterning in mice, we inactivated *Aurora A*, a gene essential for completion of the cell cycle. We discovered that inhibiting cell proliferation leads to different outcomes depending on the tissue affected. If the epiblast, the embryonic component, is compromised, it leads to gastrulation failure. However, when *Aurora A* is inactivated in extra-embryonic tissues, mutant embryos fail to properly establish the anteroposterior axis. Ablation of *Aurora A* in the epiblast eventually leads to abnormal embryos composed solely of extra-embryonic tissues. We took advantage of this phenomenon to generate embryonic stem (ES) cell-derived mice. We successfully generated newborn pups using this epiblast ablation chimera strategy. Our results highlight the importance of coordinated cell proliferation events in embryo patterning. In addition, epiblast ablation chimeras provide a novel *in vivo* assay for pluripotency that is simpler and more amenable to use by stem cell researchers.

TABLE OF CONTENTS

LIST OF TABLES

LIST OF FIGURES

CHAPTER III

APPENDIX

List of Third Party Copyright Material

Parts of this dissertation have appeared in the following publications:

Yoon Y, Cowley DO, Gallant J, Jones SN, Van Dyke T, Rivera-Perez JA. Conditional Aurora A deficiency differentially affects early mouse embryo patterning. Dev. Biol. 2012 Nov 1;171(1): 77-85.

Yoon Y, Riley J, Gallant J, Jones SN, Rivera-Perez JA. Generation of newborn mice using epiblast complementation chimeras. (Manuscript in preparation)

CHAPTER I:

GENERAL INTRODUCTION

The main goal of developmental biology is to understand how a single fertilized egg becomes an adult organism that is able to produce the offspring of the next generation. The mouse has been utilized as a model organism for developmental biologists who are interested in studying mammalian development because it is the most amenable animal model for understanding human development. The mouse takes only 9 weeks from fertilization to maturity and this is a relatively short period compared to humans. It also has been commonly utilized due to abundant genetic knowledgement and well-established methods for the generation of novel mutants.

The peri- and early post-implantation stages of the mouse development are important periods for proper embryogenesis and survival of the embryo because this is the time when the embryo establishes its basic body plan including the anteroposterior, dorsoventral, and left-right axes and gives rise to its primary germ layers, eventually producing the progenitor cells for all the tissues of the fetus. It is known that 30% of all human pregnancies stop at early post-implantation stages (Macklon et al., 2002) and that the occurrence of abnormalities during this period gives rise to embryonic lethality, or conjoined twins with heart defects (Alikani et al., 2003). Therefore, it is critical to investigate the developmental processes of embryo patterning and axial specification during early post-implantation development to create better solutions to multiple human diseases including pregnancy problems.

Pre-implantation embryonic development in the mouse

The implantation of the mouse embryo into the uterine wall of the mother is a crucial step for further development and its continued survival to birth. The pre-implantation development encompasses stages from fertilization to the implantation.

Fertilization takes place in the ampulla inside the oviduct of the female. After fertilization, the newly created zygote undergoes several cell divisions known as cleavage, then undergoes compaction and reaches the blastocyst stage at around embryonic day 3.5 (E3.5) (Fig. 1. 1A). The blastocyst consists of a fluid-filled cavity called blastocoele and two groups of cell types, the inner cell mass (ICM), which later forms the epiblast and the primitive endoderm, and the trophectoderm (TE), which forms extra-embryonic ectoderm and ectoplacental cone at early post-implantation stages. Both the extra-embryonic ectoderm and the ectoplacental cone contribute to the formation of the placenta. These tissues allow nutrient uptake, waste removal, and gas exchange through maternal tissues that connect the developing embryo to the uterine wall of the mother. The epiblast forms the fetus, while the primitive endoderm gives rise to two extra-embryonic tissues: parietal endoderm and visceral endoderm (Fig. 1. 1B). The parietal endoderm becomes part of the parietal yolk sac (PYS) and the visceral endoderm comes to lie on the outer side of the visceral yolk sac (VYS) and the epiblast and extra-embryonic ectoderm of egg cylinder stage embryos.

At around E4.0, the blastocyst hatches from the zona pellucida and attaches to the uterine wall, initiating the post-implantation period (Arnold and Robertson, 2009; Beddington and Robertson, 1999; Tam et al, 2006).

Figure 1. 1

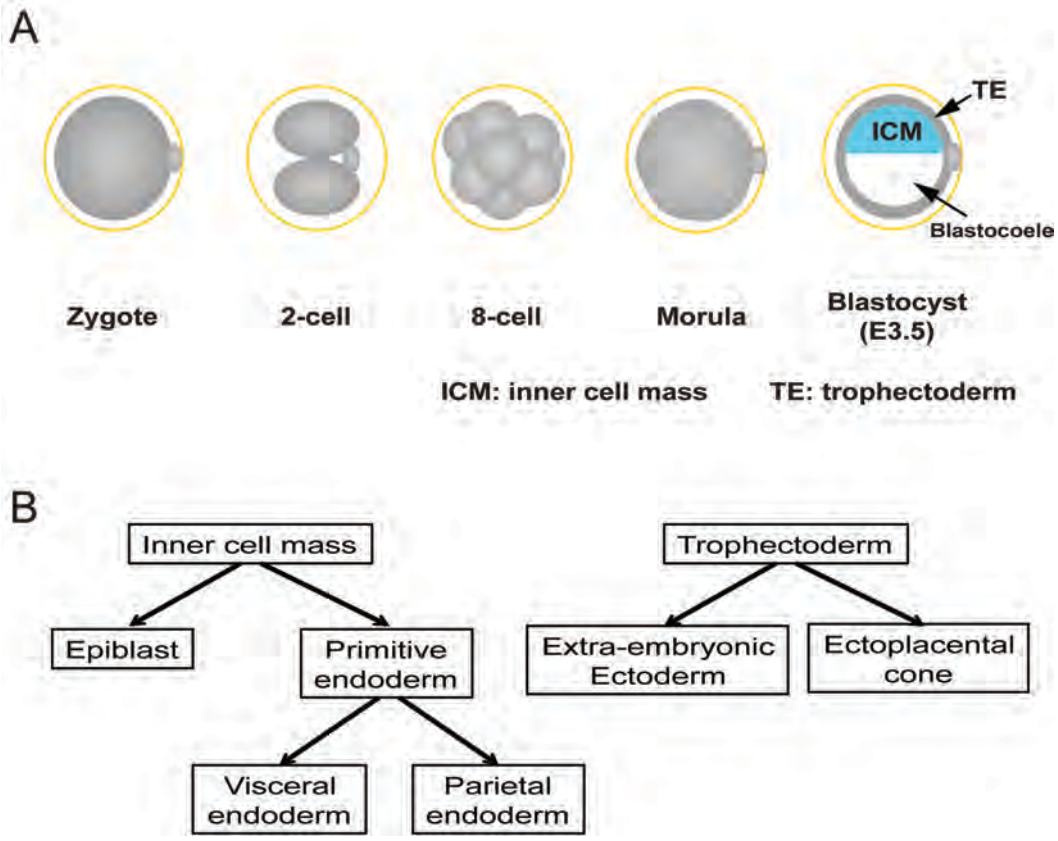

Figure 1. 1. Schematic representation of pre-implantation stages during early mouse embryogenesis. (A) Development from fertilization to blastocyst stage. (B) Summary of the derivatives of the tissues that constitute the blastocyst.

Post-implantation embryonic development in the mouse

At the time of implantation, the inner cell mass has already given rise to two cell types: the primitive ectoderm or epiblast and the primitive endoderm. The latter tissue forms an epithelium on the surface of the ICM facing the blastocoele cavity. The trophectoderm contacting the epiblast, known as polar trophectoderm, forms the ectoplacental cone and the extra-embryonic ectoderm. The mural trophectoderm, which surrounds the blastocoele, gives rise to the trophoblast giant cells, which participate in many processes essential for a successful pregnancy such as blastocyst implantation, remodeling of maternal decidua, and secretion of hormones that regulate the development of fetal and maternal compartments of the placenta (Gardner et al., 1973). At this time, the epiblast elongates distally into the blastocoele cavity and becomes a cup-shaped structure that develops an internal cavity called proamniotic cavity. The primitive endoderm expands distally to form the parietal endoderm layer that attaches to the luminal surface of the mural trophectoderm. The primitive endoderm also produces the visceral endoderm that expands concomitantly with the epiblast and the extra-embryonic ectoderm to end up covering both tissues (Fig. 1. 2). Because of its crucial functions in nurturing the embryo and mediating the activities of signaling molecules such as transforming growth factor-β (TGF-β), bone morphogenetic protein (BMP), Nodal, and Wnt3 for proper patterning of the body axis during early post-implantation development, the visceral endoderm has been highly investigated over the past two decades (Tam et al., 2006; Tam and Loebel, 2007; Rivera-Perez and Hadjantonakis, 2013). Studies of its epithelial architecture, regionalized gene expression patterns, and the pattern of morphogenetic movement during early post-implantation have shown that the visceral endoderm can be divided into several subpopulations and that these

Figure 1. 2

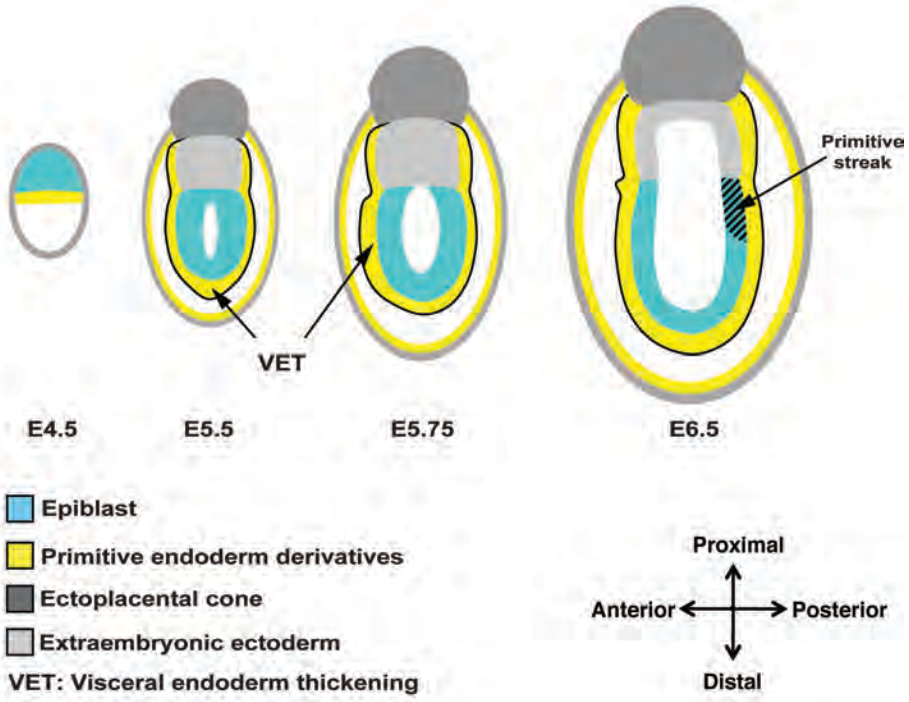

Figure 1. 2. Schematic representation of early post-implantation stages during early mouse embryogenesis.

populations act as major signaling centers for coordinating embryonic patterning and axial specification (Kemp et al., 2005; Kemp et al., 2007; Kimura-Yoshida et al., 2007; Yamamoto et al., 2004; Pfister et al., 2007; Rivera-Perez et al., 2003; Srinivas, 2006). In addition, a recent finding provided evidence that the visceral endoderm contributes to the embryonic tissues of the growing embryo (Kwon et al., 2008). This finding is surprising because it contradicts the prevailing view that the visceral endoderm contributes only to the extra-embryonic tissues and important because it suggests the existence of unknown subpopulation in the visceral endoderm that could be viewed as a fourth germ layer in mammals.

Axial specification during early mouse development

The establishment of the anteroposterior (AP) axis is a fundamental step that defines the three main axes of the embryo, which in turn serve as the frame on which the fetus is built. The establishment of the AP axis is linked to the shift of distal visceral endoderm (DVE) to become anterior visceral endoderm (AVE). At E5.5 the appearance of a local thickening of the visceral endoderm in the distal region of the egg cylinder, called visceral endoderm thickening (VET), heralds the appearance of the DVE (Fig. 1. 2). The DVE expresses Hex, a divergent homeobox gene (Thomas et al., 1998). Lineage tracing of the cells of DVE together with the analysis of gene expressions in the visceral endoderm revealed that DVE shifts to the prospective anterior pole of the conceptus where it is referred to as anterior visceral endoderm (AVE) (Rivera-Perez et al., 2003; Thomas and Beddington, 1996; Torres-Padilla et al., 2007; Srinivas et al., 2004). It has been suggested that the location of the AVE determines the position of the primitive streak at the opposite end of the epiblast, establishing AP axis in the embryo. The

location of the AP axis, together with the previously established position of the dorsoventral (DV) axis defines the left-right (LR) axis, forming the basic frame on which the rest of the fetus will be constructed.

Results from embryological studies and the analysis of mutant embryos have suggested several mechanisms that drive the anterior displacement of the DVE to form the AVE. For example, embryonic growth is shown to be associated with the movement of DVE into prospective anterior region to become AVE (Rivera-Perez et al., 2003). Time-lapse experiments of DVE cells expressing GFP have provided the evidence that DVE cells actively migrate to the future anterior region of the embryo (Srinivas et al., 2004). The shift of DVE has also been proposed to be caused by regional differences in the rate of visceral endoderm cell proliferation, which is itself associated with the level of Nodal signaling activity (Yamamoto et al., 2004). This shift appears to be from the region of high Nodal activity, which exhibits elevated cell proliferation, to the region of low Nodal activity. Wnt signaling activity also has been suggested to be involved in driving the displacement of the visceral endoderm. In this case, the DVE is displaced away from a region where Wnt activity is high towards a region of low Wnt activity where dickkopf 1 (DKK1) antagonizes Wnt signaling by blocking the function of the Wnt co-receptor LRP6 (Kimura-Yoshida et al., 2005).

Cell proliferation and embryonic patterning in model organisms

Embryonic development is composed of many different cellular behaviors such as cell proliferation, death, migration, and differentiation and it requires the coordination of these processes to execute proper embryonic patterning and morphogenesis. Cell

proliferation is essential to provide sufficient cell numbers for proper development and has been widely studied in different model organisms.

In *Caenorhabditis elegans*, an analysis of cell proliferation patterns was conducted with the purpose of getting information of embryonic cell lineages. Embryonic cell lineages were traced from fertilization to the hatched larval stages. This was possible because of the small number of total cells present during embryogenesis (671 cells) of *C. elegans* (Sulston et al., 1983). It has been found that embryonic cell lineages are highly invariant in this organism, indicating that cell proliferation has an important role in embryonic patterning and differentiation of each cell type by providing appropriate number of cells in right timing.

By contrast, in other organisms such as the fruit fly *Drosophila melanogaster* and the amphibian *Xenopus laevis*, it is difficult to trace each cell because of rapidly increasing cell numbers during embryogenesis. In the fruit fly, rapid and meta-synchronous mitotic events occur at the beginning of development and specific embryo patterning occurs with different mitotic kinetics of diverse cell types by differentiation (Foe, 1989). In the amphibian, the mitotic kinetics were not analyzed in time and space as extensively as in the fruit fly, but it has been reported that inhibition of cell proliferation before the onset of gastrulation in *Xenopus laevis* leads to severe developmental defects such as developmental arrest at mid-gastrulation, whereas inhibition after the beginning of gastrulation results in mild morphological alterations (Cooke, 1973a; Cooke, 1973b).

It also has been shown that proper cell proliferation is essential for embryonic patterning and morphogenesis in the plant *Arabidopsis thaliana* (Hemerly et al., 2000). For example, overexpression of a dominant-negative *Cdc2a* gene in *Arabidopsis* led to

altered frequency of cell divisions during embryonic development causing diverse phenotypes like distorted apical-basal patterns in seedlings.

Cell proliferation in embryonic growth and patterning during mouse development

In the mouse embryo, the initial cell cycles of the embryo and somatic cell cycles seem to follow similar general steps. For example, the lengths of the cell cycle from somatic cells and pre-implantation mouse embryos are comparable.

The mouse zygote needs 84 hours (3.5 days) to reach the blastocyst stage. During this period, the number of cells increases from one to 64 cells. This means that the average time for each cell division is approximately 14 hours (Ciemerych and Sicinski, 2005). However, the first two cell cycles are slower and each of them takes 18 to 20 hours (Flach et al., 1982). The third and fourth cell cycles are faster, each of them taking approximately 12 hours (Harlow and Quinn, 1982; Smith and Johnson, 1986), indicating that cell cycle parameters in the mouse embryo exhibit a high degree of flexibility depending on the stage. More pronounced differences in the dynamics of cell proliferation are observed at a time the embryo reaches the blastocyst stage. For example, cells of the polar trophectoderm, which are located in close contact with ICM, divide more rapidly than cells of the mural trophectoderm, which are in contact with the blastocoele.

Early post-implantation development in mice is associated with a dramatic increase in proliferation rates and with the start of differentiation within the embryo. This is concurrent with morphogenetic changes in egg cylinder structure, axial specification and gastrulation (Solter et al., 1971; Snow, 1977; MacAuley et al, 1993). Previous studies showed that there is a rapid increase in cell numbers of the epiblast and the

visceral endoderm between E5.5 and E6.5 when the embryo establishes its anteroposterior axis and gets ready for gastrulation. At E5.5, the mouse embryo contains an average of 120 epiblast and 95 visceral endoderm cells (Snow, 1977). Over the next 24 hours, the cell numbers of the epiblast and the visceral endoderm increase to 660 and 250, respectively. In fact, it was calculated that the cell cycle rate in the epiblast could be as short as four and a half hours (Snow, 1977).

During gastrulation, the three primary germ layers are generated from epiblast cells and each germ layer proliferates with different rates. The doubling time of embryonic ectoderm cells, which give rise to the skin, the brain and spinal cord, and neural crest, was estimated to be 5 hours at E6.5 and 8 hours at E7.5. The doubling time of embryonic mesoderm cells, which form the notochord, skeletal structures, muscle, connective tissue, kidney, heart, and blood etc., was calculated to be 14 hours at E7.5 (Snow, 1977). Later in development, during organogenesis, the length of the cell cycles increases again and becomes similar to those of most proliferating adult tissues (Ciemerych and Sicinski, 2005).

Utilization of mouse chimeras in biological research

A chimera is an animal composed of genetically distinct cells derived from two different zygotes. Embryonic chimeras of the mouse have been generated and established as tools for studying mouse development (Tam and Rossant, 2003). The analysis of chimeras generated from normal and mutant cells have been useful for determining the function of specific genes in the specification of certain lineages during embryogenesis. In other cases, chimeras were generated to determine the essentiality of specific genes in embryonic versus extra-embryonic tissues for proper embryo

patterning. Chimeras were also utilized to determine if specific genes function in cell-autonomous or non-cell-autonomous manner by analyzing the ability of wild type cells in a chimera to rescue a mutant phenotype.

The first experimental mouse embryonic chimeras were made more than 50 years ago by Andrzej Tarkowski (Tarkowski, 1961), who aggregated two eight-cell stage embryos after removing the zona pellucida. These aggregates became viable live chimeras after transfer into surrogate females. Another method for making mouse embryonic chimeras was devised by Richard Gardner and Ralph Brinster, who injected foreign cells into blastocysts (Gardner, 1968). The advent of pluripotent embryonic stem (ES) cells, derived from the inner cell mass of the blastocysts (Evans and Kaufman, 1981; Martin, 1981), expanded the use of this methodology coupled with gene targeting technology (Doetschman et al., 1988; Thomas and Capecchi, 1987). Generation of chimeras by using mutated ES cells, where a specific gene was targeted by homologous recombination, became a critical step for producing knockout mice (Bradley et al, 1984), accelerating the increase of our biological knowledgement of gene function.

The methods to generate mouse chimeras can be modified to manipulate the levels of chimerism in different embryonic lineages (Table 1. 1). When two diploid eight-cell stage embryos are aggregated together, chimerism is observed in both embryonic and extra-embryonic tissues. By contrast, when ES cells are utilized for the generation of chimeras by aggregation or injection, chimerism will be detected only in the embryonic tissues including germline cells and some extra-embryonic tissues such as the amnion, the allantois, and the extra-embryonic mesoderm of visceral yolk sac, which are derivatives of the epiblast.

Tetraploid embryos can also be utilized for the production of chimeras. These embryos are composed of cells that have their developmental potential compromised by the doubling of their DNA contents (Tarkowski et al, 1977). In chimeras composed of ES cells and tetraploid embryos, the ES cells contribute the embryonic components and some extra-embryonic tissues derived from the epiblast, whereas embryonic cells from tetraploid embryo only contribute to the extra-embryonic tissues, all derivatives from the primitive endoderm and the trophectoderm. This method is called tetraploid embryo complementation assay. The tetraploid complementation assay is possible not because tetraploid cells are unable to contribute to the epiblast derivatives, but because they are outcompeted by the ES cells in the epiblast lineage, which exhibits high proliferative activity.

Using tetraploid complementation chimeras, it was shown that it is possible to generate embryos derived from ES cells (Nagy et al., 1990; Nagy et al., 1993; Wang et al., 1997). This finding has led to the generation of ES cell-derived newborns or adult mice with alterations in specific genes. Mutant ES cell-derived mice can be used for the immediate analysis of phenotypes without the need of breeding between heterozygous mice, which saves time and money in the generation and maintenance of mouse lines. In a similar way, the technique to generate fully ES cell-derived mice changes the conventional system of generating knockout mice by omitting the intermediary breeding step to generate germline targeted offspring from chimeras. Recently, with the advent reprogrammed induced pluripotent stem (iPS) cell lines, this technique has received special attention from stem cell researchers, since it is considered the most stringent method to test the potency of stem cell lines.

Table 1. 1

Chimera components		Lineage composition			
A	**B**	**Embryo proper**	**Yolk sac mesoderm**	**Yolk sac endoderm**	**Placenta's trophoblast**
Diploid embryo	Diploid embryo	AB	AB	AB	AB
Tetraploid embryo	Diploid embryo	B	B	AB	AB
ES cells	Diploid embryo	AB	AB	B	B
ES cells	Tetraploid embryo	A	A	B	B

Table 1. 1. Contribution of chimera components to different embryonic lineages in different types of chimeras (Nagy et al., 2003)

Aims of this Dissertation

As described earlier in this chapter, regulation of the kinetics of cell proliferation is essential for appropriate morphogenesis during development. However, whether and how the proliferation of epiblasts or visceral endoderm cells is involved in the embryo patterning and gastrulation of the mouse embryo remains to be determined.

This dissertation describes the outcome of experiments designed to affect cell proliferation in the epiblast or in the visceral endoderm layers of the mouse conceptus during early post-implantation development using ablation of the *Aurora A* gene in a tissue-specific manner (CHAPTER II). It will also provide the description on a novel technique called epiblast complementation assay, the idea of which originated from the experimental results described in chapter II (CHAPTER III). This technique could be utilized to generate mice composed solely of ES cells and be an alternative to the tetraploid complementation assay. In addition to these two main chapters, I will describe preliminary work on the analysis of the contribution of visceral endoderm cells to fetuses and adult mice (APPENDIX I).

These studies will extend our understandings of early post-implantation mouse development by addressing how cell proliferations of the epiblast and visceral endoderm are involved in developmental processes for proper embryonic patterning. Furthermore, it will provide a useful novel technique for studies of mammalian embryogenesis and a practical approach for stem cell researchers.

CHAPTER II:

EFFECTS OF CONDITIONAL *AURORA A* DEFICIENCY ON EMBRYO PATTERNING DURING EARLY POST-IMPLANTATION MOUSE DEVELOPMENT

Preface

The work shown in this chapter has been published in the journal *Developmental Biology*. All of the work described here has been designed and performed by myself. The group of Terry Van Dyke generated *Aurora A* conditional knockout mice and provided them to us for our tissue-specific knockout experiments.

Abstract

Cell proliferation and differentiation are tightly regulated processes required for proper development of multi-cellular organisms, ensuring adequate numbers of cells at specific stages of the development. It has been reported that a threshold number of cells are required for the progression of gastrulation and that differential cell proliferation accounts for the shift of distal visceral endoderm (DVE) towards the future anterior side of the embryo at pre-gastrulation stage, suggesting that cell proliferation plays an important role in the completion of gastrulation and proper embryonic patterning.

Aurora A is a mitotic kinase essential for cell proliferation. Ablation of *Aurora A* results in mitotic arrest and pre-implantation lethality due to defects in centrosome separation and chromosome segregation. In the present study, we report the effects of *Aurora A* ablation on embryo patterning at early post-implantation stages using a tissue-specific knockout strategy.

For our analysis, we generated epiblast and visceral endoderm (VE)-specific *Aurora A* knockout embryos using *Sox2Cre*- and *TtrCre*-mediated recombination, respectively. Analysis of mutants showed that inactivation of *Aurora A* in the epiblast or visceral endoderm layers of the conceptus leads to cellular apoptosis and inhibition of embryo growth, eventually causing lethality and resorption at approximately E9.5. The effects on embryo patterning, however, were different depending on the tissue affected by the mutation of *Aurora A* gene. Embryos with an epiblast ablation of *Aurora A* properly establish the anteroposterior axis but fail to progress through gastrulation. In contrast, mutation of *Aurora A* in the visceral endoderm leads to failure to elongate the

anteroposterior axis and posteriorization of the conceptus (i.e., expansion of the primitive streak to the anterior region) due to defects in DVE movements.

In conclusion, our study suggests that Aurora A plays similar roles at pre- and post-implantation stages at the cellular level but that abolition of its function gives rise to different outcomes at the organism level depending on the tissue affected. Our study also reveals a new way to induce apoptosis and to ablate cells in a tissue-specific manner *in vivo*, providing novel opportunities for the future experiments.

Introduction

During the development of a multi-cellular organism, cell proliferation and differentiation are tightly regulated processes (Conlon and Raff, 1999). In particular, cell proliferation is essential for generating proper numbers of cells at the appropriate stages during development.

In mouse embryos, the importance of appropriate cell numbers in embryogenesis has been tested by experimental manipulations of the embryos at pre-implantation stages. For example, when one blastomere is ablated from a four-cell stage embryo, the resulting conceptus shows a 12 hour delay in gastrulation, a critical step in the formation of body plan during embryogenesis (Power and Tam, 1993). A similar result was observed when cell numbers were reduced in pre-implantation mouse embryos by treatment with Mitomycin C, an alkylating agent that kills the cells (Tam, 1988). In the converse experiment, fusion of several morulae to produce a chimera leads to reduction in the rate of cell proliferation such that gastrulation can be achieved with similar number of cells at an expected stage (E6.5) (Lewis and Rossant, 1982). It has also been suggested that DVE movement for axial specification correlates with embryonic growth at E5.5 to E6.0 (Rivera-Perez *et al.*, 2003)

The mouse embryo at early post-implantation stages is composed of the epiblast, a pseudostratified epithelium that forms the fetus at later stages, and several extra-embryonic components that include the visceral endoderm, the extra-embryonic ectoderm and the ectoplacental cone (Fig. 1. 2). These extra-embryonic components are known to play roles in nurturing the embryo during embryogenesis. At E5.5, the embryo contains an average of 120 epiblast and 95 visceral endoderm cells (Snow, 1977). Over

the next 24 hours, there is rapid cell proliferation that gives rise to 660 epiblast and 250 visceral endoderm cells before gastrulation initiates. Because of the fundamental importance of proper cell number at specific embryonic stages during embryonic development, we wondered if inhibiting cell proliferation of the mouse embryo would lead to any defect in developmental processes for embryonic patterning such as gastrulation and DVE movement for axial specification and decided to examine the effects of reduced cell number on the development of early post-implantation embryos utilizing tissue-specific genetic ablation of *Aurora A*.

Aurora A has been identified as a mitotic regulator and putative oncoprotein that is overexpressed in many human tumors (Katayama et al., 2003). Multiple *in vitro* studies showed that Aurora A kinase has roles associated with cell proliferation such as centrosome maturation, mitotic spindle assembly, mitotic entry, centrosome separation, chromosome segregation, and mitotic exit during the cell division cycle (Berdnik and Knoblich, 2002; Giet *et al*., 2002; Conte *et al*., 2003; Du *et al*., 2004; Hirota *et al*., 2003; Yang *et al*., 2005). It has also been reported that ablation of *Aurora A* in primary mouse embryonic fibroblasts leads to delayed mitotic entry and accumulation of mostly tetraploid cells (Cowley *et al.*, 2009), indicating that Aurora A is essential for cell proliferation.

Recently, several groups showed that *Aurora A* null mouse embryos have defects in mitotic spindle assembly and chromosome segregation, which leads to mitotic arrest, cell proliferation failure and embryonic lethality at pre-implantation stages (Cowley *et al*, 2009; Lu *et al*, 2008; Sasai *et al*, 2008).

Here, we take advantage of a conditional allele of *Aurora A* to bypass the early embryonic lethality of *Aurora A* mutants and investigate the essential function of Aurora

A in the development of early post-implantation embryos. We induced Cre-mediated tissue-specific null mutations to determine if the function of Aurora A is essential in the epiblast or in the visceral endoderm for proper embryonic development and furthermore to assess the effects of *Aurora A* knockouts in these tissues on axial specification and gastrulation.

Results

To determine the function of Aurora A (AurA) in the epiblast of early post-implantation embryos, we utilized a mouse line carrying a floxed allele of *AurA* (*AurA*^{fx}) (Cowley et al., 2009). In this allele, exon 2 of the *AurA* gene is flanked by LoxP sites and a null allele (*AurA*^{d2}) is generated by Cre-mediated recombination (Fig. 2. 1A). Deletion of exon 2 causes a frameshift mutation that results in a non-functional truncated protein. Mice heterozygous or homozygous for the *AurA*^{fx} allele and mice heterozygous for the *AurA*^{d2} allele are shown to be viable and fertile with no overt phenotype. To obtain epiblast-specific *AurA* knockout (Epi-KO) embryos, we crossed homozygous *AurA* floxed females (*AurA*$^{fx/fx}$) with males heterozygous for the *AurA*^{d2} null allele and heterozygous for the *Sox2Cre* transgene (*AurA*$^{d2/+}$;*Sox2*$^{Cre/o}$) (Fig. 2. 1B). The embryos carrying *Sox2Cre* transgene express *Cre recombinase* only in the epiblast at early post-implantation stages at around E5.0. In this transgenic allele, a 12.5 kb enhancer/promoter element from the Sox2 gene drives the expression of *Cre recombinase* specifically in the epiblast layer of the conceptus (Hayashi *et al*., 2002). Therefore, for the embryos with a conditional mutation of *AurA* in the epiblast (*AurA*$^{d2/fx}$;*Sox2*$^{Cre/o}$), the rest of the conceptus, which includes the visceral endoderm (VE) and extra-embryonic ectoderm, still retains a functional allele of *AurA* (*AurA*^{fx}) (Fig. 2. 1B) (Cowley *et al*., 2009).

Figure 2. 1

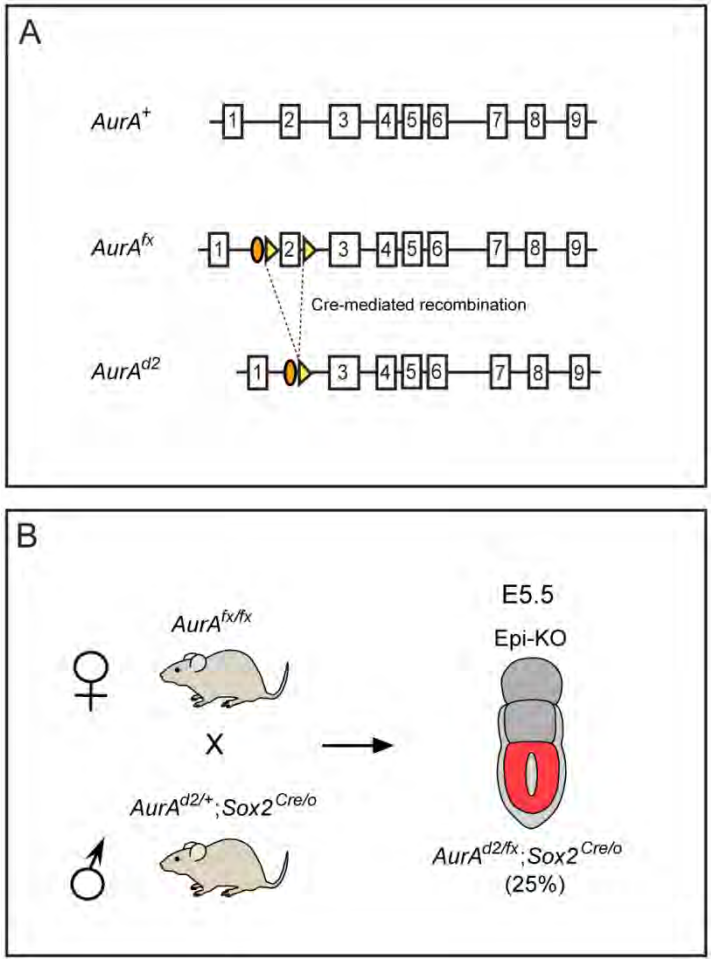

Figure 2. 1. Generation of epiblast-specific *AurA* knockout embryos.

(A) Schematic representation of *AurA* wild-type (*AurA*$^{+}$), floxed (*AurA*^{fx}), and null (*AurA*^{d2}) alleles. Yellow triangles represent LoxP site, the orange oval represents a FRT site.

(B) Mating strategy for generating epiblast-specific *AurA* knockout (Epi-KO) embryos. Red region represents the epiblast layer of the conceptus.

Aurora A is essential for epiblast growth

Using this mating strategy, we recovered multiple Epi-KO embryos and found that Epi-KO embryos were smaller than control littermates at E6.5, indicating that *AurA* ablation in the epiblast leads to the inhibition of embryo growth. Particularly, the epiblast was reduced in size and cellular debris was visible in the proamniotic cavity (Fig. 2.2A).

To determine the extent of the epiblast, we immunostained Epi-KO embryos using an antibody against Oct4, a gene known to mark the epiblast, a pluripotent tissue in early post-implantation embryo (Ovitt and Scholer, 1998). Immunofluorescence analysis revealed that the size of the epiblast in Epi-KO embryos was reduced to approximately one third of the size of control littermates and that the extra-embryonic region of these mutants appeared to be enlarged compared to ones of controls (Fig. 2. 2A,B). This morphological abnormality was also demonstrated by performing wholemount *in situ* hybridization using a probe for *Wnt7b* gene. *Wnt7b* is expressed exclusively in the extra-embryonic ectoderm layer of early post-implantation mouse embryos (Kemp et al., 2007). *Wnt7b in situ* hybridization analysis in Epi-KO embryos confirmed that the epiblast size is smaller and extra-embryonic ectoderm region was elongated distally (Fig. 2. 2C). These results demonstrate that Aurora A is essential for epiblast growth in early post-implantation embryos.

Figure 2. 2

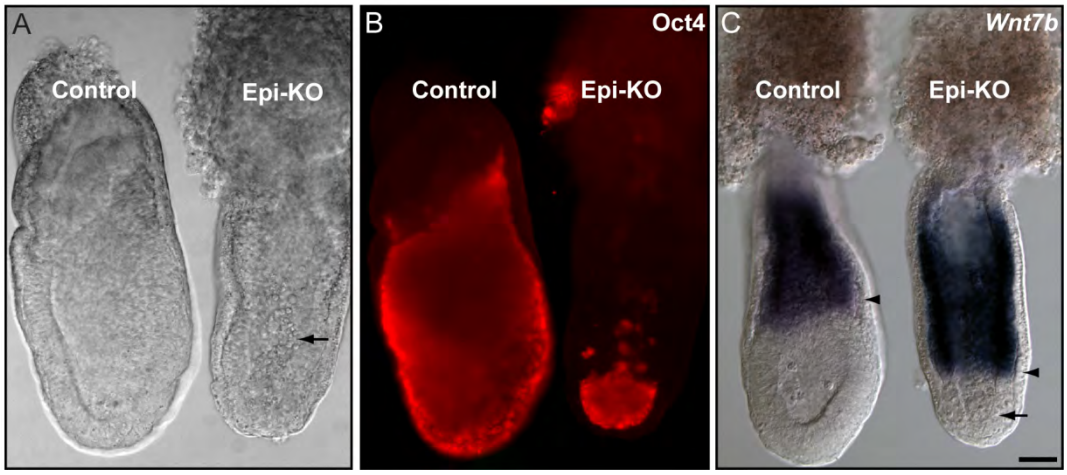

Figure 2. 2. Growth of the epiblast is inhibited in epiblast-specific *AurA* knockout embryos. (A and B) DIC (A) and fluorescent (B) images of E6.5 embryos stained with anti-Oct4 antibody to demarcate the extent of the epiblast (red). Arrow in A indicates cellular debris. (C) E6.25 embryos hybridized with a *Wnt7b* probe to detect *Wnt7b* transcripts. *Wnt7b* marks the extra-embryonic ectoderm (purple). The epiblast portion (arrow) of Epi-KO embryo is smaller than that of control embryo. The extra-embryonic ectoderm is elongated towards the embryonic region. Arrowheads indicate the boundary between embryonic region and extra-embryonic region. Embryos are shown at the same scale, scale bar, 50 µm.

Aurora A knockout in the epiblast leads to progressive cellular ablation

As demonstrated in Fig. 2, *AurA* Epi-KO embryos show the accumulation of abnormal cellular debris in the proamniotic cavity, suggesting that epiblast cells were affected by the lack of *AurA* function. To determine if this cellular debris was derived from the epiblast, we marked epiblast cells in blue using the ROSA26 reporter (*R26*^{r}) mouse line. *R26*^{r} mice carry a LoxP-STOP-LoxP-LacZ cassette targeted into the ubiquitously expressed ROSA26 locus (Zambrowicz et al., 1997; Soriano, 1999) and have been generally utilized for lineage tracing experiments. We crossed *AurA* floxed mice homozygous for *R26*^{r} allele (*AurA*$^{fx/+}$; *R26*$^{r/r}$) with mice heterozygous for the *AurA* null allele and homozygous for *Sox2Cre* (*AurA*$^{d2/+}$;*Sox2*$^{Cre/Cre}$) to generate Epi-KO embryos with epiblast cells labeled by activation of *LacZ* gene and production of β-galactosidase (*AurA*$^{d2/fx}$;*Sox2*$^{Cre/o}$;*R26*$^{r/+}$).

In E6.5 Epi-KO embryos, cellular debris positive for β-galactosidase activity was detected in the proamniotic cavity (Fig. 2. 3A), indicating that these are epiblast descendant cells and are displaced into the proamniotic cavity of Epi-KO embryos after losing the function of *Aurora A* gene in the epiblast. Furthermore, β-galactosidase activity analysis of E7.5 Epi-KO embryos revealed that few epiblast cells remained in the conceptus, indicating that the epiblast descendants were gradually ablated from the embryo with only extra-embryonic tissues remaining intact (Fig. 2. 3B). Interestingly, some remnants of epiblast cells (in blue) were found in the region of extra-embryonic ectoderm and visceral endoderm, suggesting the possibility that dying epiblast cells are eliminated by neighboring extra-embryonic ectoderm or visceral endoderm cells through the process of phagocytosis.

Figure 2. 3

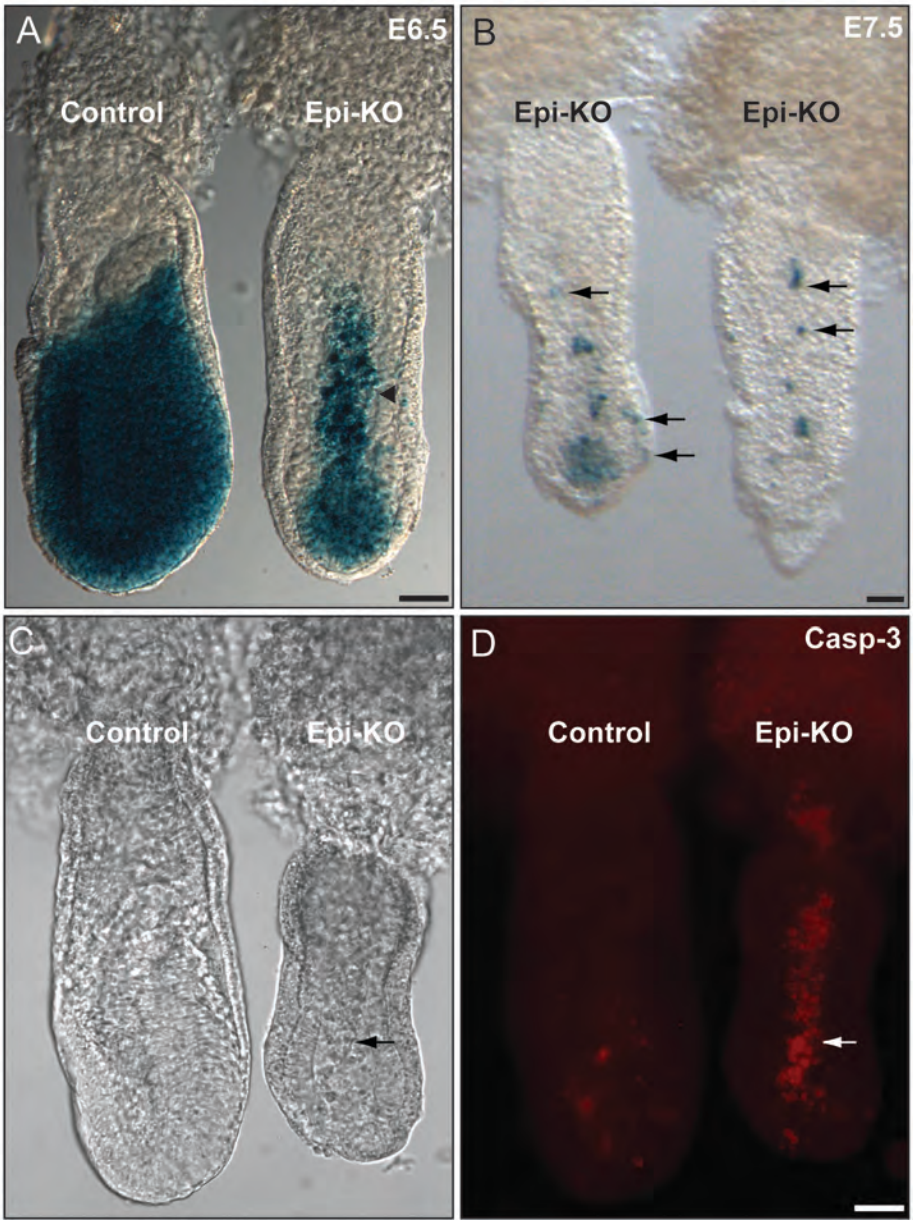
A
E6.5
Control
Epi-KO
B
E7.5
Epi-KO
Epi-KO
C
Control
Epi-KO
D
Casp-3
Control
Epi-KO

Figure 2. 3. Genetic ablation of *AurA* in the epiblast causes progressive epiblast loss through apoptosis. (A) E6.5 embryos with the epiblast component labeled by β-galactosidase activity (blue), derived from R26 reporter allele ($R26^r$). In the Epi-KO embryo, cellular debris accumulates in the proamniotic cavity (arrowhead). (B) The epiblast of Epi-KO embryos is almost ablated by E7.5. Remnants of epiblast cells (blue) were also found in the region of extra-embryonic ectoderm and visceral endoderm (arrows) (C and D) DIC (C) and fluorescent (D) images of E6.5 embryos stained with anti-cleaved Caspase-3 antibody. Apoptotic cells in Epi-KO embryo (red) were detected in the proamiotic cavity (arrows). Panels C and D are shown at the same scale. Scale bars, 50 μm.

Epiblast cells deficient for *Aurora A* function undergo apoptosis

Previous studies have reported that *AurA* knockout in mouse embryos leads to embryonic lethality at pre-implantation stage due to increased apoptosis (Cowley et al., 2009) and that RNAi-mediated knockdown of *AurA* leads to apoptosis in pancreatic cancer cells (Hata et al., 2005). Therefore, we wondered if Epi-KO embryos exhibit apoptotic events as well. To address this, we performed wholemount immunostaining experiments using an antibody against cleaved (activated) Caspase-3, a marker for apoptosis (Elmore, 2007). Interestingly, Epi-KO embryos exhibited strong staining of cleaved Caspase-3 in the proamniotic cavity (Fig. 2. 3C,D). The stained area in the proamniotic cavity exactly overlaps with the region where we detected multiple displaced epiblast cells in Epi-KO embryos, which has been demonstrated by the staining of β-galactosidase activity (Fig. 2. 3A). This indicates that these apoptotic cells are derived from the epiblast and that ablation of *AurA* leads to apoptosis in mouse embryos.

From these results, we conclude that Aurora A is essential for epiblast survival and that *AurA* knockout in the epiblast leads to cellular ablation via apoptosis, giving rise to embryos devoid of epiblast at later stages.

***Aurora A* Epi-KO embryos establish the anteroposterior axis, but fail to progress through gastrulation**

A previous study reported that embryo growth is correlated with the shift of the anterior visceral endoderm (AVE) towards the prospective anterior side of the embryo, an essential process for establishment of the anteroposterior axis (Rivera-Perez et al., 2003). The phenotype of *Cripto* mutant embryos also suggests that embryo growth is necessary for the shift of AVE towards one side of the embryo (Ding et al., 1998). The

AVE normally marks the prospective anterior side of the embryo and is located opposite to the position of the primitive streak, which marks the caudal end of the embryo at E6.5. In *Cripto* mutants, which show less mitotic index compared to control littermate embryos (Stuckey et al., 2011), the AVE fails to reach the anterior side of the embryo and remains at the distal tip of the epiblast, leading to expansion of the primitive streak to anterior regions of the epiblast (Ding et al., 1998). Cripto, a member of the epidermal growth factor-Cripto, FRL1, Cryptic (EGF-CFC) gene family, is expressed exclusively in the epiblast and is also known to be over-expressed in a number of human cancer cell lines (Salomon et al., 2000), suggesting that epiblast growth by the proliferation of epiblast cells is involved in the process of DVE shift to become AVE.

Because the size of the epiblast in Epi-KO embryos is reduced to one third of its normal size at the onset of gastrulation, we hypothesized that axial specification is affected in Epi-KO embryos. To determine if the axes of Epi-KO embryos were correctly specified, we examined the positions of the AVE and the primitive streak in *AurA* Epi-KO mutants. To examine the extent of AVE formation and its location in Epi-KO embryos, we conducted wholemount *in situ* hybridization experiments using a probe for *Hex*, a gene expressed specifically in the AVE (Thomas et al., 1998). *Hex* is also expressed at the anterior tip of the primitive streak at mid-streak stages, marking the emerging definitive endoderm lineage. Analysis of *Hex* expression in E6.5 Epi-KO embryos revealed that the AVE was properly located on one side of the epiblast, extending from the tip of the epiblast to its junction with the extra-embryonic ectoderm (Fig 2. 4A). In these embryos, however, we did not detect the expression of *Hex* on the posterior side of the embryo, suggesting a failure in gastrulation, a crucial process of generating the three primary germ layers (ectoderm, mesoderm and endoderm) during embryogenesis.

Figure 2. 4

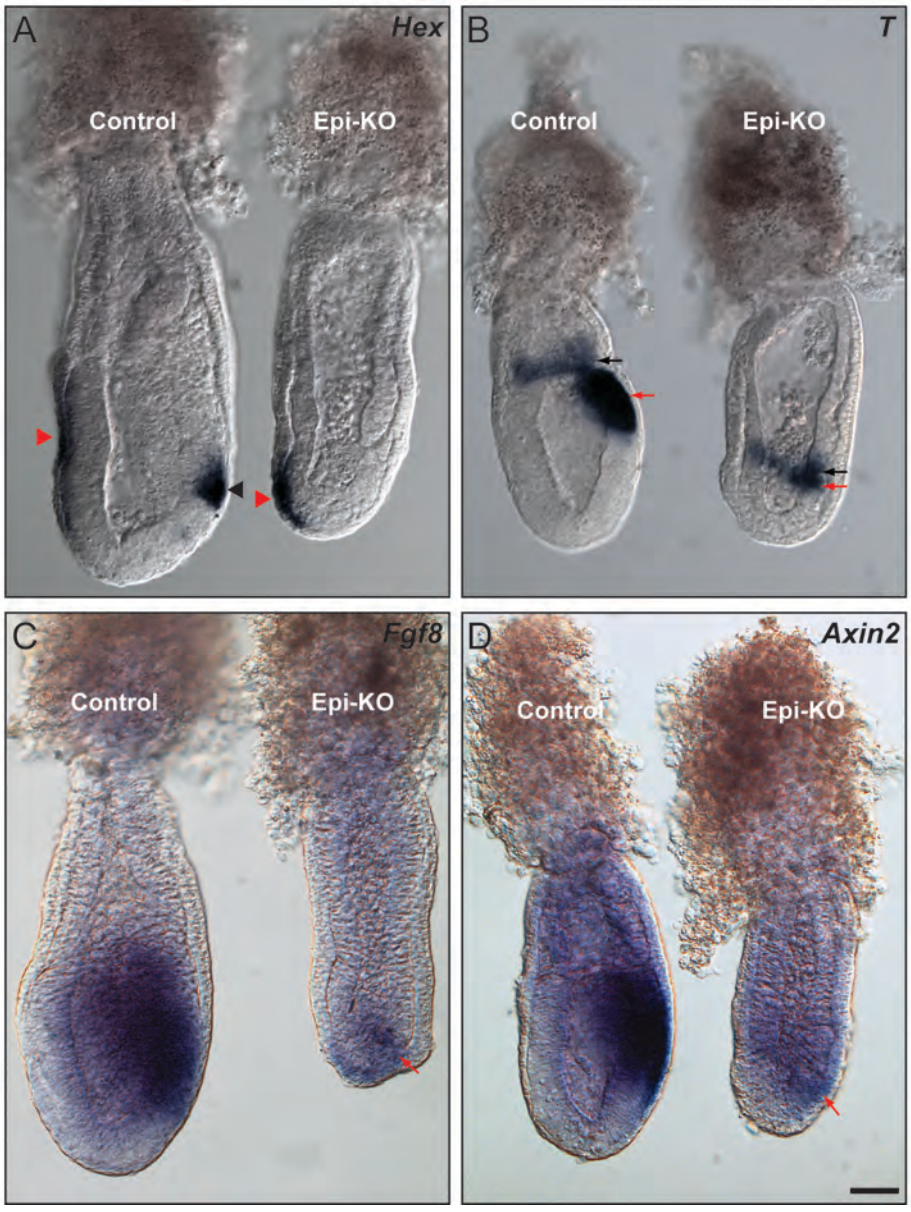
A
Hex
Control
Epi-KO
B
T
Control
Epi-KO
C
Fgf8
Control
Epi-KO
D
Axin2
Control
Epi-KO

Figure 2. 4. Epiblast-specific *AurA* knockout embryos establish the anteroposterior axis, but fail to progress through gastrulation. (A) *Hex* expression in embryos dissected at E6.5 marks the anterior visceral endoderm (AVE) (red arrowheads) and newly emerging definitive endoderm at the tip of the primitive streak (black arrowhead). The Epi-KO embryo reveals normal AVE position in one side, but absence of *Hex* expression in the primitive streak. (B) *Brachyury* (*T*) expression in embryos dissected at E6.5. Expression is evident in the extra-embryonic ectoderm (black arrows) as well as in the posterior region of epiblast, marking the primitive streak (red arrows). (C and D) Expression of *Fgf8* (C) and *Axin2* (D) mark the formation of mesoderm in the posterior region of the embryo (red arrows) at E6.5. Pictures are shown at the same scale. Scale bar, 50 μm.

Experiments in which the number of blastomeres was reduced by manipulation of four cell stage embryos at pre-implantation stage have also suggested that a specific threshold number of epiblast cells need to be reached for the gastrulation to progress completely (Power and Tam, 1993). To determine if the primitive steak was specified properly in the posterior region of Epi-KO embryos and to examine the process of gastrulation in Epi-KO embryos, we performed wholemount *in situ* hybridization using probes for *Brachyury* (*T*), a well-known marker of the primitive streak (Wilkinson et al., 1990). T also marks the distal portion of the extra-embryonic ectoderm circumferentially in early post-implantation embryos (E5.5~E6.5) (Perea-Gomez et al., 2004; Rivera-Perez and Magnuson, 2005). Analysis of *T* expression in E6.5 Epi-KO embryos revealed that *T* is expressed strongly in a small area on one side of the epiblast (Fig 2. 4B), indicating that the primitive streak was specified properly in the posterior region of Epi-KO embryos. We also observed the expression of *T* in the distal area of extra-embryonic ectoderm in those mutants, suggesting that *T* expression in that region was not affected by *Aurora A* knockout in the epiblast.

We also analyzed the expression of *Fgf8* and *Axin2*, two markers for mesoderm lineage that emerges during gastrulation at E6.5. We observed the expression of both *Fgf8* and *Axin2* in the posterior region of Epi-KO embryos, but the areas covered by this expression were smaller compared to wild type control littermates (Fig. 2. 4C,D). Thus, Epi-KO does not affect the initiation of mesoderm formation during gastrulation.

These results demonstrate that Epi-KO embryos are able to establish an anteroposterior axis properly due to no defect of AVE shift in these mutants and specify the primitive streak and mesoderm in the posterior region. However, Epi-KO embryos cannot advance to mid-streak stages and fail to complete the gastrulation likely due to

decreased number of epiblast cells. This result suggests that Aurora A is not essential in the epiblast for the initiation of mesoderm formation at the onset of gastrulation, but is required for normal progression and completion of gastrulation.

Aurora A in the visceral endoderm is essential for embryonic growth and survival

Visceral endoderm is a functional layer of the conceptus that surrounds both the epiblast (embryonic visceral endoderm) and the extra-embryonic ectoderm (extra-embryonic visceral endoderm). To determine the role of Aurora A in the visceral endoderm (VE) and how cell proliferation defects in the visceral endoderm would affect the embryonic patterning at early post-implantation stages, we generated VE-specific knockout embryos utilizing *TtrCre* transgenic mouse line. The embryos carrying *TtrCre* allele express *Cre recombinase* only in the visceral endoderm at early post-implantaton stages (E5.0) (Kwon and Hadjantonakis, 2009; Kwon et al., 2008). To generate VE-KO embryos, we crossed homozygous *AurA* floxed mice ($AurA^{fx/fx}$) with transgenic *TtrCre* mice carrying a null allele of *AurA* ($AurA^{d2/+};Ttr^{Cre/o}$) (Fig. 2. 5A). VE-KO embryos fail to express *AurA* in the visceral endoderm only, but retain a functional allele of *AurA* ($AurA^{fx}$) in the rest of the conceptus.

To determine the morphological defects in VE-KO embryos, we isolated VE-KO embryos at E6.25, E7.5 and E9.5. We found that VE-KO embryos were slightly smaller than control littermates at E6.25 (Fig. 2. 5B), indicating that genetic ablation of *Aurora A* in the visceral endoderm affects the growth of early post-implantation embryos. In mutant embryos, the visceral endoderm surface was rough and cellular debris was observed. Interestingly, the embryonic portion of the conceptus seemed to be more affected. The smaller size, representing the defect in embryo growth, was more

Figure 2. 5

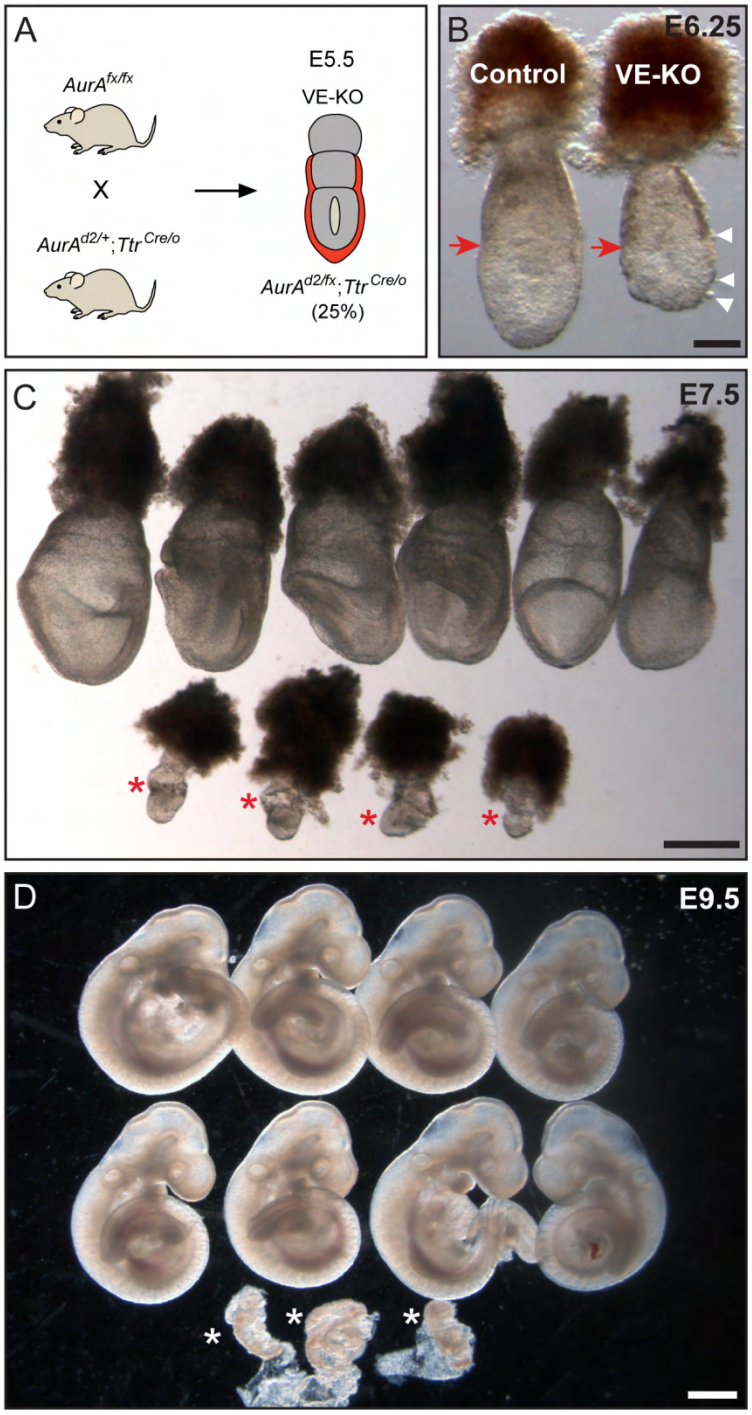
A
AurA fx/fx
X
AurA d2/+ ; Ttr Cre/o
E5.5
VE-KO
AurA d2/fx ; Ttr Cre/o
(25%)
B
E6.25
Control
VE-KO
C
E7.5
D
E9.5

Figure 2. 5. *AurA* knockout in the visceral endoderm inhibits embryo growth and causes lethality. (A) Mating strategy for generating visceral endoderm-specific knockout (VE-KO) embryos. Red region represents the visceral endoderm layer of the conceptus. (B) Control and *AurA* visceral endoderm knockout (VE-KO) embryos dissected at E6.25. The VE-KO embryo is smaller than the control embryo. Cell debris (arrowheads) was observed on the surface of the visceral endoderm. Arrows indicate the boundary between the embryonic region and extra-embryonic region.
(C) Embryos dissected at E7.5. The smaller size of VE-KO embryos (red asterisks) is evident, revealing the growth inhibition by *AurA* knockout in mutants. (D) At E9.5, VE-KO embryos (white asterisks) are in the process of resorption. Scale bars, 50 µm, 200 µm, and 500 µm in A, B, and C, respectively.

pronounced at E7.5 (Fig. 2. 5C), suggesting that mutant embryos fail to grow further due to absence of Aurora A function in the visceral endoderm. Expectedly, mutant embryos were in the process of resorption by E9.5 (Fig. 2. 5D). These results show that function of Aurora A is also essential in the visceral endoderm for embryo growth and survival of early post-implantation embryos.

A mutation of *Aurora A* in the visceral endoderm leads to cellular ablation

We labeled *AurA*-deficient VE cells using the ROSA26 reporter allele (*R26*^{r}) and *TtrCre*-mediated recombination of VE cells to investigate the fate and integrity of visceral endoderm cells. β-galactosidase activity assays of E6.5 embryos revealed that mutant visceral endoderm cells lose cell-cell contacts and mutant embryos exhibit multiple protrusions on the surface of the visceral endoderm layer (Fig. 2. 6A). Analysis for E7.5 embryos demonstrated the prevalence of mutant visceral endoderm cells in the extra-embryonic region but not in the distal area of the conceptus (embryonic region) (Fig. 2. 6B). These results indicate that most of visceral endoderm cells overlying the epiblast (embryonic visceral endoderm cells) were ablated from the embryo and that visceral endoderm cells overlying the extra-embryonic ectoderm are more tolerant to the absence of Aurora A function than visceral endoderm cells overlying the epiblast.

Figure 2. 6

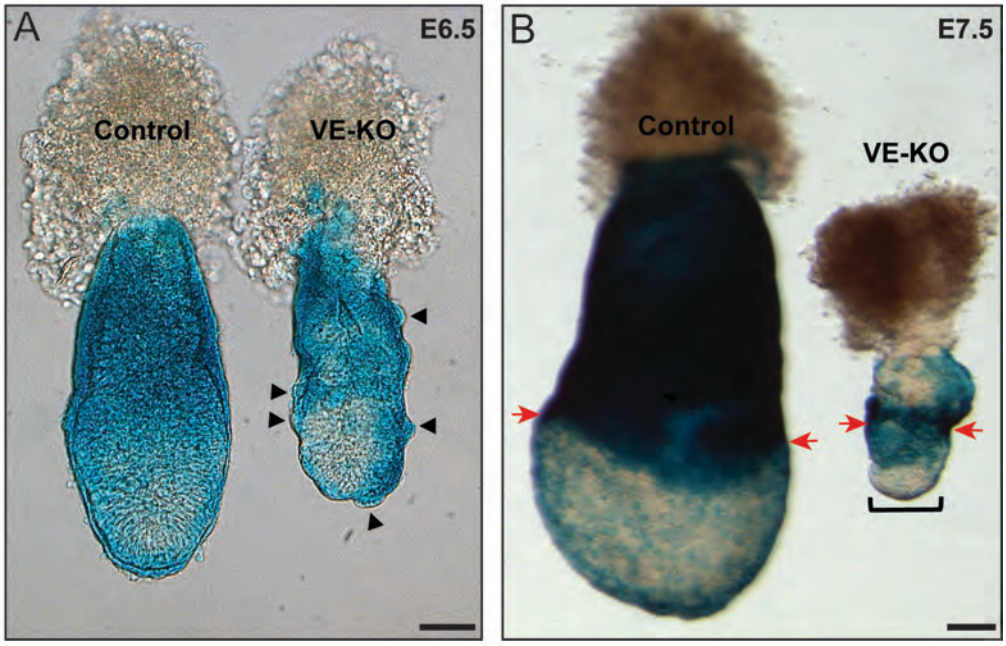

Figure 2. 6. *AurA* knockout in the visceral endoderm affects cellular integrity and leads to cellular ablation. (A) Embryos stained with X-gal after dissection at E6.5, with visceral endoderm cells marked by β-galactosidase activity (blue). The VE-KO embryo shows cellular protrusions on the surface of the visceral endoderm layer (arrowheads). (B) Embryos dissected at E7.5, with visceral endoderm cells marked by β-galactosidase activity (blue). Marked visceral endoderm cells in *AurA* VE-KO embryos are more prevalent in the visceral endoderm overlying the extra-embryonic ectoderm portion of the conceptus and mostly absent in the distal area (bracket) of the conceptus. Arrows indicate the boundary between the embryonic region and extra-embryonic region. Scale bars, 50 μm and 100 μm in A and B, respectively.

Aurora A ablation in the visceral endoderm leads to apoptosis

From the observation of cellular ablation in embryonic visceral endoderm, we wondered whether ablation of *Aurora A* leads to apoptosis in visceral endoderm cells as well. To determine if visceral endoderm cells in VE-KO embryos were undergoing apoptosis due to absence of *Aurora A*, we conducted wholemount immunofluorescence analysis using anti-cleaved Caspase-3 antibody and observed the extensive apoptosis event in the visceral endoderm layer of VE-KO embryos at E6.5 (Fig. 2. 7A,B). Interestingly, the apoptotic events demonstrated by cleaved Caspase-3 staining were mostly restricted to the embryonic portion of VE-KO mutants. This result is consistent with our previous observation that visceral endoderm cells lacking *Aurora A* are more prevalent in the extra-embryonic region of the conceptus (Fig. 2. 6B), suggesting that embryonic visceral endoderm cells are more sensitive to the absence of Aurora A function than extra-embryonic visceral endoderm cells. Furthermore, it indicates that affected mutant embryonic visceral endoderm cells are gradually eliminated from the embryo through apoptosis.

Axial development is affected in *Aurora A* VE-KO embryos

Nodal is a secreted signaling molecule of transforming growth factor-beta (TGF-β) family, involved in many essential processes during early mouse development. These include AVE formation and movement, mesoderm induction, and left-right (LR) axis specification (Brennan et al., 2001; Schier, 2003; Varlet et al., 1997).

It has been reported that Nodal signaling promotes cell proliferation in the visceral endoderm whereas Nodal antagonists such as *Lefty1* and *Cerl* inhibit cell proliferation (Yamamoto et al., 2004) and *Nodal* null embryos exhibit defects in AVE

Figure 2. 7

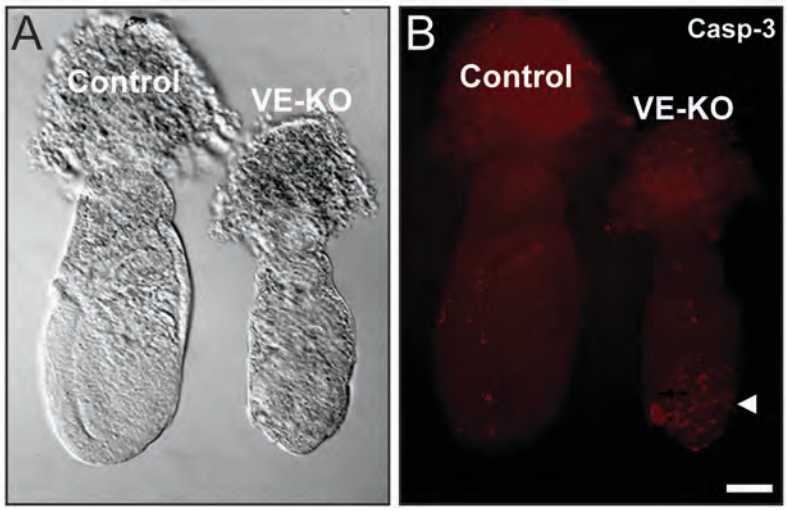

Figure 2. 7. VE-specific *AurA* knockout leads to apoptosis. (A and B) DIC (A) and fluorescent (B) microscopic images of E6.5 embryos immunostained with cleaved Caspase 3 antibody. *AurA* VE-KO embryo shows apoptotic events (red) in the visceral endoderm cells overlying the epiblast (arrowhead in B). Scale bar, 50 μm.

shift to the anterior side of the embryo (Norris et al., 2002). These studies suggest that cell proliferation in the visceral endoderm is involved in AVE movement. Therefore, we hypothesized that *AurA* VE-KO embryos would have defects in AVE movement for axial specification. To address this question, we performed wholemount *in situ* hybridization using *Hex* and *T* RNA probes. Analysis of *Hex* expression revealed that the position of the AVE in VE-KO embryos assumes two different patterns. In some embryos, it remained at the distal tip of the embryo (Fig. 2. 8A), while in the others it shifted to one side of the epiblast although it failed to reach the boundary between the epiblast and the extra-embryonic ectoderm (Fig. 2. 8D). Analysis of *T* expression exhibited the correlation with the pattern of *Hex* expression. In some mutant embryos, the primitive streak was expanded towards the anterior side around the junction of epiblast with the extra-embryonic ectoderm (Fig. 2. 8B,C), likely due to the position of AVE in the distal tip. In others, *T* expression was localized properly in the posterior side of VE-KO embryos, indicating that these mutants established the anteroposterior axis in right direction. However, these mutants exhibited a failure in the elongation of the anteroposterior axis (Fig. 2. 8E,F), which usually occurs between E6.0 and E6.5 in wildtype embryos (Mesnard et al., 2004; Perea-Gomez et al., 2004).

Together, these results support our hypothesis that ablation of *Aurora A* in the visceral endoderm leads to abnormal establishment of the anteroposterior axis of early post-implantation mouse embryo.

Figure 2. 8

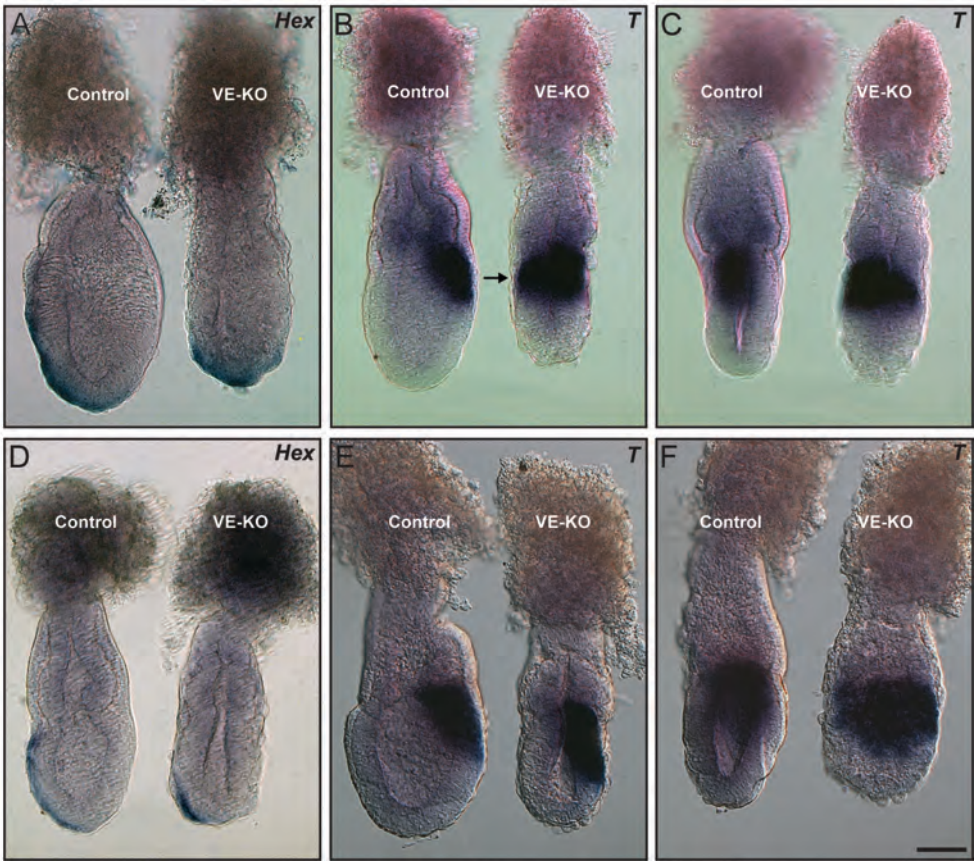
A
Hex
Control
VE-KO
B
T
Control
VE-KO
C
T
Control
VE-KO
D
Hex
Control
VE-KO
E
T
Control
VE-KO
F
T
Control
VE-KO

Figure 2. 8. VE-specific *AurA* knockout causes axial defects. (A and D) *Hex* expression in embryos dissected at E6.5. The AVE in VE-KO embryos remains at the distal tip of the embryo (A) or shifts to approximately half of the anterior epiblast (D). (B and C) Side view (B) and posterior view (C) of embryos hybridized with *Brachury* (*T*) probe to mark the primitive streak after dissection at E6.5. The *AurA* VE-KO embryo shows expansion of the primitive streak towards the anterior region of the epiblast (arrow in B). (E and F) Side view (E) and posterior view (F) of control and *AurA* VE-KO embryos hybridized with *Brachyury* (*T*) probe after dissection at E6.5. In VE-KO embryo, *T* expression remains in one side of the short axis of the conceptus, indicating that these mutants established the anteroposterior axis in right direction, but that the axis of mutants failed to elongate. All images are shown at the same scale, scale bar, 50 µm.

Discussion

Ablation of *Aurora A* in mice causes apoptosis and embryonic lethality at pre-implantation stages (Cowley et al., 2009; Lu et al., 2008; Sasai et al., 2008). Our current study reveals similar essential roles for Aurora A at early post-implantation stages of mouse embryogenesis. We found that genetic ablation of *Aurora A* in the epiblast or in the visceral endoderm layer of post-implantation embryos using the Cre-LoxP system leads to apoptosis, inhibition of embryo growth and embryonic lethality. The knockout of *Aurora A*, however, was shown to impact embryonic development differently depending on the tissue affected.

Mutation of *Aurora A* in the epiblast leads to progressive loss of epiblast cells and gastrulation defects, resulting in a conceptus composed mostly of extra-embryonic tissues by E7.5. The presence of epiblast debris in the region of extra-embryonic ectoderm and visceral endoderm suggests that dying epiblast cells in the proamniotic cavity are gradually eliminated by neighboring cells of the extra-embryonic ectoderm and the visceral endoderm through the process of phagocytosis without affecting other extra-embryonic tissues. Interestingly, despite the severe reduction of epiblast cells, the axes of the embryo are properly established, suggesting that the defects of gastrulation observed in embryos lacking *Aurora A* in the epiblast are due to a paucity of epiblast cells rather than patterning defects. Previous studies have shown that a threshold number of cells are required for the gastrulation to proceed (Power and Tam, 1993; Tam, 1988). Our results are consistent with these observations. However, the initial specification of the primitive streak, the engine of gastrulation, appears to be less dependent on a cell number threshold because we observed the expression of

Brachyury, a marker gene for the primitive streak, in the posterior region of Epi-KO mutants even though it was detected in smaller area.

In contrast, lack of Aurora A function in the visceral endoderm leads to defects in establishment of the anteroposterior axis. Analysis of *Hex* expression in VE-KO embryos revealed the position of the AVE in the distal tip, which is correlated with the expansion of the primitive streak toward anterior regions of the epiblast in mutants. This phenotype is consistent with previous observations that the AVE regulates the extent of the primitive streak by antagonizing the expansion of the primitive streak. For example, a double knockout of *Cerl1* and *Lefty1*, two known genes expressed in the AVE, leads to the formation of multiple primitive streaks (Perea-Gomez et al., 2002). Also, mutations that abolish the shift of the AVE to the anterior side of the epiblast lead to anterior expansion of the primitive streak (Ding et al., 1998; Perea-Gomez et al, 2001). We believe that the expanded or radialized primitive streak observed in *AurA* VE-KO embryos is due to improper positioning of the AVE. How the ablation of *Aurora A* in the visceral endoderm leads to the defect in shift of the AVE to one side is still an open question. One possibility is that a specific threshold number of visceral endoderm cells provided by proper cell proliferation in visceral endoderm are required to allow proper positioning or movement of the AVE towards the anterior side of the conceptus. Another possible explanation is that *AurA*-deficient visceral endoderm cells become functionally abnormal and cannot fulfill their normal roles for embryonic patterning (i.e. AVE migration) during development.

Interestingly, in some VE-KO embryos, the anteroposterior axis was specified correctly but it failed to elongate anteroposteriorly. Our analysis of *T* expression revealed that VE-KO embryos have short anteroposterior axis compared to wild type control

littermates, indicating that the elongation process does not occurs properly in mutant embryos during the pre-primitive streak stages (E6.0 ~ E6.5). This suggests that less visceral endoderm cells or affected visceral endoderm cells in VE-KO embryos constrain the growth of the epiblast due to the defects in provision of nutrients to embryonic tissues of the embryos. This constraint or inhibition of epiblast growth might prevent the elongation of the anteroposterior axis of the embryo, supporting the notion that growth of the epiblast within the visceral endoderm layer allows the elongation of the anteroposterior axis in wild type embryos (Tam, 2004).

It will be interesting to address the question of why in some VE-KO embryos the AVE remains at the distal tip of the embryo whereas other VE-KO mutants show slight shift toward one side. One possibility is that mutant embryos show different phenotypes depending on their stage of development. In other words, younger embryos might tend to show distal AVE whereas older embryos exhibit a slight shift of the AVE toward one side because older embryos have more chances of changing the position of AVE compared to younger ones. This hypothesis could be addressed in the future by comparing the AVE location of older embryos and younger embryos. Another possibility is that AVE randomly moves without any specific direction in VE-KO mutant embryos and thus each embryo has a different position of AVE. This possibility could be tested by time-lapse fluorescence microscopy of mutant embryos carrying *Hex-GFP* transgene in culture (Rodriguez et al., 2001).

Examination of the fate of mutant visceral endoderm cells in E6.5 and E7.5 *AurA* VE-KO embryos and wholemount immunofluorescence analysis of apoptosis events in E6.5 VE-KO embryos revealed the prevalence of visceral endoderm cells in the extra-embryonic region. This variability of consequences between embryonic visceral

endoderm and extra-embryonic visceral endoderm is not due to failure to ablate *Aurora A* by Cre-mediated recombination in the extra-embryonic region since recombination of the ROSA26 reporter allele (shown in blue) indicated Cre recombinase activity in VE cells of this region as well (Fig. 2. 6A). The differences in tolerance to *Aurora A* ablation may be caused by inherent differences between two groups of visceral endoderm cells, which are morphologically and molecularly distinct. This speculation is consistent with several findings for extensive cellular heterogeneity within the visceral endoderm (Pfister et al., 2007; Rivera-Perez et al., 2003; Mesnard et al., 2004; Thomas and Beddington, 1996). Another explanation is given by the observation that visceral endoderm cells in embryonic region have more proliferative capacity than ones in extra-embryonic region, which barely proliferate (Huang and Rivera-Perez, unpublished; Stuckey et al., 2011). As the apoptotic phenomenon by *Aurora A* deficiency seems to be tied to cellular proliferation events with the evidence that it is overexpressed in many human tumors and plays major roles during cell division cycle (Sen et al., 1997; Marumoto et al., 2005), lower proliferation activity in the extra-embryonic visceral endoderm cells could cause fewer apoptotic events induced by *Aurora A* deficiency and consequently lead to better survival rates of these cells.

Even though we proposed that the phenotypes of VE-KO embryos are caused by defects of cell proliferation in visceral endoderm, we did not provide evidence that cell proliferation of visceral endoderm was inhibited by *Aurora A* mutation in VE-KO embryos. To determine the cell proliferation defects in VE-KO embryos, we immunoassayed the embryos using antibody against phospho-histone H3 (PH3), a commonly used mitotic marker (Hendzel et al., 1997). We found that there is not a significant difference in the extent of PH3 staining between VE-KO mutants and wild

type control littermates (not shown). This does not necessarily indicate that there is no difference in cell proliferation level because *Aurora A* deficiency leads to mitotic arrest and arrested cells could be positive for PH3 staining even if they are not dividing. This uncertainty prevented further trials using PH3 antibody.

Analysis of VE-KO embryos also raised the possibility that the phenotype could be caused indirectly by defects in the epiblast brought about by abnormal function of visceral endoderm cells with *Aurora A* deficiency. Because the visceral endoderm plays a role in nurturing the embryo, especially the epiblast during early post-implantation stages, defective visceral endoderm by *Aurora A* mutation might lead to defects in epiblast growth or epiblast cell proliferation alongside visceral endoderm cells defects, eventually generating axial specification problems. However, it needs to be determined whether this is true.

In conclusion, our study demonstrates that Aurora A plays similar roles at pre- and post-implantation stages at the cellular level but that interference with its function by genetic ablation has different outcomes depending on the tissue affected. It also reveals that proper growth of embryonic and extra-embryonic tissues is essential for appropriate embryonic patterning during early post-implantation development and continued survival during embryogenesis.

A practical consequence of our study is that mutation of *Aurora A* can be utilized as a way to induce apoptosis in a tissue-specific manner *in vivo*. It will be interesting to examine the process of apoptotic events in live embryos in culture via time-lapse microscopy of fluorescent markers. In other hands, it will be possible to investigate the functionality of specific cell types in the embryo or in the mouse using diverse Cre lines.

Materials and Methods

Embryo staging and dissection

Embryo stages were determined morphologically as described previously (Downs and Davies, 1993; Rivera-Perez et al., 2010) after dissection or in terms of dissection time. Noon of the day when a mating plug was observed was considered embryonic day 0.5 of development (E0.5). Dissections of post-implantation embryos were performed as described previously (Nagy et al., 2003).

Mouse strains and genotyping

The *AurA*^{fx} conditional mouse line was previously described (Cowley et al., 2009). Females carrying *AurA*^{fx} allele were crossed to *Sox2Cre* transgenic males to generate mice carrying *AurA*^{d2} allele. In this allele, exon 2 is excised, leading to a null allele. *Sox2Cre* (Hayashi et al., 2002) and ROSA26 reporter (*R26*^{r}) (Soriano, 1999) mice were purchased from the Jackson Laboratory (Stock No. 003309 and 004783, respectively). *TtrCre* transgenic mouse line was previously described (Kwon and Hadjantonakis, 2009) and was kindly provided by Dr. Anna-Katerina Hadjantonakis. Mice were genotyped using PCR on genomic DNA samples obtained from tail tips. For genomic DNA sample preparation from each mouse, a piece of tail tip was placed into 200 µl of PCR lysis buffer (50 mM KCl, 10 mM Tris-HCl, 10 mM Tris-HCl, 2.5 mM $MgCl_2$, 0.1 mg/ml Gelatin, 0.45% v/v IGEPAL and 0.45% v/v Tween-20, 100 µg/ml Proteinase K) and incubated overnight at 56°C. The next day, after heat inactivation of the Proteinase K at 95°C for 5-8 min, half or one microlitter of samples was used for PCR amplification.

Embryos were genotyped retrospectively after wholemount *in situ* hybridization, immunostaining or β-galactosidase assay procedures. For each conceptus, the ectoplacental cone was removed using forceps and placed in 20 µl of PCR lysis buffer and incubated overnight at 56°C. After heat inactivation of the Proteinase K at 95°C for 5-8 min, one or two microlitters of spin-downed samples were used for PCR amplification. Each allele was confirmed using the following primers: $AurA^{fx}$ and $AurA^{+}$ alleles, forward primer: 5′-CCT GTG AGT TGG AAA GGG ACA TGG CTG-3′, reverse primer: 5′-CCA CCA CGA AGG CAG TGT TCA ATC CTA AA-3′, 2). $AurA^{d2}$ allele, forward primer: 5′-CAG AGT CTA AGT CGA GAT ATC ACC TGA GGG TTG A-3′, reverse primer: 5′-GAT GGA AAC CCT GAG CAC CTG TG AAC-3′ 3). *Sox2Cre* and *TtrCre* alleles, forward primer: 5′-TCC AAT TTA CTG ACC GTA CAC CAA-3′, reverse primer: 5′-CCT GAT CCT GGC AAT TTC GGC TA-3′

Wholemount immunofluorescence analysis

Dissected embryos were fixed for 1 hour in 4% paraformaldehyde in phosphate buffered saline (PBS) right after the dissection. After fixation, embryos were washed three times in PBS for 10 min each and once in PBT (1% BSA and 5% Triton X-100 in PBS) for 10 min. After incubating in blocking solution (5% normal goat serum in PBT) for 1 hour, embryos were incubated with primary antibodies in blocking solution for overnight in 4°C. Then, embryos were washed three times in PBT for 10 min each, and incubated with secondary antibodies for 1 hour. After secondary antibody incubation, embryos were washed three times in PBT for 10 min each, once in PBS for 5 min, equilibrated in serial Glycerol/PBS solutions (25%, 50%), and analyzed in an inverted fluorescence microscope (Leica. DMI4000). The following antibodies were utilized. Primary antibodies: rabbit anti-Oct4 (Abcam, Cat. No. ab19857) diluted with 1:1000;

rabbit anti-cleaved Caspase-3 (Cell Signaling, Cat. No. 9664) diluted with 1:500. Secondary antibody: Alexa Fluor 594 goat anti-rabbit antibody (Invitrogen, Cat. No. A31631) diluted with 1:2000 in PBT.

Wholemount *in situ* hybridization

The wholemount *in situ* procedure was adapted and modified from the protocol of Henrique and co-workers (Henrique et al., 1995). Dissected embryos were fixed overnight in 4% paraformaldehyde in PBS at 4°C. After fixation, embryos were dehydrated in a methanol/PBT (0.1% Tween-20 in PBS) series (25%, 50%, 75% and 100%) and stored at -20°C in 100% methanol. For rehydration, embryos were washed with the opposite direction.

Embryos were treated with Proteinase K for 8 min, pre-hybridized at 70°C for a minimum 2 hours, and incubated with RNA probes overnight at 70°C. The next day, embryos were washed in MABT (50 mM maleic acid, 75 mM NaCl, 0.1% tween-20), incubated in blocking solution (10% blocking reagent in MAB) for 1 hour, incubated in NGS-blocking solution (10% normal goat serum in blocking solution) for a minimum of 2 hours, and incubated overnight with alkaline phosphate-conjugated antibody against digoxigenin (Roche Cat. No. 11 093 274 910) diluted 1:2000 in NGS-blocking solution at 4°C. After overnight incubation with antibody, embryos were washed four times in MABT for 30 min each, washed twice in NTMT (0.1 M NaCl, 0.1 M Tris-HCl pH 9.5, 50 mM MgCl, 0.1% tween-20) for 10 min each and stained with 20 µl/ml NBT/BCIP stock solution (Roche Cat. No.681451) in NTMT for color reaction. The color reaction was allowed to proceed for 12-48 hours. After that, embryos were washed twice in PBT for 10 min each, fixed in 4% paraformaldehyde for 20 min, and cleared in glycerol/PBT.

Preparation of RNA probes

The following probes were utilized: Hex (291-818 cDNA; 528bp) (Thomas et al., 1998); Brachyury (T) (full length cDNA; 1784bp) (Herrmann, 1991); Wnt7b (full length cDNA; 3396bp) (Image consortium, ID 6817404); Fgf8 (full length cDNA; 1100bp) (Guo and Li, 2007) and Axin2 (2420bp cDNA piece containing part of exon 2, exons 3-9 and a portion of exon 10) (Jho et al., 2002). For RNA probe preparations, DNA constructs containing cDNA were linearized by overnight reaction with restriction enzymes. DNA constructs were kindly provided by Drs. Frank Costantini (*Axin2*), James Li (*Fgf8*), and Tristan Rodriguez (*Hex*). 1 µg of linearized DNA were used as a template in 20 µl *in vitro* transcription reactions (1X Transcription buffer, 1X digoxigenin RNA labeling mix (Roche Cat. No. 1277073), 0.01 M DTT, 1 U/µl RNAse inhibitor (RNAsin, Promega N2611), 2 U/µl T3, T7 or SP6 RNA Polymerase).

Wholemount β-galactosidase activity assay

Dissected embryos were fixed in fixation solution (0.2% glutaraldehyde, 2% formalin, 5 mM EGTA, 2 mM MgCl2 in 0.1 M phosphate buffer, pH 7.3) for 5-10 min, washed three times in rinse solution (0.1% deoxycholate, 0.2% IGEPAL, 2 mM MgCl2 in 0.1 M phosphate buffer, pH 7.3), and stained overnight in staining solution (1 mg/ml X-gal, 5 mM potassium ferricyanide, 5 mM potassium ferrocyanide in rinse solution) at 37°C. The next day, embryos were washed twice in rinse solution for 5 min each, twice in PBS for 10 min each, fixed in 4% paraformaldehyde in PBS at room temperature for 20 min and cleared in glycerol/PBS.

CHAPTER III:

GENERATION OF EMBRYONIC STEM CELL-DERIVED MICE USING EPIBLAST-ABLATION CHIMERAS

Preface

The idea for the work shown in this chapter originated from the results described in Chapter II. This work was in collaboration with the laboratory of Dr. Steve Jones. I collected embryos, generated tetraploid embryos and analyzed the data. The laboratory of Dr. Jones provided embryonic stem (ES) cells, injected ES cells into blastocysts and conducted embryo transfer surgeries. Joy Riley, our lab member, took over blastocyst injections and embryo transfers after she joined our laboratory. All the chimeras were obtained with the combined effort of Joy Riley, Judith Gallant, Marilyn Keeler, and myself. I collected and analyzed the chimeras and interpreted the data. Statistical analysis of chimera data was performed with the help of Dr. Oliver King, an assistant professor in our department.

Abstract

In the past, many researchers have been interested in generating embryos or mice composed solely of pluripotent cells such as embryonic stem (ES) cells or induced pluripotent stem (iPS) cells. There are multiple advantages for the generation of ES cell or iPS cell-derived embryos or mice. First, it saves time and money during the generation of knockout mouse lines. Second, it makes possible the direct analysis of embryos derived completely from mutant ES cells. Third, it is the most stringent way to test the potency of newly derived or reprogrammed ES or iPS cell lines.

Previously, we found that mutation of *Aurora A* in the epiblast leads to progressive depletion of the epiblast lineage through apoptosis, resulting in a conceptus composed only of extra-embryonic tissues that remain basically intact. From these results, we hypothesized that epiblast-specific *Aurora A* knockout (Epi-KO) embryos (that is, the genetically unaffected extra-embryonic tissues of mutants) were able to support the development of ES cell-derived embryos to term. We tested this hypothesis by injecting ES cells into host Epi-KO blastocysts. Four different ES cell lines, AB1, R1, KT4 and v6.5, were used in these experiments and we were able to generate E9.5 ES cell-derived embryos as well as ES cell-derived pups at E18.5. The majority of these pups died at birth and only one survived to adulthood and sired 4 pups, demonstrating that it was fertile.

As an alternative strategy, we took advantage of inducible Diphtheria toxin A (DTA)-mediated epiblast ablation to generate epiblast-ablated embryos. This strategy recapitulates the events of progressive epiblast depletion, observed in *Aurora A* epiblast-specific knockout mutants. Using this strategy, we were able to recover multiple E18.5

pups derived from two ESC lines tested (v6.5 and PC3) at 29% and 17%, respectively. However, none of the newborn pups survived to adulthood and interestingly, the majority exhibited abnormal features that included open eyelids, craniofacial defects and extra digits in the forelimbs.

We also have treated pregnant females with folic acid diet supplementation to test the hypothesis that folic acid supplementation would change the genomic methylation pattern and help fix the morphogenetic defects. However, folic acid supplementation did not rescue the phenotypic defects.

In conclusion, we were able to generate newborn mice derived from ES cells using our novel technique, called ‘epiblast complementation assay’. This technique suffices as a stringent tool for testing the pluripotency of any newly derived or reprogrammed line of ES cells or iPS cells and offers a simpler alternative to the tetraploid embryo complementation method. However, it is still necessary to conduct additional experiments to successfully generate adult mice composed of ES cells using the epiblast complementation chimera technique.

Introduction

A chimera is an animal composed of genetically distinct cells derived from two different zygotes. Since the first chimera experiment was performed to generate mouse chimeras by aggregating two eight-cell mouse embryos in the 1960s (Tarkowski et al., 1961), chimeras have been utilized as valuable tools for studying mouse genetics and development. Currently, the most important use of chimeras is in the generation of knockout mice. Traditionally, targeted ES cells produced by homologous recombination have been aggregated with diploid embryos (Wagner et al., 1985; Nagy et al., 1990; Wood et al., 1993) or have been injected into diploid host blastocysts to achieve germline transmission of the mutated allele to the offspring (Bradley et al., 1984).

Because the generation of knockout mice using targeted ES cells takes considerable amount of effort, several researchers have tried to generate embryos or mice derived fully from pluripotent cells. The tetraploid complementation assay is one of the methodologies that have been utilized for this purpose (Nagy et al., 1990; Nagy et al., 1993; Wang et al., 1997) and is considered to be the most stringent tool to test the pluripotency of stem cells.

There are multiple advantages for generating mice solely from stem cells. First, it saves time for generating knockout mouse lines because it does not require the generation of intermediate chimeras to get gene-targeted offspring. Second, it is more economical because less monetary resources would be required for husbandry expenses. Third, it is possible to analyze the embryos derived completely from mutant ES cells without any breeding steps to generate mutant embryos. Fourth, it is the most

stringent methodology to test the pluripotency of any newly derived or reprogrammed lines of ES cells or induced pluripotent stem (iPS) cells.

As described in chapter II, we observed that genetic ablation of *Aurora A* in the epiblast layer of the conceptus (Epi-KO) leads to gradual epiblast depletion through apoptosis at early post-implantation stages, resulting in a conceptus composed solely of extra-embryonic tissues that remain basically intact. We hypothesized that the extra-embryonic tissues of *Aurora A* Epi-KO embryos would sustain the capacity to direct the differentiation of stem cells for appropriate embryonic patterning and development.

In the current study, we addressed this hypothesis by injecting pluripotent stem cells into host Epi-KO blastocysts. In essence, we created chimeras composed of ES cells and embryos devoid of epiblast tissue and asked if the injected ES cells could substitute for epiblast-derived tissues. Using this strategy, we were able to generate ES cell-derived embryos and mice. We also used an alternative strategy in which the epiblast of post-implantation embryos was depleted by conditional expression of *Diphtheria toxin A* specifically in the epiblast (Epi-DTA). Using this strategy, we were able to generate ES cell-derived embryos and newborn mice. We found that this alternative strategy is easier to perform and more efficient in producing ES cell-derived newborns than the tetraploid complementation assay, which has been commonly used for *in vivo* assay for pluripotency.

Results

Extra-embryonic tissues of *AurA* Epi-KO embryos support the development of embryonic stem cell-derived embryos

As described in Chapter II, mutation of *Aurora A* in the epiblast leads to progressive epiblast ablation through apoptosis, giving rise to a conceptus composed of extra-embryonic tissues that remain basically intact (Fig. 2. 3B). This observation made us hypothesize that the extra-embryonic tissues of *AurA* Epi-KO embryos are functionally capable of supporting ES cell-derived embryos to develop to term.

To address this question and to test whether we could generate ES cell-derived embryos or mice by making chimeras between *AurA* Epi-KO embryos and pluripotent embryonic stem (ES) cells, we devised and performed the strategy illustrated in Fig. 3.1. First, we generated *AurA* Epi-KO blastocysts by mating females homozygous for a floxed allele of *AurA* (*AurA*$^{fx/fx}$) to males heterozygous for a null allele of *AurA* and homozygous for *Sox2Cre* transgene (*AurA*$^{d2/+}$;*Sox2*$^{Cre/Cre}$). Then, we injected pluripotent ES cells into these blastocysts and transferred them into pseudopregnant recipients, allowing them to develop to the desired embryonic stages or to develop to term.

To generate chimera intermediates, we first injected wild-type AB1 and R1 ES cells into Epi-KO blastocysts marked by the recombination of R26 reporter allele (*AurA*$^{d2/fx}$;*R26*$^{r/+}$;*Sox2*$^{Cre/o}$) using the mating strategy described in Table 3.1. The AB1 cell line was established from the blastocysts generated by 129/Sv cross (McMahon and Bradley, 1990) and results in agouti coat color in chimera pups. The R1 ES cells were derived from (129X1/SvJ x 129S1) F1 blastocysts and also give rise to agouti coat color in chimera mice (Nagy et al., 1993).

Figure 3. 1

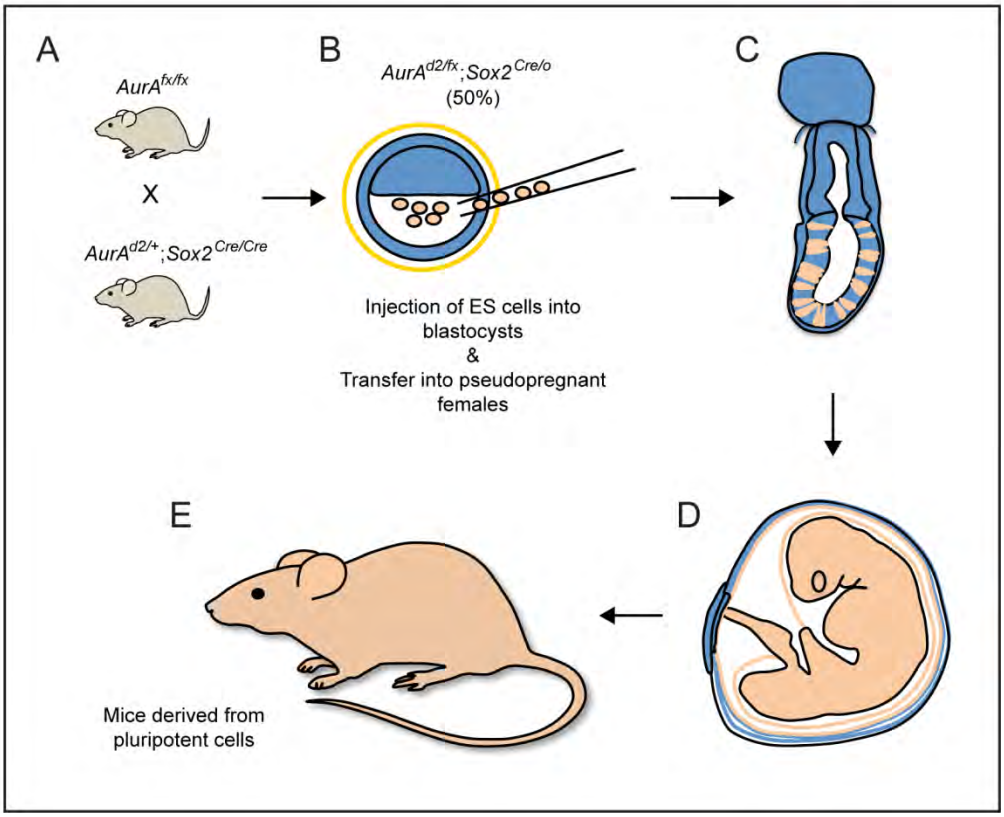
A
AurA fx/fx
X
AurA d2/+;Sox2 Cre/Cre
B
AurA d2/fx;Sox2 Cre/o
(50%)
Injection of ES cells into
blastocysts
&
Transfer into pseudopregnant
females
C
D
E
Mice derived from
pluripotent cells

Figure 3. 1. Strategy for generating ES cell-derived embryos or mice using *AurA* Epi-KO embryos. (A) First, we generated *AurA* Epi-KO blastocysts from the cross between females homozygous for a floxed allele of *AurA* (*AurA*$^{fx/fx}$) and males heterozygous for a null allele of *AurA* and homozygous for *Sox2*^{Cre} transgene (*AurA*$^{d2/+}$;*Sox2*$^{Cre/Cre}$). (B) After collecting *AurA* Epi-KO blastocysts at E3.5, we injected ES cells (marked in beige) into these blastocysts and transferred them into pseudopregnant recipient females (E2.5), allowing them to develop. (C) At E6.5, the epiblast is composed of epiblast cells derived from injected ES cell (beige) and host epiblast (blue). (D) We could recover embryos at E9.5 or (E) allow them to develop to term, generating fully ES cell-derived mice.

Table 3. 1

Cross	Male	Female	Injected ES cell line	Chimerism assay
1	*AurA*$^{d2/+}$; *Sox2Cre/Sox2Cre*	*AurA*$^{fx/fx}$; *R26*$^{r/r}$	AB1, R1	Contribution by host blastocyst (β-galactosidase activity assay)
2	*AurA*$^{d2/+}$; *Sox2Cre/Sox2Cre*	*AurA*$^{fx/fx}$	KT4 (*R26*^{LacZ})	Contribution by ES cells (β-galactosidase activity assay)
3 (Coat color)	*AurA*$^{d2/+}$; *Sox2Cre/Sox2Cre* (Albino)	*AurA*$^{fx/fx}$ *R26*$^{mT\text{-}mG/mT\text{-}mG}$ (Albino)	v6.5 (Agouti)	Coat color (Agouti) by ES cells Green fluorescence by host blastocyst

Table 3. 1. Mating strategies for generating ES cell-derived mice and the chimerism analysis.

Initially, we created chimeras by injecting AB1 and R1 ES cells into LacZ-marked blastocysts. β-galactosidase activity assays for embryonic chimeras dissected at E9.5 revealed that the injected ES cells rescue the developmental defects of *AurA* Epi-KO embryo, which usually exhibits empty yolk sac with no embryonic s tissue at E9.5 (Fig. 3. 2A), to generate normal AB1 and R1 ES cell-derived embryos at organogenesis stages. Compared to control chimeras, which exhibited high percentage of stained cells derived from host blastocyst, ES cell-derived embryos (experimental chimeras) contained only few stained cells in embryonic tissues, indicating that injected non-*LacZ* ES cells substitute most of the ablated epiblast, derived from host embryos (Fig. 3. 2B, C).

In the converse experiments, we injected KT4 ES cells into non-*LacZ* Epi-KO blastocysts ($AurA^{d2/fx};R26^{+/+};Sox2^{Cre/o}$) (See the Table 3.1). KT4 ES cells, derived from mouse blastocysts carrying the ROSA26 *LacZ* gene trap (Tremblay et al., 2000), constitutively express a cytoplasmic form of β-galactosidase and their contribution in chimeras can be traced by β-galactosidase assays. Using this strategy, we were also able to generate normal KT4 ES cell-derived embryos of organogenesis stages at E9.5. β-galactosidase assays revealed that the whole embryonic tissues were derived from injected KT4 ES cells (Fig. 3. 3B). Even extra-embryonic mesoderm tissue, which would be derived from the epiblast lineage during embryogenesis, was completely derived from injected KT4 ES cells, indicating that injected KT4 ES cells took over the roles of host epiblast that had already been ablated due to knockout of *Aurora A*.

These results demonstrate that the extra-embryonic tissues of *AurA* Epi-KO embryos can support the development of ES cell-derived embryos through gastrulation and early organogenesis stages and that injected pluripotent ES cells were able to

Figure 3. 2

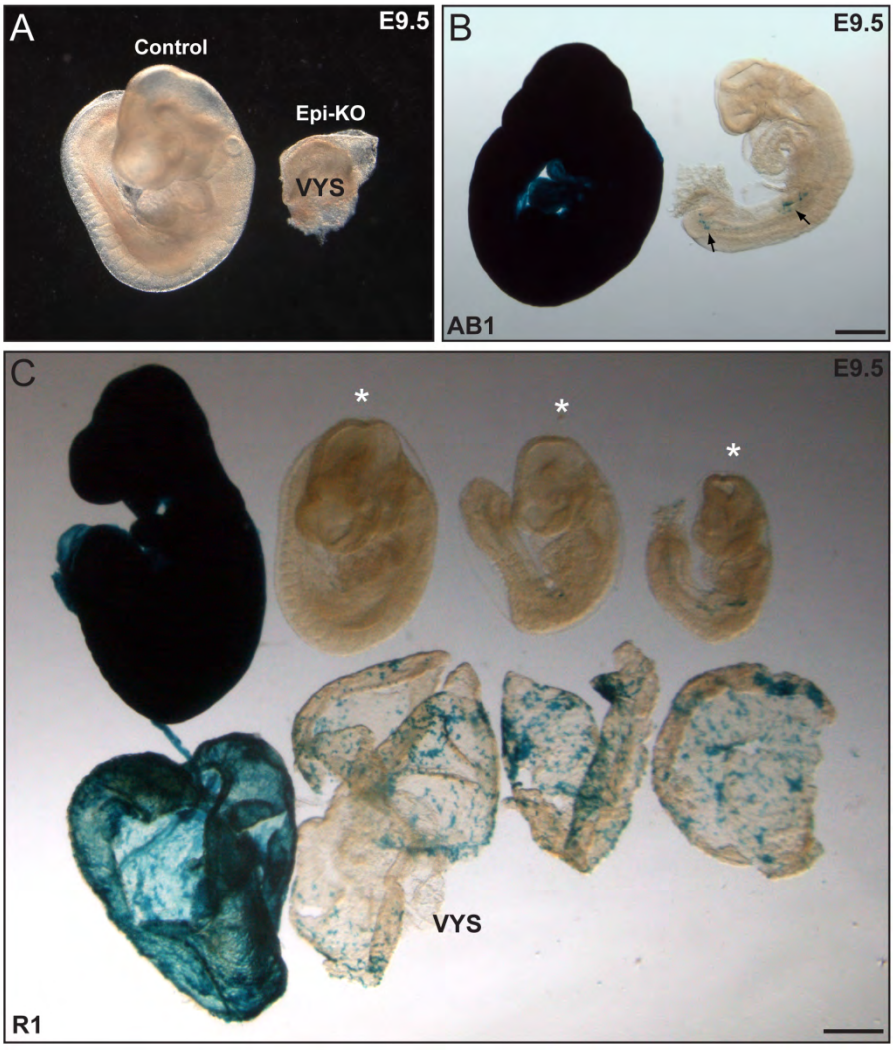

Figure 3. 2. Extra-embryonic tissues of *AurA* Epi-KO embryos support the development of ES cell-derived embryos to organogenesis stages.

(A) Control and *AurA* epiblast knockout embryos dissected at E9.5. The *AurA* Epi-KO embryo has been resorbed leaving the extra-embryonic components intact and giving rise to an empty visceral yolk sac (VYS). (B) Chimeric embryos generated by injection of AB1 ES cells into control blastocysts (left) or *AurA* Epi-KO blastocysts (right). The descendants of the host blastocyst are marked by $R26^{lacZ}$ in the epiblast (blue). The chimera derived from an *AurA* Epi-KO blastocyst is composed mostly of injected AB1 ES cell-derived tissuess (non-blue), whereas the chimera derived from a control blastocyst is composed mostly of the host blastocyst-derived tissues (blue). A few blastocyst-derived cells, marked by β-galactosidase activity, are visible in the gut region of the Epi-KO chimeras (arrows). (C) Chimeric embryos generated by injection of R1 ES cells into control blastocysts (left) or *AurA* Epi-KO blastocysts (white asterisks). The descendant cells of the host blastocysts are marked by activation of $R26^{lacZ}$ in the epiblast (blue). Chimeras derived from *AurA* Epi-KO blastocysts are composed mostly of injected R1 ES cell-derived tissues (non-blue), whereas chimeras derived from control blastocyst are composed mostly of host blastocyst-derived tissues (blue). A few blastocyst-derived cells, marked by β-galactosidase activity, are still visible in the gut region and visceral yolk sacs (VYS). Images are shown at the same scale. Scale bar, 500 μm.

Figure 3. 3

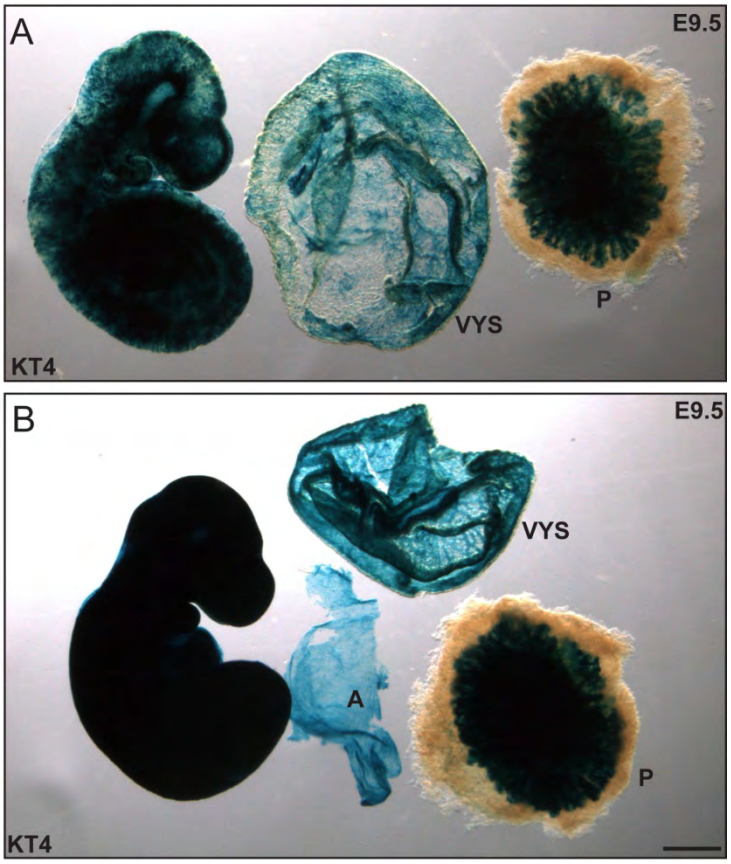

Figure 3. 3. Extra-embryonic tissues of *AurA* Epi-KO embryos support the development of KT4 ES cell-derived embryos to organogenesis stages.

(A and B) A chimeric embryo with its extra-embryonic tissues, visceral yolk sac (VYS), amnion (Am) and placenta (P) generated by injection of KT4 ES cells into control blastocysts (A) or *AurA* Epi-KO blastocyst (B). Descendants of injected KT4 ES cells are marked by the presence of the $R26^{lacZ}$ allele (blue). A chimera derived from an *AurA* Epi-KO blastocyst is composed mostly of injected KT4 ES cell-derived tissues (blue), whereas a control chimera is composed of both host blastocyst-derived tissues (non-blue) and injected KT4 ES cell-derived tissues (blue), revealing a normal chimeric embryo. Images are shown at the same scale. Scale bar, 500 µm.

rescue the gastrulation failure and embryonic lethality at E9.5, previously observed in *AurA* Epi-KO embryos.

Extra-embryonic tissues of AurA Epi-KO embryos support the development of ES cell-derived embryos to term

After the successful generations of E9.5 ES cell-derived embryos using multiple ES cell lines (AB1, R1, KT4), we decided to test if ES cell-derived embryos could develop to term. For this purpose, we injected KT4 ES cells into *AurA* Epi-KO blastocysts, transferred them into pseudopregnant recipients and recovered them at E18.5 by Caesarean section (C-section). Surprisingly, we found that most of ES cell-derived embryos were resorbed before E18.5. A few of the pups were stillborn and were composed solely of injected KT4 ES cells, as shown by β-galactosidase assays in all the tissues of the pups including the skin (Fig. 3. 4A) and internal organs (Fig. 3. 4B). However, we were not able to recover any live KT4 ES cell-derived pup at E18.5 using this strategy.

Since the lack of survival to term may be due to problems with the potency of KT4 ES cells, we utilized another ES cell line called v6.5. This is a C57BL/6 x 129/sv F1 hybrid line that has already been reported to generate live ES cell-derived pups via tetraploid embryo complementation and nuclear transfer cloning methods (Rideout et al., 2000; Eggan et al., 2001). To detect the contribution of injected v6.5 ES cells, we used coat color and GFP fluorescence to distinguish the contribution of ES cells and host blastocyst to the chimera.

Figure 3. 4

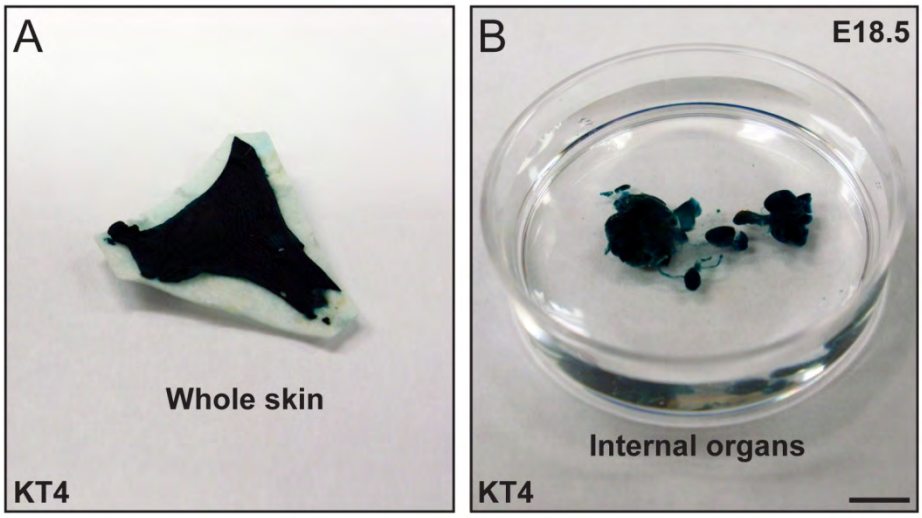

Figure 3. 4. Extra-embryonic tissues of *AurA* Epi-KO embryos support the development of KT4 ES cell-derived embryos to term. (A and B) β-galactosidase assay for the skin (A) and internal organs (B) from a KT4 ES cell-derived pup recovered at E18.5. This pup was generated by injection of KT4 ES cells into *AurA* Epi-KO blastocysts. Analysis of β-galactosidase activity reveals that the whole pup is fully composed of injected KT4 ES cell descendants.

(See Table 3.1). The coat color of ES cell-derived pups should be completely agouti without albino coat contribution from the host blastocyst. These pups also should not contain green fluorescent tissues, derived from the host blastocyst, which carries the *R26*$^{mT\text{-}mG}$ and *Sox2*^{Cre} transgenes. Based on this strategy, we were able to demonstrate the birth of v6.5 ES cell-derived pups recovered by C-section at E18.5. However, except for one male mouse, the majority did not survive to adulthood. This mouse was entirely agouti as demonstrated by coat color examination (Fig. 3. 5A, B), and had no green fluorescent tissue (Fig. 3. 5C, D). This animal sired 4 pups after mating with wild-type CD1 females (Fig. 3. 5E), revealing that it was fertile.

Diphtheria toxin A expression in the epiblast recapitulates the epiblast ablation phenotype of *AurA* Epi-KO embryos

The generation of ES cell-derived mice using *AurA* Epi-KO embryos (Fig. 3.1) is inconvenient in that it requires a genotyping step to identify the chimeras derived from *AurA* Epi-KO blastocysts (*AurA*$^{fx/d2}$;*Sox2*$^{Cre/o}$) or control littermates (*AurA*$^{fx/+}$;*Sox2*$^{Cre/o}$). This strategy is also inefficient because *AurA* Epi-KO blastocysts represent only half of the embryos collected and control chimeras have higher survival rates over epiblast-ablated ES cell-derived ones.

To correct these problems, we devised an alternative strategy, depicted in Fig. 3. 6. In this strategy, we take advantage of diphtheria toxin A (DTA)-mediated cellular ablation to generate epiblast-ablated embryos using *R26*^{DTA} and Sox2^{Cre} mice. The *R26*^{DTA} line carries a floxed *Diphtheria toxin fragment A* cassette targeted to the ROSA26

Figure 3. 5

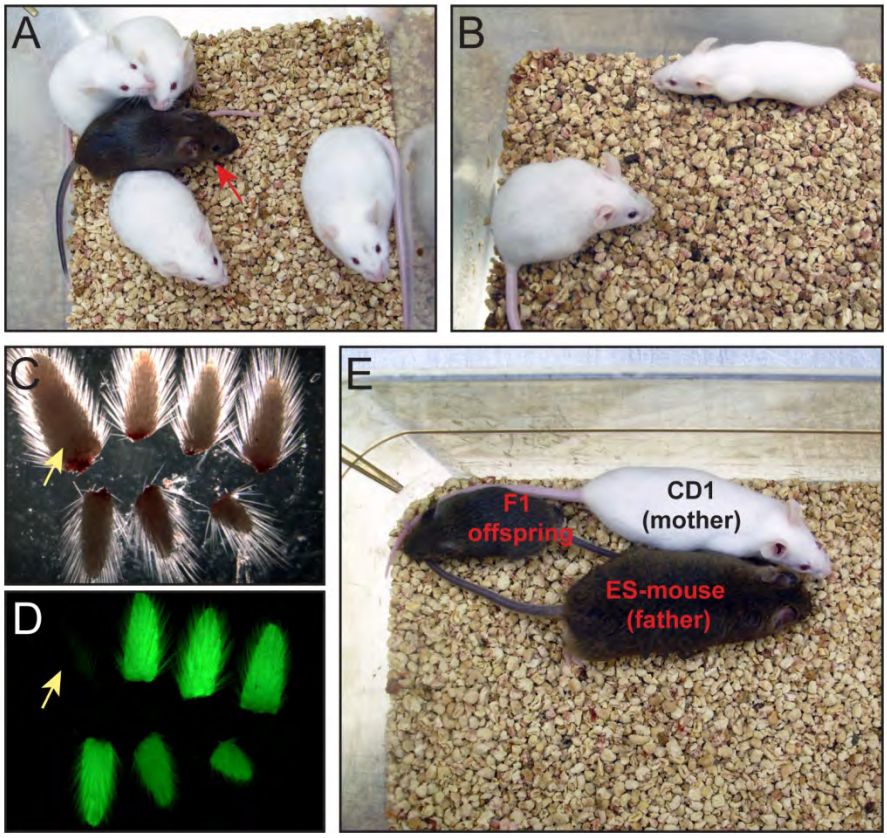

Figure 3. 5. *AurA* Epi-KO embryos support the development of v6.5 ES cell-derived embryos to term. (A) Male pups recovered at E18.5. One mouse (red arrow) exhibits agouti color, indicating that it is a v6.5 ES-derived pup. The rest exhibit a few patches of agouti color, revealing that they are chimeras derived from control blastocysts. (B) Female pups recovered at E18.5. Both show little agouti color. (C) Tail tips from pups shown in A and B. The yellow arrow indicates the tail from the agouti mouse shown in A. (D) Fluorescence visualization of the tail tips shown in C. The tail from the agouti mouse does not exhibit any green fluorescence signal, indicating that there is no contribution from the host blastocyst. The rest show strong green fluorescence, an indicator of host blastocyst contribution. (E) v6.5 ES cell-derived pup produced live agouti offspring, demonstrating its fertility and germline transmission.

Figure 3. 6

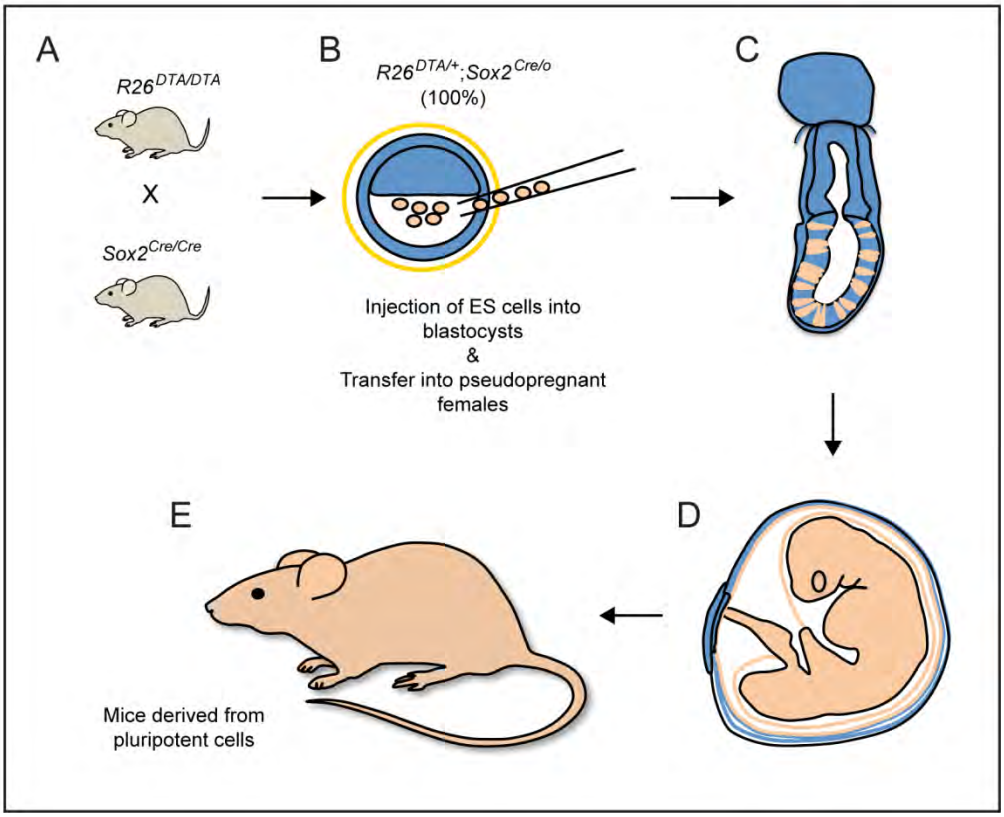
A
R26DTA/DTA
X
Sox2Cre/Cre
B
R26DTA/+;Sox2Cre/o
(100%)
Injection of ES cells into
blastocysts
&
Transfer into pseudopregnant
females
C
D
E
Mice derived from
pluripotent cells

Figure 3. 6. Alternative strategy for generating ES cell-derived embryos or mice using epiblast-ablated embryos generated by *DTA* expression. (A) First, we generate blastocysts, expressing *DTA* in the epiblast, from crosses between females homozygous for a floxed allele of *DTA* ($R26^{DTA/DTA}$) and males homozygous for the $Sox2^{Cre}$ transgene ($Sox2^{Cre/Cre}$). (B) Blastocysts collected at E3.5 (marked in blue), will be injected with ES cells and transfered into pseudopregnant recipients. (C) In E6.5 chimeras, the epiblast is composed of injected ES cells (beige) and host epiblast cells (blue). The epiblast cells would be ablated from the chimera due to the expression of *DTA* in this tissue. (D) By E9.5, ES cells take over the embryo with no host epiblast contributing to the embryonic tissue. (E) Injected blastocysts will be allowed to develop to term, generating ES cell-derived mice.

locus (Voehringer et al., 2008). The cross between females homozygous for *R26*^{DTA} allele (*R26*$^{DTA/DTA}$) and males homozygous for *Sox2*^{Cre} (Sox2$^{Cre/Cre}$) would give rise only to double heterozygous blastocysts (*R26*$^{DTA/+}$;*Sox2*$^{Cre/o}$), obviating the need to genotype each chimera.

To confirm that this strategy recapitulates the phenotype of *AurA* Epi-KO embryos and leads to empty yolk sac at E9.5, we performed morphological analysis of double heterozygous embryos (*R26*$^{DTA/+}$;*Sox2*$^{Cre/o}$) at E6.5, E7.5 and E9.5. As expected, E6.5 and E7.5 mutant concepti exhibited less epiblast (Fig. 3. 7A, C) and E9.5 mutants consisted of empty yolk sacs with no embryonic tissue (Fig 3. 7D), mimicking the phenotype of *AurA* Epi-KO mutants (Fig 3. 2A). This was also confirmed by wholemount immunostaining experiment using an Oct4 antibody. Interestingly, the epiblast ablation in Epi-DTA mutants seems to progress more quickly than the one in *AurA* Epi-KO mutants. More than half of the epiblast has been already ablated in E6.5 Epi-DTA embryos (Fig. 3. 7A, B).

Epiblast-ablated embryos generated by *DTA* expression can support the development of ES cell-derived embryos to term

After confirming that the Epi-DTA strategy leads to epiblast ablation, we tested the ability of Epi-DTA embryos to support the development of ES cell-derived pups using two ES cell lines, v6.5 and PC3. As shown before, the v6.5 cell line has been tested in *AurA* Epi-KO embryos and proved to have the potential to produce ES cell-derived adult mice. The PC3 line has been utilized in the generation of chimeras (Sluss et al., 2004) and tested without success in tetraploid embryo complementation assay by the

Figure 3. 7

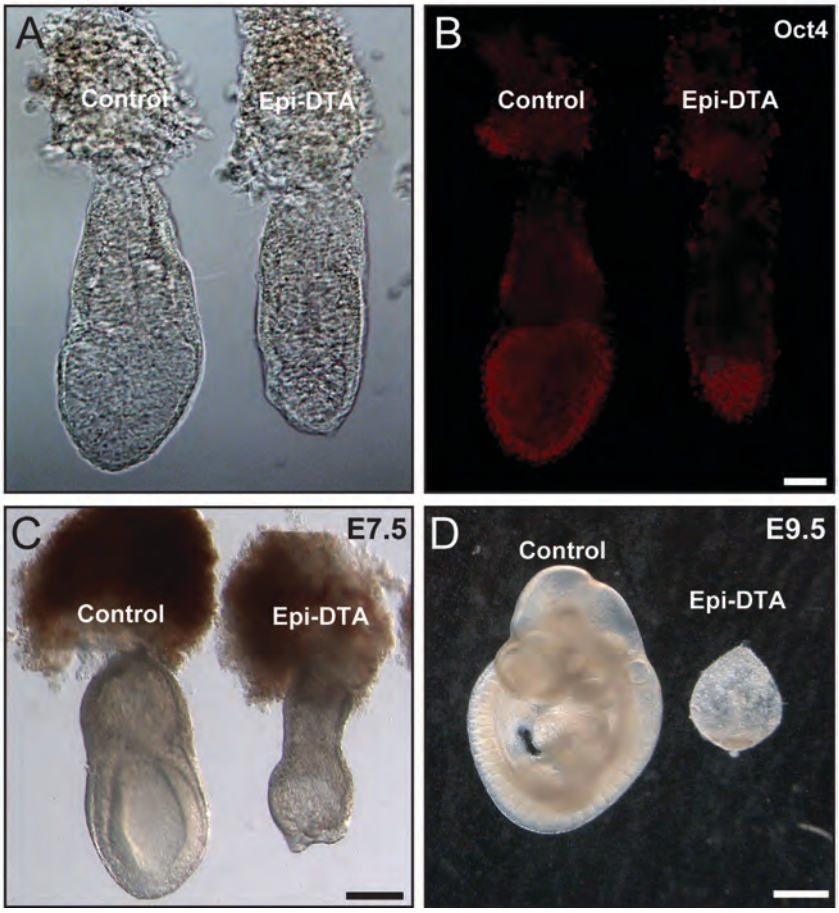
A
Control
Epi-DTA
B
Oct4
Control
Epi-DTA
C
E7.5
Control
Epi-DTA
D
E9.5
Control
Epi-DTA

Figure 3. 7. *DTA* expression in the epiblast recapitulates the epiblast depletion phenotype of *AurA* Epi-KO embryos. (A and B) DIC (A) and fluorescence (B) images of E6.5 embryos stained with anti-Oct4 antibody to mark the epiblast. The epiblast of Epi-DTA embryo is reduced to about one third of the size of control embryo. (C) Embryos dissected at E7.5. In Epi-DTA embryos, the epiblast has been depleted but extra-embryonic tissues are intact. (D) Epi-DTA embryos progress into empty yolk sacs by E9.5. Scale bars, 50 µm in A and B, 200 µm in C, and 500 µm in D.

laboratory of Steve Jones previously. After multiple trials, we found that both lines were able to give rise to E18.5 ES cell-derived pups at a rate of 29% and 17%, respectively (See the Table 3. 2), indicating that the new strategy works successfully in both cell lines without significant difference ($p>0.05$). ES cell-derived pups were identified easily by examining the eye pigmentation of pups recovered by C-section at E18.5 because both ES cells were established from pigmented mice and were injected into blastocysts derived from albino parents. Some of pups were recovered alive and looked morphologically normal (Fig. 3. 8A, C).

We also found that the increase in the number of injected ES cells (from 10-15 to 18-20) led to significant improvement in recovery rate of newborn pups ($p<0.05$).

ES cell-derived pups exhibit morphological defects

The majority of recovered ES cell-derived pups died at birth (Fig. 3. 8B, D) and exhibited abnormal features such as abnormally big placenta, post-axial polydactyly specifically in the forelimbs, craniofacial defects and open eyelids (Fig. 3. 9; also table 3. 3). The penetration and expressivity of these phenotypes varied. For the large placenta phenotype (Fig. 3. 9A), the v6.5 cell line showed 100% penetration (3/3) whereas PC3 had 50% penetration rate (4/8). The penetration rates for open eyelid phenotype (Fig. 3. 9B) were 82% (9/11) in v6.5-derived pups and 11% (1/9) in PC3-derived pups. The polydactyly phenotype consisted of one digit-like protrusion on the posterior side of the forelimbs that could be bilateral or restricted to one forepaw. The extra digit phenotype (Fig. 3. 9 C, D) was present in 80% (12/15) of the v6.5-derived pups and in 70% (7/10) of the PC3-derived pups.

Table 3. 2

Experimental condition	ES cell line (No. of cells injected)	No. of injected / transferred embryos	No. of pups at E18.5	Recovery rate (%)	Survival rate (%)
1	v6.5 (10-15)	51	5	10	0
2	v6.5 (18-20)	48	14	29[a]	0
3	PC3 (18-20)	59	10	17[b]	0
4*	v6.5 (18-20)	50	11	22[c]	0

v6.5: F1 129Sv X C57BL ES cell line, PC3: 129Sv ES cell line

* Folic acid diet supplementation

a. Exp. 1 vs. Exp. 2. Fisher's exact test. $p<0.05$

b. Exp. 2 vs. Exp. 3. Fisher's exact test, $p>0.05$

c. Exp. 2 vs. Exp. 4. Fisher's exact test. $p>0.05$

Table 3. 2. Summary of Epi-DTA chimera experiments

Figure 3. 8

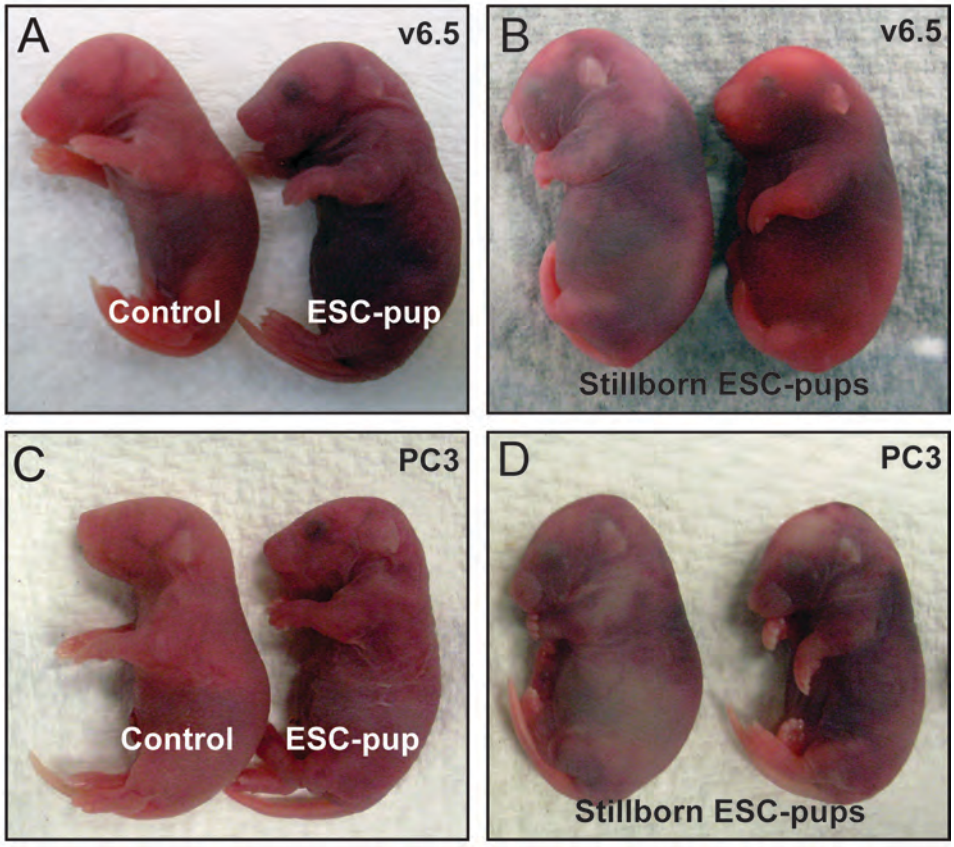

Figure 3. 8. Epiblast-ablated embryos generated by *DTA* expression can support the development of ES cell-derived newborn pups. (A) Control and v6.5 ES cell-derived pups recovered at E18.5. (B) Stillborn v6.5 ES cell-derived pups. (C) Control and PC3 ES cell-derived pups recovered at E18.5. (D) Stillborn PC3 ES cell-derived pups.

Figure 3. 9

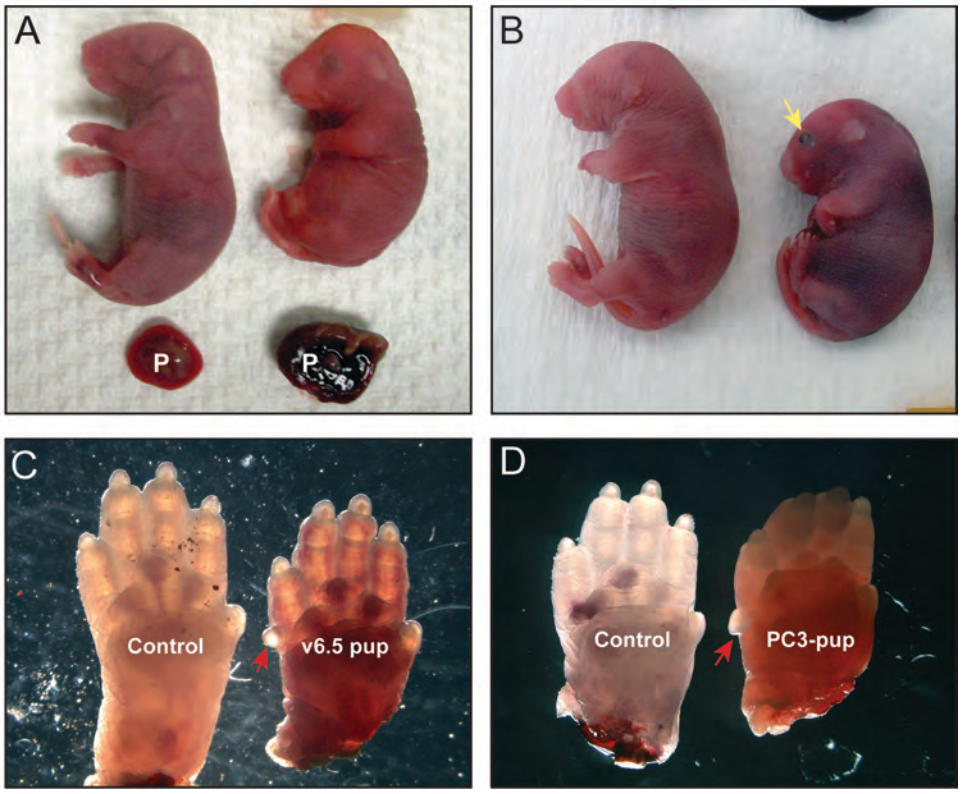

Figure 3. 9. ES cell-derived pups show developmental defects. (A) Control (left) and v6.5 ES cell derived (right) pups recovered at E18.5. ES cell-derived pup shows bigger placenta (P). (B) Control (left) and ES cell derived (right) pups recovered at E18.5. ES cell-derived pup show eyelid-closing defects. (C and D) Right forelimbs from control and ES cell-derived pups. Both v6.5 and PC3 ES cell-derived pups exhibit post-axial polydactyly in forelimbs (red arrows).

Table 3. 3

ES cell line	No. of pups recovered at E18.5 (%)	Morphological abnormalities		
		Bigger Placenta (%)	Extra digits in forelimbs (%)	Open eyelid (%)
v6.5	14/48 (29.2)	3/3 (100)	12/15 (80)	9/11 (81.8)
PC3	10/59 (16.9)	4/8 (50)	7/10 (70)	1/9 (11.1)

Table 3. 3. Morphological abnormalities in ES cell-derived pups recovered at E18.5

Folic acid supplementation diet does not rescue the defects of ES cell-derived pups

Previous studies have shown that the anomalies observed in ES cell-derived pups are likely due to epigenetic alterations in imprinted genes of ES cell lines (Dean et al, 1998). One example is the extra digits phenotype, which has been observed in mutants for *Igf2*, one of well-studied imprinted gene (Wang et al., 1994). In addition, open eyelids were reported in cloned mice (Shimozawa et al., 2002), where aberrant gene expressions or methylation of imprinted genes are responsible for this phenotype.

Folate is a methyl donor in biological methylation reactions such as the DNA methylation process (Lucock, 2000; Crider et al., 2012) and dietary folate deficiency has been reported to decrease genome-wide methylation both in human and animal models (Choi and Mason, 2002). On the other hand, folic acid supplementation has been observed to increase genomic DNA methylation globally and has been shown to help prevent neural tube closure defects (Pufulete et al., 2005; Gonda et al., 2012; Zhao et al., 1996).

In an attempt to prevent the morphological defects of ES cell-derived pups, we supplemented the surrogate mothers with folic acid from the day of embryo transfer surgery to pup recovery at E18.5. However, our results revealed that folic acid supplementation did not significantly rescue the morphological defects of v6.5 ES cell-derived pups and that the recovery rate was not improved compared to regular food supplementation (Table 3. 2). On the contrary, it seemed to have adverse effects in that pups recovered at E18.5 were much more affected (Fig. 3. 10).

Figure 3. 10

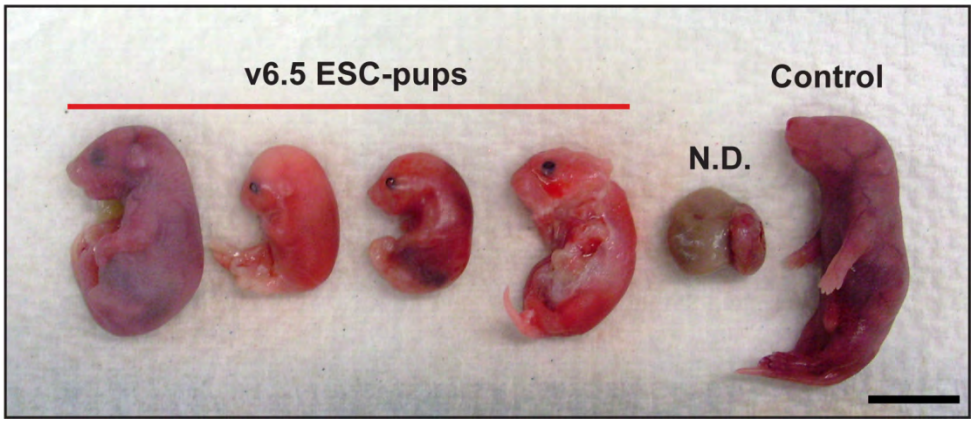

Figure 3. 10. Folic acid supplementation does not rescue the defects of ES cell-derived pups. v6.5 ES cell-derived pups recovered at E18.5 after dietary supplementation with folic acid during pregnancy. The first 4 pups are derived from v6.5 ES cells, as shown by eye pigmentation. The three pups in the right were stillborn and more developmentally compromised. Scale bar, 1 cm.

The **epiblast complementation assay is more efficient than the tetraploid complementation assay**

The main reason for our interest in developing epiblast complementation technology is the need of an alternative protocol to tetraploid embryo complementation assay, which is currently the most stringent assay for pluripotency. Compared to the tetraploid complementation assay (depicted in Fig. 3. 11A), our epiblast complementation assay is technically simpler. It does not require electrofusion or embryo culture to blastocysts for chimera production. Therefore, it is important to determine if this novel technology is more efficient to generate ES cell-derived embryos or mice than the tetraploid complementation assay.

To address this question, we generated tetraploid complementation chimeras using the same ES cell lines (v6.5 and PC3) that we tested to generate epiblast complementation chimeras and analyzed the resulting pups after recovering them by C-section at E18.5. In these experiments, we utilized *R26*$^{mT\text{-}mG}$ mice to generate the host tetraploid embryos, making it possible to distinguish the tissues derived from the injected ES cells from the ones derived from the host tetraploid embryo.

In experiments using the PC3 cell line, we were not able to generate any E18.5 pups (0/12). We observed only resorbing embryos consisting of placental tissues that were identified by the presence of red fluorescence (not shown). In experiments using the v6.5 ES cell line, we were able to generate only one live ES cell-derived pup (1/24), which was found dead the day after fostering to a surrogate mother (Fig. 3. 11B). Interestingly, we observed post-axial polydactyly in this pup, similar to the phenotype of epiblast complementation chimeras (Fig. 3. 11C, D). Consequently, the

Figure 3. 11

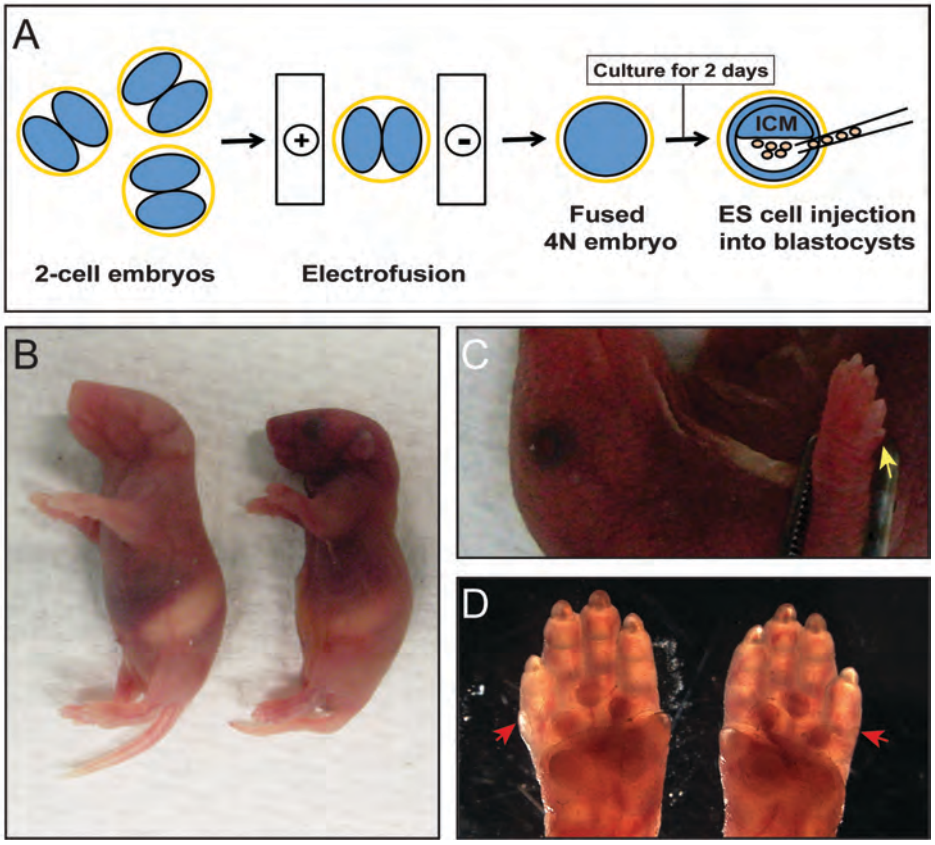
A
Culture for 2 days
ICM
2-cell embryos
Electrofusion
Fused
4N embryo
ES cell injection
into blastocysts
B
C
D

Figure 3. 11. Generation of ES cell-derived pups using the tetraploid complementation assay. (A) Schematic representation of tetraploid embryo complementation method. Two-cell stage embryos were collected at E1.5 and electrofused to generate tetraploid (4N) embryos. After 2 days in culture, we injected embryonic stem cells into the 4N blastocysts generated. ICM, inner cell mass. (B) Control (left) and ES cell derived (right) pups generated by tetraploid complementation assay. (C) ES cell-derived pup exhibited post-axial polydactyly in the forelimb (yellow arrow). (D) Both forelimbs have extra digit (red arrows).

recovery rate of the tetraploid complementation assay is lower than our epiblast complementation assay (29% vs. 4%).

In conclusion, our novel epiblast complementation assay suffices for generating stem cell-derived pups and provides a practical method for testing the pluripotency of newly derived or reprogrammed ES cells or iPS cell lines, replacing the tetraploid complementation assay.

Discussion

In this chapter, we show that it is possible to generate ES cell-derived newborns using host embryos deprived of epiblast either by *AurA* knockout or *DTA* expression. These results reveal that the extra-embryonic tissues of post-implantation embryos, devoid of the epiblast, are sufficient to guide and support the development of ES cells into fetuses. This observation is consistent with the notion that extra-embryonic tissues are responsible for patterning the embryo as well as for nutrition and protection during early post-implantation stages (Stern and Downs, 2012). However, we could not rule out the possibility that residual epiblast cells existing at earlier stages of development provide injected ES cells with non-cell autonomous signals which direct the differentiation of ES cells into a fully patterned embryo. It will be interesting to determine how epiblast cells from host embryo and injected ES cells communicate or compete with each other in chimeric embryos.

We also found that we could not generate adult mice derived solely from ES cells with one exception using *AurA* Epi-KO embryos and that ES cell-derived pups exhibited major defects including a larger placenta, open eyelids and post-axial polydactily. These findings raised two questions: 1) Why are the ES cell-derived pups generated through our epiblast complementation assay not able to survive to adulthood? 2) Why do these pups show morphological defects?

Previous reports give some clues to answer these questions. The defects found in our newborn pups were also observed in ES cell-derived fetuses produced by tetraploid complementation assay and these abnormalities have been reported to be associated with aberrant expression of imprinted genes such as *Igf2r*, *H19*, *Igf2*, and

U2af1-rs1 in ES cells and ES cell-derived fetuses (Dean et al., 1998). The finding that mutants for *Igf2* gene exhibited the post-axial polydactyly in the forelimbs supports this notion (Wang et al., 1994). Thus, it suggests the possibility that the ES cells utilized in our experiments might have alterations in the expression of imprinted genes and that abnormal expression of these genes is responsible for the defects observed in ES cell-derived pups produced by epiblast complementation assay. However, whether the ES cell lines that we utilized in our studies have alterations in the expression of imprinted genes remains to be determined in the future.

There is also a possibility that our epiblast complementation assay leads to defects of ES cell-derived pups because of limited capability to support the ES cell-derived embryos. The capacity of extra-embryonic tissues left behind after ablating Aurora A function or after inducing the expression of *DTA* in the epiblast might not be enough to differentiate the injected ES cells into ES cell-derived pups in a proper manner during embryogenesis. This possibility is supported by the fact that we were able to generate an adult ES cell-derived mouse using the *Aurora A* Epi-KO strategy. The Epi-DTA strategy seems to ablate epiblast cells at earlier stages and in a faster manner. This likely created a different environment than that of *AurA* Epi-KO chimeras. It is also important to mention that the sole pup surviving to adulthood in *AurA* Epi-KO chimeras, could have been derived from a control chimera that was overtaken by ES cells.

There is also a possibility that the *Sox2Cre* transgene is activated ectopically in the extra-embryonic tissues of epiblast-ablation chimeras leading to compromised development of support tissues such as the placenta. *DTA* expression swiftly kills the cells expressing this gene whereas *Aurora A* deficiency in extra-embryonic cells would

be more tolerated because its effect is more severe in proliferating cells and extra-embryonic cells divide more slowly than epiblast cells. An alternative to solve this problem would be to use a different driver of Cre in the epiblast.

It also remains to be determined whether a diminished potency of the ES cell lines or limited capacity of the extra-embryonic tissues of *AurA* Epi-KO embryos or Epi-DTA embryos prevents the survival of ES cell-derived pups. This question could be addressed by using intact inner cell mass (ICM) cells isolated from blastocysts via immunosurgery (Solter and Knowles, 1975). The ICM is the source of ES cells and is regarded as a pure pluripotent tissue. Depending on the results of this ICM cell test, we would be able to attribute the failure to generate surviving ES cell-derived adult mice to our ES cell lines or the epiblast ablated embryo host.

We observed similarity in the patterns of abnormalities in pups derived from two different cell lines, v6.5 and PC3. These results suggest that the ES cell lines are affected in similar ways during manipulations in culture. In other words, these results suggest epigenetic rather than genetic defects in ES cells. To prevent these defects, we supplemented the diet of surrogate mothers with folic acid expecting that folic acid would change the methylation patterns of affected imprinted genes such as *Igf2* or others favorably and rescue the morphological defects (Pufulete et al., 2005; Gonda et al., 2012). However, this treatment did not prevent the lethality of ES cell-derived pups and the survival rate was not improved (Table 3. 2). Therefore a more reliable method is required to determine if fixing the methylation pattern of imprinting genes would fix the defects of ES cell-derived fetuses or pups. One exciting possibility is the treatment of ES cells with vitamin C. A recent study reported that vitamin C could revert the methylation

pattern of ES cells in culture to a more similar state to that encountered in ICM cells (Blaschke et al., 2013).

To compare our epiblast complementation technique with the tetraploid complementation assay, we performed tetraploid complementation assays using the same ES cell lines. Using the PC3 ES cell line, we could not generate any ES cell-derived pups through tetraploid complementation assay. In experiments using the v6.5 ES cell line, we were able to generate only one live ES-cell derived pup, which died the next day. These results indicate that our epiblast complementation assay is much more efficient than tetraploid complementation in the generation of newborn pups.

In conclusion, we were able to generate newborns derived from two different pluripotent ESC lines (v6.5 and PC3) using our novel technique of epiblast ablation, which is called ‘epiblast complementation assay’. Despite several drawbacks, this technique suffices for testing the pluripotency of newly derived or reprogrammed line of ES cells or iPS cells and offers a simple alternative to the tetraploid complementation technique, generally accepted as a most stringent *in vivo* assay for pluripotency.

Materials and Methods

Mouse strains and genotyping

The *AurA*^{fx} conditional mouse line was obtained from Dr. Terry Van-Dyke (Cowley et al., 2009). Females carrying the *AurA*^{fx} allele were crossed to *Sox2*^{Cre} transgenic males to generate *AurA*^{d2} mice. The *AurA*^{d2} allele lacks exon 2 and it is a null allele of *AurA* . *Sox2*^{Cre} (Hayashi et al., 2002), ROSA26 reporter (*R26*^{r}) (Soriano, 1999), and *R26*$^{DTA/DTA}$ (Voehringer et al., 2008) mice were purchased from the Jackson Laboratory (Stock No. 003309, 004783, and 009669, respectively). The *R26*$^{mT\text{-}mG}$ mouse line was previously described (Muzumdar et al., 2007) and genotyped by the presence of red fluorescence in a tail tip biopsy. The rest of the mice were genotyped using PCR on genomic DNA samples obtained from tail tips. For genomic DNA sample preparation a piece of tail tip was placed into 200 µl of PCR lysis buffer (50 mM KCl, 10 mM Tris-HCl, 10 mM Tris-HCl, 2.5 mM $MgCl_2$, 0.1 mg/ml Gelatin, 0.45% v/v IGEPAL and 0.45% v/v Tween-20, 100 µg/ml Proteinase K) and incubated overnight at 56°C. The next day, after heat inactivation of the Proteinase K at 95°C for 5-8 min, a half or one microlitter of sample was used for PCR amplification.

Embryos were genotyped retrospectively after wholemount *in situ* hybridization, immunostaining or β-galactosidase assay procedures. For each conceptus, the ectoplacental cone was removed using forceps and placed in 20 µl of PCR lysis buffer and incubated overnight at 56°C. After heat inactivation of the Proteinase K at 95°C for 5-8 min, one or two microliters were used for PCR amplification. Each allele was confirmed using the following primers: 1) *AurA*^{fx} and *AurA*$^{+}$ alleles, forward primer: 5′-CCT GTG AGT TGG AAA GGG ACA TGG CTG-3′, reverse primer: 5′-CCA CCA CGA

AGG CAG TGT TCA ATC CTA AA-3′, 2) *AurA*^{d2} allele, forward primer: 5′-CAG AGT CTA AGT CGA GAT ATC ACC TGA GGG TTG A-3′, reverse primer: 5′-GAT GGA AAC CCT GAG CAC CTG TG AAC-3′ 3) *Sox2Cre* allele, forward primer: 5′-TCC AAT TTA CTG ACC GTA CAC CAA-3′, reverse primer: 5′-CCT GAT CCT GGC AAT TTC GGC TA-3′ 4) *R26*^{DTA} and *R26*$^{+}$ alleles, forward primers: 5'-CGA CCT GCA GGT CCT CG-3', 5'-CGT GAT CTG CAA CTC CAG TC-3', reverse primers: 5'-CTC GAG TTT GTC CAA TTA TGT CAC-3', 5'-GGA GCG GGA GAA ATG GAT ATG-3'.

Collection of blastocysts and embryonic stem (ES) cell injection

Blastocysts were collected from uteri of pregnant females on E3.5 or generated by culturing electrofused tetraploid embryos. Collection of blastocysts was performed as described previously (Nagy et al., 2003). Noon of the day when a mating plug was observed was considered embryonic day 0.5 of development (E0.5).

Collection of two-cell stage embryos and electrofusion

Two-cell stage (E1.5) embryos were collected from oviducts of pregnant females in the morning on day 2. To generate tetraploid embryos, two-cell stage embryos were electrofused as described previously (Nagy et al., 2003). Two-cell embryos were equilibrated in 0.3 M mannitol solution (0.3 M mannitol, (Sigma M4125), 0.3% BSA (Sigma A3311)) before being placed between two platinum electrodes (GSS-250, Biochemical Laboratory Service, Budapest, Hungary) in 0.3 M mannitol solution. Two-cell stage blastomeres were given an electric pulse at 30 V for 40 μsec using CF-150B pulse generator (Biochemical Laboratory Service, Budapest, Hungary). The resulting fused embryos (tetraploid embryos) were placed in a tissue culture incubator (5% CO2, 5% O2) and cultured for 2 or 3 days.

Wholemount immunofluorescence analysis

Dissected embryos were fixed for 1 hour in 4% paraformaldehyde in phosphate buffered saline (PBS) right after dissection. After fixation, embryos were washed three times in PBS for 10 min each and once in PBT (1% BSA and 5% Triton X-100 in PBS) for 10 min. After incubating in blocking solution (5% normal goat serum in PBT) for 1 hour, embryos were incubated with primary antibodies in blocking solution overnight in 4°C. Then embryos were washed three times in PBT for 10 min each, and incubated with secondary antibodies for 1 hour. After secondary antibody incubation, embryos were washed three times in PBT for 10 min each, once in PBS for 5 min, equilibrated in serial Glycerol/PBS solutions (25%, 50%), and analyzed in an inverted fluorescence microscope (Leica. DMI4000). The following antibodies were utilized. Primary antibodies: rabbit anti-Oct4 (Abcam, Cat. No. ab19857) diluted with 1:1000. Secondary antibody: Alexa Fluor 594 goat anti-rabbit antibody (Invitrogen, Cat. No. A31631) diluted with 1:2000 in PBT.

Wholemount β-galactosidase activity assay

Dissected embryos were fixed in fixation solution (0.2% glutaraldehyde, 2% formalin, 5 mM EGTA, 2 mM MgCl2 in 0.1 M phosphate buffer, pH 7.3) for 5-10 min, washed three times in rinse solution (0.1% deoxycholate, 0.2% IGEPAL, 2 mM MgCl2 in 0.1 M phosphate buffer, pH 7.3), and stained overnight in staining solution (1 mg/ml X-gal, 5 mM potassium ferricyanide, 5 mM potassium ferrocyanide in rinse solution) at 37°C. The next day, embryos were washed twice in rinse solution for 5 min each, twice in PBS for 10 min each, fixed in 4% paraformaldehyde in PBS at room temperature for 20 min and cleared in glycerol/PBS.

Statistical analysis

We used Fisher's exact test to compare the different experimental conditions used to generate chimeras.

CHAPTER IV:

GENERAL DISCUSSION

The study of developmental biology encompasses the processes of cellular growth, differentiation and morphogenesis that give rise to all the tissues and organs of an organism (Wolpert et al., 1998). The peri- and early post-implantation stages are extremely important for proper embryogenesis and continued survival of the embryo this is because abnormalities happening during this period of time would give rise to major developmental defects. In the worst case, they will lead to embryonic lethality but in other cases, they can cause conjoined twins or other major abnormalities such as heart defects or spina bifida. Therefore, it is paramount to investigate the early developmental processes that shape the embryo such as axial specification and gastrulation.

As a vital part of embryo growth, cell proliferation has major roles in embryogenesis. For example, it was previously shown that reducing the number of cells or inhibiting cell proliferation at pre-implantation stages leads to failure or delay of gastrulation (Tam, 1988; Power and Tam, 1993). Several reports also suggested the possibility that cell proliferation defects would have devastating consequences during early post-implantation development (Ding et al., 1998; Rivera-Perez et al., 2003; Yamamoto et al., 2004). The genetic analysis of the effects of abnormal cell proliferation at post-implantation stages has been precluded in the past by the lethality caused by mutations that affect the cell cycle. These mutations typically arrest embryo development at the time of implantation when the maternal supply of proteins and RNA is depleted. In addition, there have been no efforts to study the effects of cell proliferation arrest in the different components of the post-implantation embryo. The recent generation of a conditional floxed allele of Aurora A, a molecule essential to complete the cell cycle, and the availability of novel Cre driver lines now provide the reagents to address these questions.

The first part of my thesis focused on understanding the effects of deregulated cell proliferation on axial specification and embryonic patterning in early post-implantation mouse development. We hypothesized that defects in cell proliferation in the epiblast or the visceral endoderm would affect the process of axial specification and gastrulation, the two major patterning events of early post-implantation stages. To address this hypothesis we utilized a conditional allele of *Aurora A* to induce cell proliferation defects specifically in the epiblast or in the visceral endoderm components of the early mouse conceptus.

Analysis of tissue-specific mutant embryos showed that inactivation of *Aurora A* leads to apoptosis, failure of embryonic growth and eventually embryonic lethality. These results are identical to the effects of *AurA* ablation in pre-implantation embryos (Cowley et al., 2009; Lu et al., 2008; Sasai et al., 2008), indicating that Aurora A is essential for cellular growth and survival regardless of the tissue affected.

The effects on embryonic patterning were different between *AurA* Epi-KO and VE-KO mutants. The ablation of Aurora A in the epiblast led to drastic depletion of epiblast cells and gastrulation failure but it did not affect the initial establishment of the anteroposterior axis. In contrast, embryos with a mutation of *AurA* in the visceral endoderm failed to properly establish their anteroposterior axis and exhibited posteriorization of the conceptus resulting in the expansion of the primitive streak to the anterior region. These axial defects are associated with defects of DVE movement. These results are quite interesting if we consider that the in both cases it is the same mutation that led to such different outcomes. In the case of *Aurora* A ablation in the epiblast, the failure to complete gastrulation can be directly linked to low numbers of epiblast cells. This is similar to experiments in which the number of blastomeres is

reduced at pre-implantation stages, leading to delayed gastrulation, that suggest that the embryo pauses during development until a critical number of cells is reached to allow the progression of gastrulation. In *AurA* Epi-KO mutants, however, the events that initiate gastrulation are in place but the embryo cannot complete gastrulation because it is not able to compensate for the sudden and massive cell death brought about by the absence of *Aurora A* in the epiblast.

The patterning defects observed in VE-KO embryos may be indirectly related to cell death in the visceral endoderm. During the analysis of mutant embryos, we noticed that the AVE failed to shift or only partially shifted toward the anterior side of the embryo. The AVE is known to prevent the expansion of the primitive streak to the anterior side of the embryo, restricting the location of the primitive streak to the posterior region of the embryo. One possibility is that visceral endoderm cell death leads to reduction in visceral endoderm cell numbers, leading to failure to reach the critical cell numbers necessary to support the movement of the AVE. Eventually, this defect would allow the expansion of the primitive streak towards the anterior epiblast region, causing the posteriorization of the embryo.

Intriguingly, the analysis of *AurA* VE-KO mutants also revealed that the embryonic visceral endoderm, the visceral endoderm overlying the epiblast, was more severely affected than the extra-embryonic visceral endoderm, the layer of tissue that envelops the extra-embryonic ectoderm. We believe that these differences may be due to differences in the rate of cell proliferation between these two subpopulations of visceral endoderm with the extra-embryonic VE proliferating at a slower rate and thus leading to fewer apoptotic events in these cells and prolonged survival of the tissue. An interesting implication of this possibility is that inactivation of *Aurora A* in combination

with a floxed reporter and specific Cre drivers could be used to identify stem cells *in vivo*. This is because stem cells are quiescent and unlike proliferating cells would be resistant to the apoptotic effects produced by *Aurora A* inactivation.

One of the original goals of our study was to determine if inhibiting cell proliferation in the VE or epiblast would affect the shift of the AVE to the anterior side of the embryo. This required us to generate embryos in which cells of the VE or epiblast are unable to divide but otherwise normal. Unfortunately, we were unable to achieve this goal because ablation of *AurA* resulted in cell death. This question still remains and requires further investigation using novel strategies. One possibility is to utilize the conditional knockout of *HDAC1.* HDAC1 is a protein that has histone deactylase (HDAC) activity (Vidal and Gaber, 1991; Taunton et al., 1996) and it has been reported that HDAC1 knockout embryos have proliferation defects and exhibit increased level of cyclin-dependent kinase (CDK) inhibitors such as p21 and p27 (Lagger et al., 2002). Interestingly, HDAC1-deficient embryos do not exhibit elevated apoptosis levels when compared to wild type embryos. Therefore, it would be exciting to pursue our original aim using *HDAC1* conditional mice in place of mice with an *AurA* conditional allele. Another possible strategy is to lessen cellular death in the epiblast using the $Mox2^{Cre}$ allele (Tallquist and Soriano, 2000) in combination with the *AurA* floxed allele. This approach will lead to mosaic recombination in the epiblast at E5.0, resulting in reduced epiblast cell numbers and allowing us to study the link between cell numbers and anterior AVE movement. There are some caveats to this possibility; for example, it remains to be determined if the activity of $Mox2^{Cre}$ transgene results in reduced epiblast cell numbers or whether the non-recombined epiblast cells would compensate for the reduced cell number and produce a normal embryo.

The second part of my thesis was devoted to test a novel idea to generate mice completely derived from stem cells. This idea arouse from our *AurA* Epi-KO studies. In this technique termed “epiblast complementation chimera assay”, blastocysts in which the epiblast is genetically ablated are injected with ES cells and allowed to develop to term to determine if the injected ES cells can take over the epiblast lineage and produce viable offspring. Currently, the only way to achieve this goal is through the use of tetraploid complementation chimeras. This technique, however, is laborious and inefficient because it requires two critical steps: the generation of tetraploid embryos by electrofusion at the two-cell stage and the culture of tetraploid embryos in the incubator. In our experience, this technique has high attrition numbers and leads to delayed development of blastocysts.

In this study, we were able to generate newborns completely derived from ES cells by using our novel epiblast complementation assay. Unfortunately, with the exception of one case, we could not generate an ES cell-derived adult mouse by utilizing the ES cell lines that have been proved to be pluripotent previously. ES cell-derived pups died at birth and exhibited morphological defects such as post-axial polydactyly in forelimbs, open eyelids and overgrown placenta. Why are ES cell-derived pups generated through epiblast complementation not able to survive to adulthood? This question can likely be addressed by answering the next question; what is the source of the morphological defects of ES cell-derived pups? Previous findings provide some hints for the answers. Mutants for *Igf2,* one of well-studied imprinted genes, exhibit post-axial polydactyly in the forelimbs, a phenotype highly similar to the phenotype of our pups (Wang et al., 1994). This morphological defect has also been found in tetraploid complementation chimeras alongside enlarged placenta.

The hypertrophic placenta in ES cell-derived pups points out a malfunctioning embryonic-maternal connection. This could lead to nutritional deficiency in the embryo, methylation defects and aberrant expression of imprinted genes such as *Igf2r*, *H19*, *Igf2*, and *U2af1-rs1* (Dean et al., 1998). Also, it is known that the neural crest, a tissue responsible for the formation of most of the components of the head, is particularly sensitive to nutritional defects because of its accelerated rates of cell proliferation during embryogenesis (Crane and Trainor, 2006; Gray and Ross, 2009; Trainor, 2010). Thus, the defects observed in ES cell-derived pups could be due to abnormal function in the extra-embryonic tissues of epiblast ablated host embryos. This, in turn, may point to the defects in the potency of ES cells because as replacement of the epiblast lineage, ES cells are the source of several extra-embryonic tissues including extra-embryonic mesoderm, which gives rise to important components of the visceral yolk sac, placenta and umbilical chord (Nagy et al., 2003).

Our results indicate that the morphological defects of ES cell-derived pups are independent of the ES cell lines utilized. Thus, it is possible that epigenetic anomalies of ES cell lines acquired in culture or that occur in ES cell-derived fetuses during embryogenesis are responsible for the morphological abnormalities. Future investigation should focus on determining if methylation patterns in imprinted genes are altered in ES cells or embryos and if aberrant expression is really responsible for the abnormalities observed in ES cell-derived pups. If this were the case, the ability to produce adult mice derived from ES cells routinely would depend on our ability to correct epigenetic defects in ES cells in culture or in the developing embryo. This would provide another significant criterion for determining the level of the pluripotency or quality of experimentally and clinically applicable ES cells and iPS cells in the future.

It is important to note that although the cell lines used in our experiments were previously shown to be pluripotent, they had been used at lower passage stages compared to our experimental ES cells. This indicates that the ES cells used in our experiments have drifted farther from the normal epigenetic state encountered in the ICM, their tissue of origin resulting in embryo malformations. One way to address this possibility would be to use cell lines with low passage number or to utilize inner cell mass-derived cells in our epiblast complementation experiments because ICM is the tissue that ES cells are originally derived from and regarded as a pure pluripotent tissue.

Despite the drawbacks encountered in our epiblast complementation experiments, one significant ramification of our experiments is that epiblast complementation chimeras can be used to test the potency of ES cells or iPS cells by determining if they are be able to generate fully ES or iPS cell-derived newborn pups. Because of its simplicity, this assay should be highly advantageous over the tetraploid complementation assay that many researchers currently depend on for testing pluripotency.

Altogether, the work described in this dissertation thesis has already extended our understanding of early post-implantation development in mammals and provided a novel technique to generate stem cell-derived newborn mice. Our studies have generated multiple novel questions that offer exciting challenges for mouse developmental biologists and the stem cell researchers in the future.

APPENDIX:
ANALYSIS OF VISCERAL ENDODERM FATE AT FETAL AND ADULT STAGES

Preface

The work described in this chapter was initiated and executed by myself. It describes preliminary data that needs to be expanded in the future.

Introduction

During development, gastrulation is one of the most important events and has been highly investigated by many developmental biologists. In the mouse, the process of gastrulation gives rise to three primary germ layers from the pluripotent epiblast cells. These are the mesoderm, endoderm and ectoderm that generate all the tissues of the adult individual, allowing its survival and proper development. Before the initiation of gastrulation, the embryonic component of the early post-implantation mouse conceptus consists of the epiblast and the overlying visceral endoderm. The epiblast gives rise to the fetus and extra-embryonic membranes such as the amnion and the extra-embryonic mesoderm, which contributes to the visceral yolk sac. The visceral endoderm has been reported to be involved in patterning the epiblast (Stern and Downs, 2012) as well as in nutrient uptake and transport during early post-implantation stages (Cross et al, 1994).

According to previous cell fate studies, definitive endoderm cells, which give rise to the embryonic gut tube, emerge from the anterior primitive streak and displace the visceral endoderm into the extra-embryonic region where it becomes part of the visceral yolk sac (Lawson et al., 1986; Tam and Beddington, 1987). Therefore, the visceral endoderm is considered an extra-embryonic component of the conceptus because it contributes only to the outer endoderm layer of the visceral yolk sac.

Surprisingly, a recent paper reported that visceral endoderm descendants contribute to the embryonic gut tube of the embryos at stages earlier than 20 somites (~E8.75) (Kwon et al., 2008). This study argues that visceral endoderm cells intercalate with newly emerging definitive endoderm cells during the process of gastrulation and differentiate into embryonic tissues together with neighboring definitive endoderm cells

instead of being displaced completely into the extra-embryonic area. This finding contradicts the prevailing view that the VE cell lineage does not become part of the embryo and that it only contributes to extra-embryonic tissues. However, it still remains to be determined whether the visceral endoderm cell descendants in embryonic tissues are maintained in fetuses or adult mice and if they play essential roles during mouse embryogenesis and after birth.

Here, we took advantage of genetic labeling strategies to trace the descendants of visceral endoderm cells during embryogenesis and to the adulthood. We provide the evidence that visceral endoderm-derived cells contribute to the liver, pancreas, lung, stomach and heart of fetus, perinatal and adult mice, revealing that visceral endoderm cells can contribute to the fetuses and survive even to the adulthood.

Results

Analysis of visceral endoderm cell descendants in the fetus, newborns and adult mice using genetic labeling

To determine the fate of visceral endoderm descendants in fetuses and mice, we utilized the reporter line called *R26*$^{mT\text{-}mG}$. This mouse line carries a floxed tandem dimmer Tomato (tdTomato) fluorescent protein, one of the RFP variants targeted to membrane (mT), followed by membrane targeted GFP (mG) in the ROSA 26 locus (Muzumdar et al., 2007) (Fig. A. 1A). The *R26*$^{mT\text{-}mG}$ allele labels all the cells of the embryo or mouse with red fluorescence in the absence of Cre-mediated recombination. Once Cre-mediated recombination occurs, all recombined cells become labeled with green fluorescence protein (GFP). To differentially label VE and epiblast cell descendants, we took advantage of a cross between *R26*$^{mT\text{-}mG}$ and *Sox2*$^{Cre/o}$ transgenic mice, which drive the expression of *Cre recombinase* specifically in the epiblast. This mating strategy would result in labeling epiblast cell descendants with green fluorescence by the expression of GFP and labeling the descendant cells of visceral endoderm with red fluorescence by the expression of membrane targeted tdTomato gene (Fig. A.1B).

Using the above mating strategy, we were able to generate *R26*$^{mT\text{-}mG}$ and *Sox2*$^{Cre/o}$ double heterozygous mice, identified by looking at the presence of green fluorescence in the tail tip. We collected liver, pancreas, stomach, heart, lung and other organs from these mice and analyzed them under fluorescence microscopy.

Analysis of organs from perinatal mice (5 days old) demonstrated that liver, pancreas, heart and stomach contain some red fluorescent cells in their tissues (Fig. A.

Figure A. 1

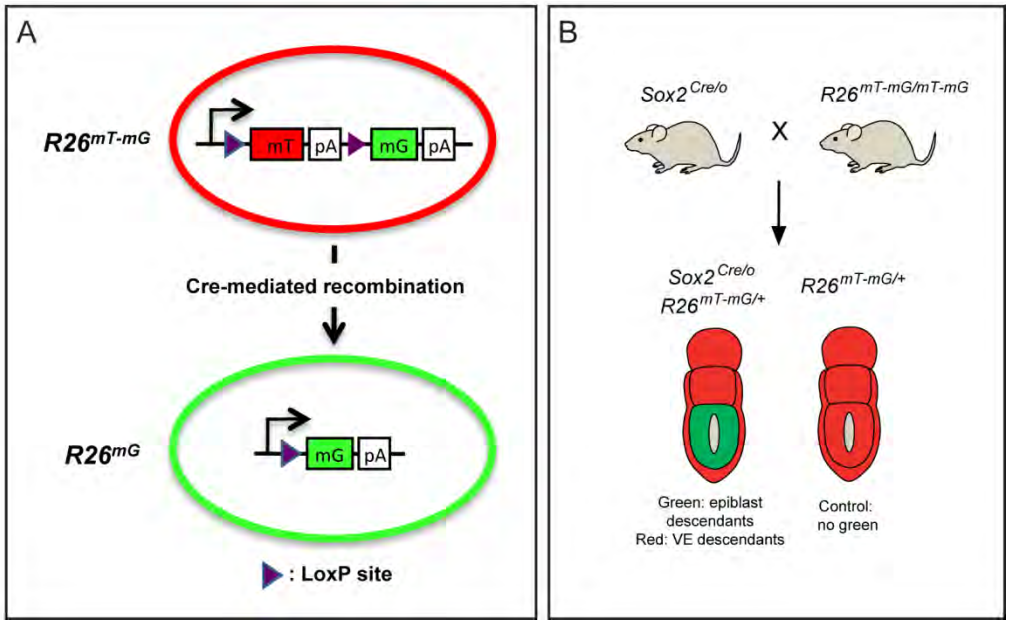

Figure A. 1. Schematic representation of the strategy to differentially label visceral endoderm and epiblast cells using *R26*$^{mT\text{-}mG}$ reporter line. (A) Schematic representation of *R26*$^{mT\text{-}mG}$ transgenic cassette. *R26*$^{mT\text{-}mG}$ carries a floxed membrane-targeted Tomato gene (mT), followed by membrane-targeted GFP (mG) in the *ROSA26* locus. Cre-mediated recombination drives expression of the mG gene, making the cell fluoresce green. (B) Mating strategy for labeling visceral endoderm descendants and epiblast descendants differentially using *Sox2Cre* and *R26*$^{mT\text{-}mG}$ mouse lines. *Sox2Cre* and *R26*$^{mT\text{-}mG}$ double heterozygous embryos or mice would contain epiblast cell descendants marked with green fluorescence and visceral endoderm cell descendants marked with red fluorescence.

2A), indicating that visceral endoderm cells contribute to these embryonic tissues of mouse embryo and that these cells still persist even after birth. These results expand the previous view that visceral endoderm descendants contribute to the gut tube at stages earlier than 20 somites (~E8.75). We also found that even the heart contained a few visceral endoderm cell descendants. Interestingly, we found that the liver and the pancreas contained much more visceral endoderm cell descendants compared to other organs, suggesting that these cells have a critical function in these organs.

To confirm that these visceral endoderm cell descendants perdure the adulthood, we performed similar analysis for adult mice (3 months old). Similarly, we observed that the liver, pancreas, lung and stomach contain some of red fluorescent cells in their tissues (Fig. A. 2B). In these tissues of adult mice, the visceral endoderm cell descendants appear to be more scattered compared to the ones from perinatal mice, suggesting the possibility that visceral endoderm-derived cells present in young mice are gradually diluted and distributed by intermingling with epiblast-derived cells during growth. This also indicates that VE descendants are proliferating at a slower rate than other epiblast descendants.

To independently confirm our previous results, we utilized another reporter line called *Tg*(*Z/EG*), which expresses *LacZ* gene ubiquitously in the absence of Cre-mediated recombination and expresses enhanced GFP (eGFP) upon Cre-mediated recombination (Novak et al., 2000) (Fig. A. 3A). By crossing between *Tg*(*Z/EG*) and $Sox2^{Cre/o}$ transgenic mice, we were able to label the epiblast cell descendants labeled with green fluorescence by the expression of eGFP and the VE descendant cells labeled in blue using β-galactosidase assay (Fig. A. 3B).

Figure A. 2

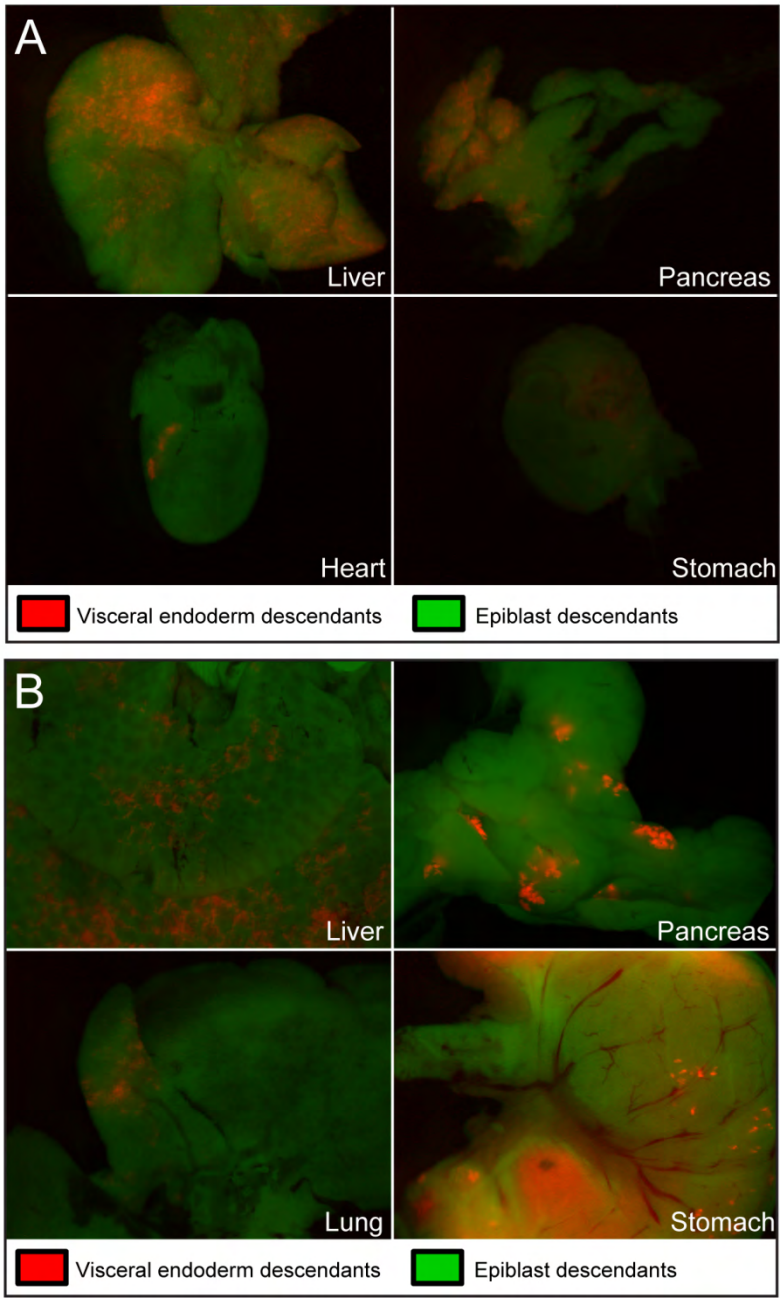
A
Liver
Pancreas
Heart
Stomach
Visceral endoderm descendants
Epiblast descendants
B
Liver
Pancreas
Lung
Stomach
Visceral endoderm descendants
Epiblast descendants

Figure A. 2. Visceral endoderm cells contribute to the embryonic tissues of perinatal and adult mice (*Sox2$^{Cre/o}$; R26$^{mT\text{-}mG/+}$*). Merged images of analyzed organs for 5 days old (A) and 3 months old mice (B) carrying *Sox2$^{Cre/o}$; R26$^{mT\text{-}mG/+}$* double heterozygous alleles. Both mice contain visceral endoderm cell descendants in the liver, pancreas, heart and stomach. Red fluorescence and green fluorescence represent visceral endoderm descendants and epiblast descendants, respectively.

Figure A. 3

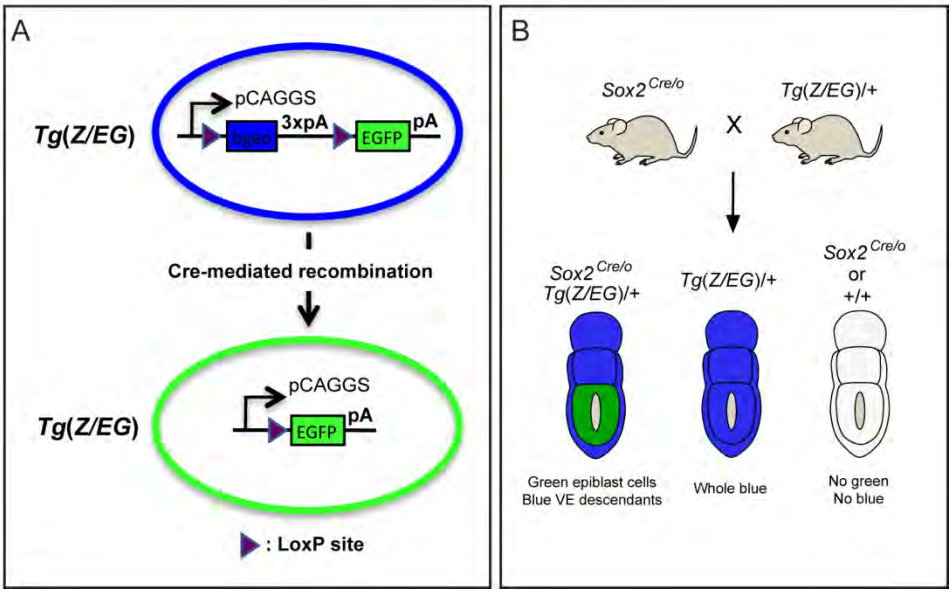

Figure A. 3. Schematic representation of the strategy to differentially label visceral endoderm and epiblast cells using *Tg(Z/EG)* reporter line. (A) A schematic representation of *Tg*(*Z/EG*) reporter line. *Tg*(*Z/EG*) line carries β-galactosidase-neomycin fusion gene (β-geo), followed by enhanced GFP (eGFP) gene under the control of the ubiquitous pCAGGS promoter. (B) Mating strategy for labeling visceral endoderm descendants and epiblast descendants differentially using *Sox2Cre* and *Tg*(*Z/EG*) mouse lines. *Sox2Cre* and *Tg*(*Z/EG*) double heterozygous embryos or mice would contain epiblast cell descendants marked with green fluorescence and visceral endoderm cell descendants marked by *LacZ* gene expression.

Using this strategy, we were able to collect *Tg*(*Z/EG*) and *Sox2*$^{Cre/o}$ double heterozygous embryos, identified by the presence of green fluorescence in the whole embryonic body (Fig. A. 4A, B). β-galactosidase activity assay for these embryos demonstrated the presence of non-recombined visceral endoderm cell descendants in embryonic tissues of E9.5, E10.5 and E11.5 embryos (Fig. A. 4C, D, E, respectively). Interestingly, most of visceral endoderm cell descendants were detected in the liver and heart, consistent with our previous observations that visceral endoderm cells contribute to the tissues in the liver and the heart of perinatal mice (Fig. A. 2A).

We also investigated organs such as liver, pancreas, stomach, heart, lung of *Tg*(*Z/EG*) and *Sox2*$^{Cre/o}$ double heterozygous perinatal and adult mice. Analysis of β-galactosidase activity in the organs of perinatal mice (5 days old) demonstrated that the liver (not shown), pancreas, heart, lung and stomach contain some cells with blue spots (Fig. A. 5A), indicating that visceral endoderm cells contribute to perinatal mice, confirming the results obtained using *R26*$^{mT\text{-}mG}$ reporter line (Fig A. 2A).

We performed similar analysis for adult mice (3 months old) and found that pancreas, heart, lung and stomach contain some cells stained blue (Fig. A. 5B). In these tissues from adult mice, visceral endoderm cell descendants appear to be more scattered compared to the ones observed in perinatal mice, similar to the studies using *R26*$^{mT\text{-}mG}$ mice. However, we were not able to detect any visceral endoderm-derived cells in the liver. This may be due to the fact that *Tg*(*Z/EG*) transgene is not expressed in the liver of adult mice (Novak et al., 2000).

In the experiments described above, the VE was passively labeled because the *Sox2Cre* allele recombines the reporter only in the epiblast. Therefore, we decided to do the reciprocal experiment by expressing Cre in the VE using *TtrCre* mice, which express

Figure A. 4

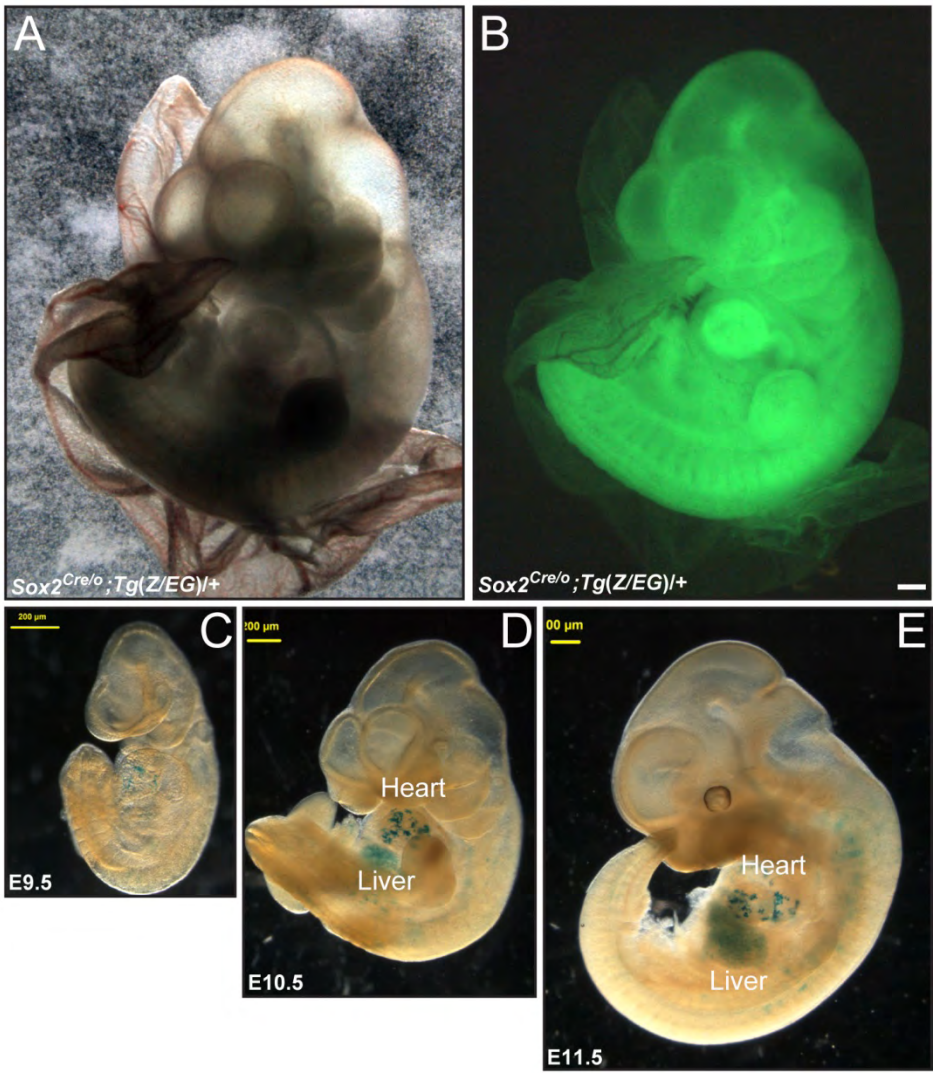
A
B
Sox2Cre/o;Tg(Z/EG)/+
Sox2Cre/o;Tg(Z/EG)/+
C
D
E
E9.5
Heart
Liver
E10.5
Heart
Liver
E11.5

Figure A. 4. Visceral endoderm cells contribute to the embryonic tissues of mouse fetuses (*Sox2$^{Cre/o}$; Tg*(*Z/EG*)). Bright field (A) and green fluorescence (B) images of E10.5 *Sox2$^{Cre/o}$; Tg*(*Z/EG*) double heterozygous embryo. Sox2Cre allele drives the expression of Cre recombinase in the epiblast, leading to green fluorescence in all of epiblast cell descendants. In this embryo, only visceral endoderm cell descendants express *LacZ* gene because of the absence of Cre recombinase activity in this tissue. Analysis of β-galactosidase activity in E9.5 (C), E10.5 (D), and E11.5 (E) *Sox2$^{Cre/o}$; Tg*(*Z/EG*) double heterozygous embryos. Blue spots indicate visceral endoderm cell descendants. Scale bars, 100 μm in A and B, 200 μm in C, D, and E, respectively.

Figure A. 5

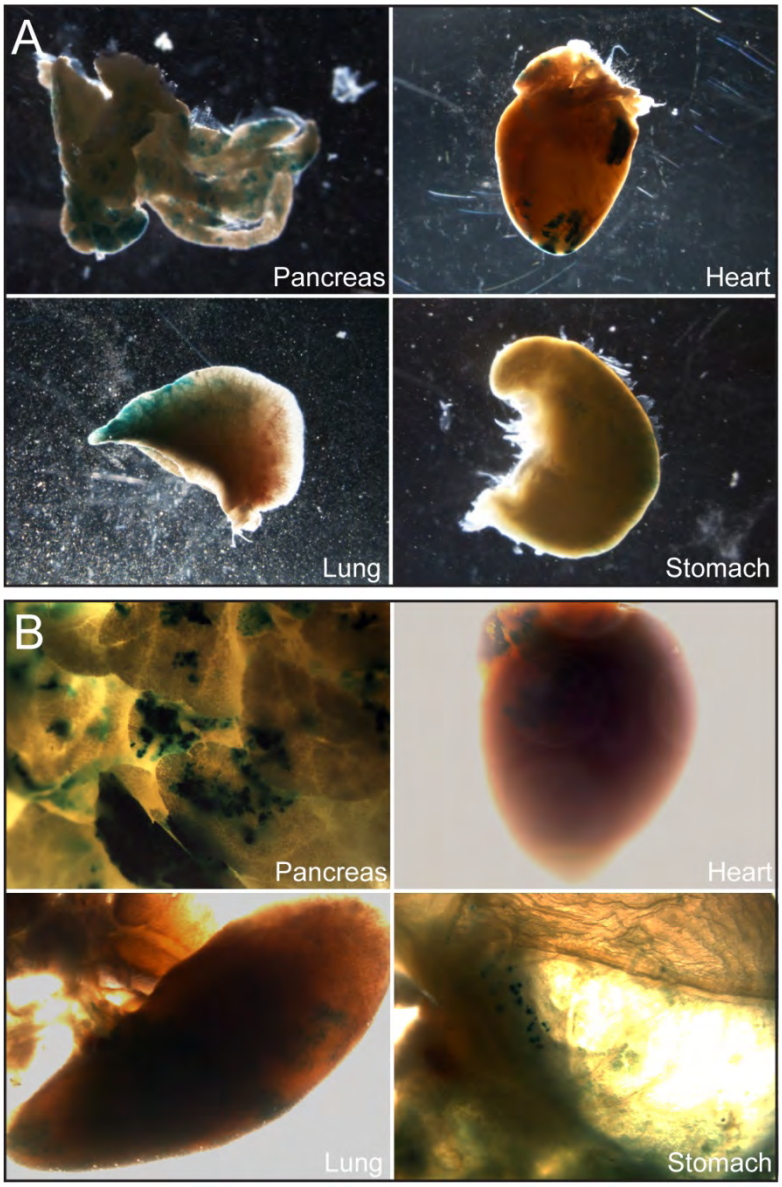
A
Pancreas
Heart
Lung
Stomach
B
Pancreas
Heart
Lung
Stomach

Figure A. 5. Visceral endoderm cells contribute to the embryonic tissues of perinatal and adult mice (*Sox2*$^{Cre/o}$*; Tg*(*Z/EG*)). Analysis of β-galactosidase activity in tissues of 5 days old (A) and 3 months old mice (B) double heterozygous for *Sox2*$^{Cre/o}$ and *Tg*(*Z/EG*) alleles. Both mice contained visceral endoderm cell descendants in the tissues of pancreas, heart, lung and stomach. Blue spots in the tissues indicate the presence of visceral endoderm cell descendants.

Cre recombinase only in the visceral endoderm at around E5.0. Using this approach, when we cross *Ttr*^{Cre} mice with *R26*$^{r/r}$ or *R26*$^{mT\text{-}mG/mT\text{-}mG}$ reporter lines, the visceral endoderm-derived cells would be recombined directly by the presence of Cre recombinase at early post-implantation stages (~E5.0) and would be marked by the presence of blue precipitates after β-galactosidase assay or green fluorescence.

Analysis of β-galactosidase activity of E11.5 *Ttr*$^{Cre/o}$*; R26*$^{r/+}$ double heterozygous mouse embryos demonstrated the blue staining in visceral yolk sac (VYS), a well-known tissue derived from visceral endoderm component (left in Fig. A. 6A), confirming the validity of this approach. The existence of blue staining in the heart and liver of the same embryo (right in fig. A. 6A) supports the notion that visceral endoderm cells contribute to these tissues in mouse fetus.

Similar results were obtained by analyzing E14.5 embryos carrying the *Ttr*$^{Cre/o}$*; R26*$^{mT\text{-}mG/+}$ alleles. We found that these embryos contain green fluorescence in the tissues of visceral yolk sac, liver, pancreas, stomach and heart (Fig. A. 6B), indicating the contribution of visceral endoderm cell descendants to these tissues.

In conclusion, these results demonstrate that visceral endoderm-derived cells contribute to the tissues of the liver, pancreas, lung, stomach and heart of fetuses, perinatal and adult mice, suggesting that visceral endoderm cells play an important role in these tissues.

Analysis of visceral endoderm cell fate using transient Cre-mediated visceral endoderm labeling strategy

The experiments described above provided the evidence that visceral endoderm cells contribute to the fetus and perinatal and adult mice. However, the *Ttr*^{Cre} transgene

Figure A. 6

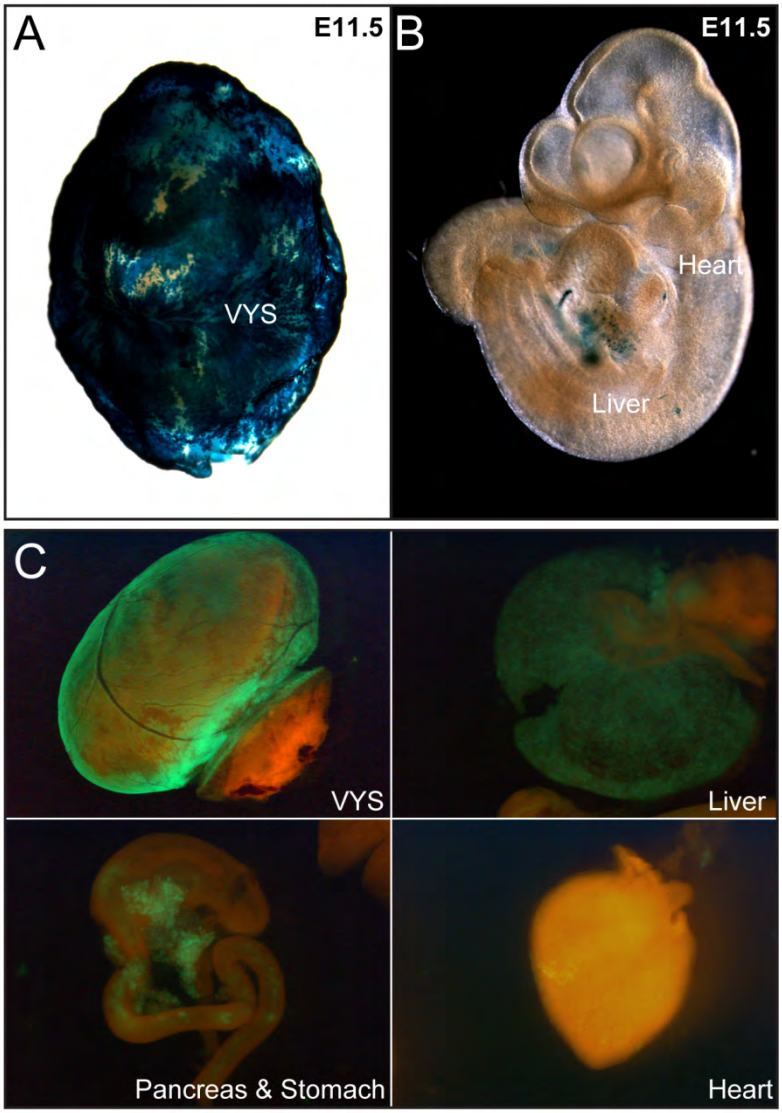
A
E11.5
VYS
B
E11.5
Heart
Liver
C
VYS
Liver
Pancreas & Stomach
Heart

Figure A. 6. Visceral endoderm cells contribute to the embryonic tissues of mouse embryos. (A) Analysis of β-galactosidase activity of E11.5 *Ttr*$^{Cre/o}$*; R26*$^{r/+}$ double heterozygous mouse embryos. Blue staining in visceral yolk sac (VYS) (left) confirm the visceral endoderm lineage identity and blue staining in the heart and liver (right) represent visceral endoderm descendants in these tissues. (B) *Ttr*$^{Cre/o}$*; R26*$^{mT\text{-}mG/+}$ double heterozygous E14.5 mouse embryo contain green fluorescence in the VYS, liver, pancreas, stomach and heart. Green fluorescence in the tissues represents the presence of visceral endoderm cell descendants.

is expressed in the liver and potentially other tissues of the fetus and adult mouse. Hence, it is possible that the putative labeled visceral endoderm cells observed in the fetus or adult mouse are not descendants of the visceral endoderm cells but rather are produced by reactivation of *Ttr*^{Cre} transgene in epiblast descendants at later stages.

To exclude this possibility, it is necessary to exclusively label visceral endoderm cells during a limited time period using transient expression of *Cre* recombinase only in the visceral endoderm layer of the conceptus between E5.5 and E6.5. The idea for this strategy came from a previous report, which shows that most of the plasmid DNA/lipid complexes delivered to post-implantation embryos through tail vein injection of pregnant females are trapped in the visceral endoderm lineage (Kikuchi et al, 2002).

To test this idea, we performed tail vein injection of a plasmid containing a Cre expression cassette into pregnant females carrying embryos heterozygous for the reporter alleles (*R26*^{r}, *R26*$^{mT\text{-}mG}$) at E5.5. We anticipated that only visceral endoderm cells of post-implantation embryos would take up the plasmid DNA and that those cells would be labeled by Cre-mediated recombination after the expression of Cre recombinase. We were able to detect the injected plasmid DNA in embryos by PCR (not shown), indicating that plasmid DNA was taken by the embryo.

However, we were not able to detect Cre-mediated recombination events in the embryos carrying the reporter alleles (*R26*^{r}, *R26*$^{mT\text{-}mG}$), suggesting that there is no Cre activity or expression of Cre recombinase in those cells where the plasmid DNA was delivered.

Discussion

A recent paper reported that visceral endoderm cells contribute to the embryonic gut tube of mouse embryo; however, the question remained on whether these cells persist to adulthood.

To address this question, we utilized several reporter lines for the analysis of the visceral endoderm lineage. We also took advantage of *Sox2*^{Cre} and *Ttr*^{Cre} transgenic mice to label visceral endoderm and epiblast cells differentially and observed that fetuses, perinatal and adult mice contain visceral endoderm cell descendants. Our results support the original finding that visceral endoderm cells contribute to the gut tube of embryos with less than 20 somites and led to the suggestion that visceral endoderm cells contribute even to the tissues of adult mice.

However, our study depends on transgenic *Cre* lines such as *Sox2*^{Cre} for inducting the recombination specifically in the epiblast lineage and *Ttr*^{Cre} for the recombination specifically in the visceral endoderm lineage. Therefore, if the activity and specificity of these transgenes were not as expected, the resulting findings would give rise to false-positive or false-negative events. For example, if the *Sox2*^{Cre} transgene does not induce the recombination in all of the epiblast cells and gives rise to non-recombined epiblast cells at early post-implantation stages, the descendants of these non-recombined cells are not distinguishable from non-recombined visceral endoderm cell descendants at later stages, leading to false-positive results. In a similar way, if the *Ttr*^{Cre} transgene induces the recombination in epiblast cell descendants at later stages during development, newly labeled epiblast-derived cells are not distinguishable from already recombined visceral endoderm-derived cells, producing false-positives.

Therefore, although our experiments indicate that VE cell descendants contribute to fetuses, perinatal and adult mice, we cannot prove conclusively these results.

We tried to solve this problem by delivering plasmid DNA into visceral endoderm cells of early post-implantation embryos through the maternal circulation to the embryos, but failed to genetically label visceral endoderm cell descendants, preventing further investigation.

In future experiments, more efficient methods for delivering plasmid DNA into visceral endoderm of early post-implantation mouse embryos or methods for making delivered DNA expressed efficiently in visceral endoderm cells would be required. Another possibility is to use an inducible *Ttr*^{Cre} mouse line such as *TtrCre-ER*, making it possible to induce recombination only in visceral endoderm during a specific time period by intraperitoneal injection of tamoxifen. This experiment would provide the best alternative to fate the visceral endoderm, because early post-implantation embryos develop rapidly, it is very difficult to control the effects of injected tamoxifen in a spatio-temporal manner at early post-implantation stages.

Even if the presence of VE in adults can be determined inequivocally in the near future utilizing more reliable techniques, the role that the tissues derived from visceral endoderm cells play during embryogenesis or in adult tissues, will remain.

Materials and Methods

Mouse strains and genotyping

Sox2^{Cre} transgenic (Hayashi et al., 2002) and ROSA26 reporter (*R26*^{r}) (Soriano, 1999) mice were purchased from the Jackson Laboratory (Stock No. 003309 and 004783, respectively). The *Ttr*^{Cre} transgenic mouse line was previously described (Kwon and Hadjantonakis, 2009) and was kindly provided by Dr. Anna-Katerina Hadjantonakis. *Tg*(*Z/EG*) transgenic reporter mice (Norvak et al., 2000) were kindly provided by Dr. JeanMarie Houghton. *R26*$^{mT\text{-}mG}$ mouse line was previously described (Muzumdar et al., 2007) and identified by the presence of red fluorescence in a tail tip. The other mice were genotyped by PCR using genomic DNA samples obtained from tail tips. For genomic DNA sample preparation from each mouse, the tail tip was placed into 200 µl of PCR lysis buffer (50 mM KCl, 10 mM Tris-HCl, 10 mM Tris-HCl, 2.5 mM $MgCl_2$, 0.1 mg/ml Gelatin, 0.45% v/v IGEPAL and 0.45% v/v Tween-20, 100 µg/ml Proteinase K) and incubated overnight at 56°C. The next day, after heat inactivation of the Proteinase K at 95°C for 5-8 min, a half or one microlitter of sample was used for PCR amplification. Each allele was confirmed using the following primers: 1) *Sox2Cre* and *TtrCre* alleles, forward primer: 5′-TCC AAT TTA CTG ACC GTA CAC CAA-3′, reverse primer: 5′-CCT GAT CCT GGC AAT TTC GGC TA-3′ 2) *R26*^{r} and *R26*$^{+}$ alleles, forward primers: 5’-AAA GTC GCT CTG AGT TGT TAT-3’, 5’-GCG AAG AGT TTG TCC TCA ACC-3’, reverse primer: 5’-GGA GCG GGA GAA ATG GAT ATG-3’. 3) *Tg*(*Z/EG*) allele, forward primer: 5’-AAG TTC ATC TGC ACC ACC G-3’, reverse primer: 5’-TGC TCA GGT AGT GGT TGT CG-3’.

Wholemount fluorescence microscopy

Dissected embryos or tissues from mice were washed three times in PBS for 5 min each and analyzed in an inverted fluorescence microscope (Leica, DMI4000) for red fluorescence (RFP) and green fluorescence (GFP).

Wholemount β-galactosidase activity assay

Dissected embryos or tissues from mice were fixed in fixation solution (0.2% glutaraldehyde, 2% formalin, 5 mM EGTA, 2 mM MgCl2 in 0.1 M phosphate buffer, pH 7.3) for 5-10 min or 30 min, respectively, washed three times in rinse solution (0.1% deoxycholate, 0.2% IGEPAL, 2 mM MgCl2 in 0.1 M phosphate buffer, pH 7.3), and stained overnight in staining solution (1 mg/ml X-gal, 5 mM potassium ferricyanide, 5 mM potassium ferrocyanide in rinse solution) at 37°C. The next day, embryos were washed twice in rinse solution for 5 min each, twice in PBS for 10 min each, fixed in 4% paraformaldehyde in PBS at room temperature for 20 min and cleared in glycerol/PBS.

Tail vein injection of plasmid DNA

For ubiquitous expression of the injected Cre gene, we utilized *pCreEGFPNuc* plasmid DNA, generated by Dr. Jaime Rivera. In this construct, Cre expression is under the control of the CMV promoter, which drives expression of CreEGFP fusion protein containing a nuclear localization signal (NLS) sequence. To prepare the solution containing *pCreEGFPNuc* DNA/lipid complex, 40 µl of FuGENE HD transfection reagent (Promega, E231B) was diluted with 60 µl of PBS without Ca^{2+} and Mg^{2+}, pH7.2 and 20 µg of DNA plasmid was dissolved in 100 µl of PBS.

200 µl of the solution with the mixture of 100 µl ofpCreEGFPNuc DNA and 100 µl of FuGENE HD transfection reagent were injected into the tail vein of each pregnant female carrying the $R26^{mT\text{-}mG/+}$ or $R26^{r/+}$ embryos at E5.5 after anesthetizing them with

avertin. At E7.5 or E9.5, the embryos were dissected and analyzed for the presence of plasmid DNA by PCR and recombination events by fluorescence microscopy or β-galactosidase assay of the embryos.

BIBLIOGRAPHY

Alikani, M., Cekleniak, N.A., Walters, E., and Cohen, J. (2003). Monozygotic twinning following assisted conception: an analysis of 81 consecutive cases. Hum Reprod *18*, 1937-1943.

Arnold, S.J., and Robertson, E.J. (2009). Making a commitment: cell lineage allocation and axis patterning in the early mouse embryo. Nat Rev Mol Cell Biol *10*, 91-103.

Beddington, R.S., and Robertson, E.J. (1999). Axis development and early asymmetry in mammals. Cell *96*, 195-209.

Berdnik, D., and Knoblich, J.A. (2002). Drosophila Aurora-A is required for centrosome maturation and actin-dependent asymmetric protein localization during mitosis. Curr Biol *12*, 640-647.

Blaschke, K., Ebata, K.T., Karimi, M.M., Zepeda-Martinez, J.A., Goyal, P., Mahapatra, S., Tam, A., Laird, D.J., Hirst, M., Rao, A*., et al.* (2013). Vitamin C induces Tet-dependent DNA demethylation and a blastocyst-like state in ES cells. Nature *500*, 222-226.

Bradley, A., Evans, M., Kaufman, M.H., and Robertson, E. (1984). Formation of Germ-Line Chimeras from Embryo-Derived Teratocarcinoma Cell-Lines. Nature *309*, 255-256.

Brennan, J., Lu, C.C., Norris, D.P., Rodriguez, T.A., Beddington, R.S., and Robertson, E.J. (2001). Nodal signalling in the epiblast patterns the early mouse embryo. Nature *411*, 965-969.

Choi, S.W., and Mason, J.B. (2002). Folate status: Effects on pathways of colorectal carcinogenesis. J Nutr *132*, 2413S-2418S.

Ciemerych, M.A., and Sicinski, P. (2005). Cell cycle in mouse development. Oncogene *24*, 2877-2898.

Conlon, I., and Raff, M. (1999). Size control in animal development. Cell *96*, 235-244.

Conte, N., Delaval, B., Ginestier, C., Ferrand, A., Isnardon, D., Larroque, C., Prigent, C., Seraphin, B., Jacquemier, J., and Birnbaum, D. (2003). TACC1-chTOG-Aurora A protein complex in breast cancer. Oncogene *22*, 8102-8116.

Cooke, J. (1973a). Morphogenesis and Regulation in Spite of Continued Mitotic Inhibition in Xenopus Embryos. Nature *242*, 55-57.

Cooke, J. (1973b). Properties of Primary Organization Field in Embryo of Xenopus-Laevis .4. Pattern Formation and Regulation Following Early Inhibition of Mitosis. J Embryol Exp Morph *30*, 49-62.

Cowley, D.O., Rivera-Perez, J.A., Schliekelman, M., He, Y.J., Oliver, T.G., Lu, L., O'Quinn, R., Salmon, E.D., Magnuson, T., and Van Dyke, T. (2009). Aurora-A kinase is essential for bipolar spindle formation and early development. Mol Cell Biol *29*, 1059-1071.

Crane, J.F., and Trainor, P.A. (2006). Neural crest stem and progenitor cells. Annu Rev Cell Dev Bi *22*, 267-286.

Crider, K.S., Yang, T.P., Berry, R.J., and Bailey, L.B. (2012). Folate and DNA Methylation: A Review of Molecular Mechanisms and the Evidence for Folate's Role. Adv Nutr *3*, 21-38.

Cross, J.C., Werb, Z., and Fisher, S.J. (1994). Implantation and the placenta: key pieces of the development puzzle. Science *266*, 1508-1518.

Dean, W., Bowden, L., Aitchison, A., Klose, J., Moore, T., Meneses, J.J., Reik, W., and Feil, R. (1998). Altered imprinted gene methylation and expression in completely ES cell-derived mouse fetuses: association with aberrant phenotypes. Development *125*, 2273-2282.

Ding, J., Yang, L., Yan, Y.T., Chen, A., Desai, N., Wynshaw-Boris, A., and Shen, M.M. (1998). Cripto is required for correct orientation of the anterior-posterior axis in the mouse embryo. Nature *395*, 702-707.

Doetschman, T., Maeda, N., and Smithies, O. (1988). Targeted Mutation of the Hprt Gene in Mouse Embryonic Stem-Cells. P Natl Acad Sci USA *85*, 8583-8587.

Downs, K.M., and Davies, T. (1993). Staging of gastrulating mouse embryos by morphological landmarks in the dissecting microscope. Development *118*, 1255-1266.

Du, J., and Hannon, G.J. (2004). Suppression of p160ROCK bypasses cell cycle arrest after Aurora-A/STK15 depletion. Proc Natl Acad Sci U S A *101*, 8975-8980.

Eggan, K., Akutsu, H., Loring, J., Jackson-Grusby, L., Klemm, M., Rideout, W.M., 3rd, Yanagimachi, R., and Jaenisch, R. (2001). Hybrid vigor, fetal overgrowth,

and viability of mice derived by nuclear cloning and tetraploid embryo complementation. Proc Natl Acad Sci U S A *98*, 6209-6214.

Elmore, S. (2007). Apoptosis: a review of programmed cell death. Toxicol Pathol *35*, 495-516.

Evans, M.J., and Kaufman, M.H. (1981). Establishment in Culture of Pluripotential Cells from Mouse Embryos. Nature *292*, 154-156.

Everett, C.A., and West, J.D. (1996). The influence of ploidy on the distribution of cells in chimaeric mouse blastocysts. Zygote *4*, 59-&.

Flach, G., Johnson, M.H., Braude, P.R., Taylor, R.A., and Bolton, V.N. (1982). The transition from maternal to embryonic control in the 2-cell mouse embryo. EMBO J *1*, 681-686.

Foe, V.E. (1989). Mitotic Domains Reveal Early Commitment of Cells in Drosophila Embryos. Development *107*, 1-22.

Gardner, R.L. (1968). Mouse Chimaeras Obtained by Injection of Cells into Blastocyst. Nature *220*, 596-&.

Gardner, R.L., Papaioannou, V.E., and Barton, S.C. (1973). Origin of the ectoplacental cone and secondary giant cells in mouse blastocysts reconstituted from isolated trophoblast and inner cell mass. J Embryol Exp Morphol *30*, 561-572.

Giet, R., Petretti, C., and Prigent, C. (2005). Aurora kinases, aneuploidy and cancer, a coincidence or a real link? Trends Cell Biol *15*, 241-250.

Gonda, T.A., Kim, Y.I., Salas, M.C., Gamble, M.V., Shibata, W., Muthupalani, S., Sohn, K.J., Abrams, J.A., Fox, J.G., Wang, T.C.*, et al.* (2012). Folic acid increases global DNA methylation and reduces inflammation to prevent Helicobacter-associated gastric cancer in mice. Gastroenterology *142*, 824-833 e827.

Gray, J.D., and Ross, M.E. (2009). Mechanistic insights into folate supplementation from Crooked tail and other NTD-prone mutant mice. Birth Defects Res A Clin Mol Teratol *85*, 314-321.

Harlow, G.M., and Quinn, P. (1982). Development of preimplantation mouse embryos in vivo and in vitro. Aust J Biol Sci *35*, 187-193.

Hata, T., Furukawa, T., Sunamura, M., Egawa, S., Motoi, F., Ohmura, N., Marumoto, T., Saya, H., and Horii, A. (2005). RNA interference targeting aurora kinase a suppresses tumor growth and enhances the taxane chemosensitivity in human pancreatic cancer cells. Cancer Res *65*, 2899-2905.

Hayashi, S., Lewis, P., Pevny, L., and McMahon, A.P. (2002). Efficient gene modulation in mouse epiblast using a Sox2Cre transgenic mouse strain. Mech Dev *119 Suppl 1*, S97-S101.

Hemerly, A.S., Ferreira, P.C.G., Van Montagu, M., Engler, G., and Inze, D. (2000). Cell division events are essential for embryo patterning and morphogenesis: studies on dominant-negative cdc2aAt mutants of Arabidopsis. Plant J *23*, 123-130.

Hendzel, M.J., Wei, Y., Mancini, M.A., VanHooser, A., Ranalli, T., Brinkley, B.R., BazettJones, D.P., and Allis, C.D. (1997). Mitosis-specific phosphorylation of histone H3 initiates primarily within pericentromeric heterochromatin during G2 and spreads in an ordered fashion coincident with mitotic chromosome condensation. Chromosoma *106*, 348-360.

Hirota, T., Kunitoku, N., Sasayama, T., Marumoto, T., Zhang, D., Nitta, M., Hatakeyama, K., and Saya, H. (2003). Aurora-A and an interacting activator, the

LIM protein Ajuba, are required for mitotic commitment in human cells. Cell *114*, 585-598.

James, R.M., Klerkx, A.H.E.M., Keighren, M., Flockhart, J.H., and West, J.D. (1995). Restricted Distribution of Tetraploid Cells in Mouse Tetraploid[--]Diploid Chimeras. Developmental Biology *167*, 213-226.

Katayama, H., Brinkley, W.R., and Sen, S. (2003). The Aurora kinases: role in cell transformation and tumorigenesis. Cancer Metastasis Rev *22*, 451-464.

Kemp, C., Willems, E., Abdo, S., Lambiv, L., and Leyns, L. (2005). Expression of all Wnt genes and their secreted antagonists during mouse blastocyst and postimplantation development. Dev Dyn *233*, 1064-1075.

Kemp, C.R., Willems, E., Wawrzak, D., Hendrickx, M., Agbor Agbor, T., and Leyns, L. (2007). Expression of Frizzled5, Frizzled7, and Frizzled10 during early mouse development and interactions with canonical Wnt signaling. Dev Dyn *236*, 2011-2019.

Kikuchi, N., Nakamura, S., Ohtsuka, M., Kimura, M., and Sato, M. (2002). Possible mechanism of gene transfer into early to mid-gestational mouse fetuses by tail vein injection. Gene Ther *9*, 1529-1541.

Kimura-Yoshida, C., Nakano, H., Okamura, D., Nakao, K., Yonemura, S., Belo, J.A., Aizawa, S., Matsui, Y., and Matsuo, I. (2005). Canonical Wnt signaling and its antagonist regulate anterior-posterior axis polarization by guiding cell migration in mouse visceral endoderm. Dev Cell *9*, 639-650.

Kimura-Yoshida, C., Tian, E., Nakano, H., Amazaki, S., Shimokawa, K., Rossant, J., Aizawa, S., and Matsuo, I. (2007). Crucial roles of Foxa2 in mouse anterior-posterior axis polarization via regulation of anterior visceral endoderm-specific genes. Proc Natl Acad Sci U S A *104*, 5919-5924.

Kwon, G.S., and Hadjantonakis, A.K. (2009). Transthyretin mouse transgenes direct RFP expression or Cre-mediated recombination throughout the visceral endoderm. Genesis *47*, 447-455.

Kwon, G.S., Viotti, M., and Hadjantonakis, A.K. (2008). The endoderm of the mouse embryo arises by dynamic widespread intercalation of embryonic and extraembryonic lineages. Dev Cell *15*, 509-520.

Lagger, G., O'Carroll, D., Rembold, M., Khier, H., Tischler, J., Weitzer, G., Schuettengruber, B., Hauser, C., Brunmeir, R., Jenuwein, T.*, et al.* (2002).

Essential function of histone deacetylase 1 in proliferation control and CDK inhibitor repression. Embo Journal *21*, 2672-2681.

Lawson, K.A., Meneses, J.J., and Pedersen, R.A. (1986). Cell fate and cell lineage in the endoderm of the presomite mouse embryo, studied with an intracellular tracer. Dev Biol *115*, 325-339.

Lewis, N.E., and Rossant, J. (1982). Mechanism of size regulation in mouse embryo aggregates. J Embryol Exp Morphol *72*, 169-181.

Lu, L.Y., Wood, J.L., Ye, L., Minter-Dykhouse, K., Saunders, T.L., Yu, X., and Chen, J. (2008). Aurora A is essential for early embryonic development and tumor suppression. J Biol Chem *283*, 31785-31790.

Lucock, M. (2000). Folic acid: Nutritional biochemistry, molecular biology, and role in disease processes. Mol Genet Metab *71*, 121-138.

Mac Auley, A., Werb, Z., and Mirkes, P.E. (1993). Characterization of the unusually rapid cell cycles during rat gastrulation. Development *117*, 873-883.

Macklon, N.S., Geraedts, J.P., and Fauser, B.C. (2002). Conception to ongoing pregnancy: the 'black box' of early pregnancy loss. Hum Reprod Update *8*, 333-343.

Martin, G.R. (1981). Isolation of a Pluripotent Cell-Line from Early Mouse Embryos Cultured in Medium Conditioned by Teratocarcinoma Stem-Cells. P Natl Acad Sci-Biol *78*, 7634-7638.

Marumoto, T., Zhang, D., and Saya, H. (2005). Aurora-A - a guardian of poles. Nat Rev Cancer *5*, 42-50.

McMahon, A.P., and Bradley, A. (1990). The Wnt-1 (int-1) proto-oncogene is required for development of a large region of the mouse brain. Cell *62*, 1073-1085.

Mesnard, D., Filipe, M., Belo, J.A., and Zernicka-Goetz, M. (2004). The anterior-posterior axis emerges respecting the morphology of the mouse embryo that changes and aligns with the uterus before gastrulation. Curr Biol *14*, 184-196.

Muzumdar, M.D., Tasic, B., Miyamichi, K., Li, L., and Luo, L. (2007). A global double-fluorescent Cre reporter mouse. Genesis *45*, 593-605.

Nagy, A., Gocza, E., Diaz, E.M., Prideaux, V.R., Ivanyi, E., Markkula, M., and Rossant, J. (1990). Embryonic stem cells alone are able to support fetal development in the mouse. Development *110*, 815-821.

Nagy, A., Rossant, J., Nagy, R., Abramow-Newerly, W., and Roder, J.C. (1993). Derivation of completely cell culture-derived mice from early-passage embryonic stem cells. Proc Natl Acad Sci U S A *90*, 8424-8428.

Norris, D.P., Brennan, J., Bikoff, E.K., and Robertson, E.J. (2002). The Foxh1-dependent autoregulatory enhancer controls the level of Nodal signals in the mouse embryo. Development *129*, 3455-3468.

Novak, A., Guo, C., Yang, W., Nagy, A., and Lobe, C.G. (2000). Z/EG, a double reporter mouse line that expresses enhanced green fluorescent protein upon Cre-mediated excision. Genesis *28*, 147-155.

Ovitt, C.E., and Scholer, H.R. (1998). The molecular biology of Oct-4 in the early mouse embryo. Mol Hum Reprod *4*, 1021-1031.

Perea-Gomez, A., Camus, A., Moreau, A., Grieve, K., Moneron, G., Dubois, A., Cibert, C., and Collignon, J. (2004). Initiation of gastrulation in the mouse embryo

is preceded by an apparent shift in the orientation of the anterior-posterior axis. Curr Biol *14*, 197-207.

Perea-Gomez, A., Rhinn, M., and Ang, S.L. (2001). Role of the anterior visceral endoderm in restricting posterior signals in the mouse embryo. Int J Dev Biol *45*, 311-320.

Perea-Gomez, A., Vella, F.D., Shawlot, W., Oulad-Abdelghani, M., Chazaud, C., Meno, C., Pfister, V., Chen, L., Robertson, E., Hamada, H*., et al.* (2002). Nodal antagonists in the anterior visceral endoderm prevent the formation of multiple primitive streaks. Dev Cell *3*, 745-756.

Pfister, S., Steiner, K.A., and Tam, P.P. (2007). Gene expression pattern and progression of embryogenesis in the immediate post-implantation period of mouse development. Gene Expr Patterns *7*, 558-573.

Power, M.A., and Tam, P.P. (1993). Onset of gastrulation, morphogenesis and somitogenesis in mouse embryos displaying compensatory growth. Anat Embryol (Berl) *187*, 493-504.

Pufulete, M., Al-Ghnaniem, R., Khushal, A., Appleby, P., Harris, N., Gout, S., Emery, P.W., and Sanders, T.A.B. (2005). Effect of folic acid supplementation on genomic DNA methylation in patients with colorectal adenoma. Gut *54*, 648-653.

Rideout, W.M., 3rd, Wakayama, T., Wutz, A., Eggan, K., Jackson-Grusby, L., Dausman, J., Yanagimachi, R., and Jaenisch, R. (2000). Generation of mice from wild-type and targeted ES cells by nuclear cloning. Nat Genet *24*, 109-110.

Rivera-Perez, J.A., Jones, V., and Tam, P.P. (2010). Culture of whole mouse embryos at early postimplantation to organogenesis stages: developmental staging and methods. Methods Enzymol *476*, 185-203.

Rivera-Perez, J.A., Mager, J., and Magnuson, T. (2003). Dynamic morphogenetic events characterize the mouse visceral endoderm. Dev Biol *261*, 470-487.

Rivera-Perez, J.A., and Magnuson, T. (2005). Primitive streak formation in mice is preceded by localized activation of Brachyury and Wnt3. Dev Biol *288*, 363-371.

Rodriguez, T.A., Casey, E.S., Harlan, R.M., Smith, J.C., and Beddington, R.S.P. (2001). Distinct enhancer elements control Hex expression during gastrulation and early organogenesis. Developmental Biology *234*, 304-316.

Salomon, D.S., Bianco, C., Ebert, A.D., Khan, N.I., De Santis, M., Normanno, N., Wechselberger, C., Seno, M., Williams, K., Sanicola, M.*, et al.* (2000). The EGF-CFC family: novel epidermal growth factor-related proteins in development and cancer. Endocr-Relat Cancer *7*, 199-226.

Sasai, K., Parant, J.M., Brandt, M.E., Carter, J., Adams, H.P., Stass, S.A., Killary, A.M., Katayama, H., and Sen, S. (2008). Targeted disruption of Aurora A causes abnormal mitotic spindle assembly, chromosome misalignment and embryonic lethality. Oncogene *27*, 4122-4127.

Schier, A.F. (2003). Nodal signaling in vertebrate development. Annu Rev Cell Dev Bi *19*, 589-621.

Sen, S., Zhou, H., and White, R.A. (1997). A putative serine/threonine kinase encoding gene BTAK on chromosome 20q13 is amplified and overexpressed in human breast cancer cell lines. Oncogene *14*, 2195-2200.

Shimozawa, N., Ono, Y., Kimoto, S., Hioki, K., Araki, Y., Shinkai, Y., Kono, T., and Ito, M. (2002). Abnormalities in cloned mice are not transmitted to the progeny. Genesis *34*, 203-207.

Sluss, H.K., Armata, H., Gallant, J., and Jones, S.N. (2004). Phosphorylation of serine 18 regulates distinct p53 functions in mice. Mol Cell Biol *24*, 976-984.

Smith, R.K., and Johnson, M.H. (1986). Analysis of the third and fourth cell cycles of mouse early development. J Reprod Fertil *76*, 393-399.

Snow, M.H.L. (1977). Gastrulation in Mouse - Growth and Regionalization of Epiblast. J Embryol Exp Morph *42*, 293-303.

Solter, D., and Knowles, B.B. (1975). Immunosurgery of mouse blastocyst. Proc Natl Acad Sci U S A *72*, 5099-5102.

Solter, D., Skreb, N., and Damjanov, I. (1971). Cell cycle analysis in the mouse EGG-cylinder. Exp Cell Res *64*, 331-334.

Soriano, P. (1999). Generalized lacZ expression with the ROSA26 Cre reporter strain. Nat Genet *21*, 70-71.

Srinivas, S. (2006). The anterior visceral endoderm-turning heads. Genesis *44*, 565-572.

Srinivas, S., Rodriguez, T., Clements, M., Smith, J.C., and Beddington, R.S. (2004). Active cell migration drives the unilateral movements of the anterior visceral endoderm. Development *131*, 1157-1164.

Stern, C.D., and Downs, K.M. (2012). The hypoblast (visceral endoderm): an evo-devo perspective. Development *139*, 1059-1069.

Stuckey, D.W., Clements, M., Di-Gregorio, A., Senner, C.E., Le Tissier, P., Srinivas, S., and Rodriguez, T.A. (2011). Coordination of cell proliferation and anterior-posterior axis establishment in the mouse embryo. Development *138*, 1521-1530.

Sulston, J.E., Schierenberg, E., White, J.G., and Thomson, J.N. (1983). The Embryonic-Cell Lineage of the Nematode Caenorhabditis-Elegans. Developmental Biology *100*, 64-119.

Tallquist, M.D., and Soriano, P. (2000). Epiblast-restricted Cre expression in MORE mice: A tool to distinguish embryonic vs. extra-embryonic gene function. Genesis *26*, 113-115.

Tam, P.P. (1988). Postimplantation development of mitomycin C-treated mouse blastocysts. Teratology *37*, 205-212.

Tam, P.P. (2004). Embryonic axes: the long and short of it in the mouse. Curr Biol *14*, R239-241.

Tam, P.P., and Beddington, R.S. (1987). The formation of mesodermal tissues in the mouse embryo during gastrulation and early organogenesis. Development *99*, 109-126.

Tam, P.P., and Loebel, D.A. (2007). Gene function in mouse embryogenesis: get set for gastrulation. Nat Rev Genet *8*, 368-381.

Tam, P.P., Loebel, D.A., and Tanaka, S.S. (2006). Building the mouse gastrula: signals, asymmetry and lineages. Curr Opin Genet Dev *16*, 419-425.

Tam, P.P., and Rossant, J. (2003). Mouse embryonic chimeras: tools for studying mammalian development. Development *130*, 6155-6163.

Tarkowski, A.K. (1961). Mouse chimaeras developed from fused eggs. Nature *190*, 857-860.

Tarkowski, A.K., Witkowska, A., and Opas, J. (1977). Development of Cytochalasin B-Induced Tetraploid and Diploid-Tetraploid Mosaic Mouse Embryos. J Embryol Exp Morph *41*, 47-64.

Taunton, J., Hassig, C.A., and Schreiber, S.L. (1996). A mammalian histone deacetylase related to the yeast transcriptional regulator Rpd3p. Science *272*, 408-411.

Thomas, K.R., and Capecchi, M.R. (1987). Site-Directed Mutagenesis by Gene Targeting in Mouse Embryo-Derived Stem-Cells. Cell *51*, 503-512.

Thomas, P., and Beddington, R. (1996). Anterior primitive endoderm may be responsible for patterning the anterior neural plate in the mouse embryo. Curr Biol *6*, 1487-1496.

Thomas, P.Q., Brown, A., and Beddington, R.S. (1998). Hex: a homeobox gene revealing peri-implantation asymmetry in the mouse embryo and an early transient marker of endothelial cell precursors. Development *125*, 85-94.

Torres-Padilla, M.E., Richardson, L., Kolasinska, P., Meilhac, S.M., Luetke-Eversloh, M.V., and Zernicka-Goetz, M. (2007). The anterior visceral endoderm

of the mouse embryo is established from both preimplantation precursor cells and by de novo gene expression after implantation. Dev Biol *309*, 97-112.

Trainor, P.A. (2010). Craniofacial birth defects: The role of neural crest cells in the etiology and pathogenesis of Treacher Collins syndrome and the potential for prevention. Am J Med Genet A *152A*, 2984-2994.

Tremblay, K.D., Hoodless, P.A., Bikoff, E.K., and Robertson, E.J. (2000). Formation of the definitive endoderm in mouse is a Smad2-dependent process. Development *127*, 3079-3090.

Varlet, I., Collignon, J., and Robertson, E.J. (1997). nodal expression in the primitive endoderm is required for specification of the anterior axis during mouse gastrulation. Development *124*, 1033-1044.

Vidal, M., and Gaber, R.F. (1991). Rpd3 Encodes a 2nd Factor Required to Achieve Maximum Positive and Negative Transcriptional States in Saccharomyces-Cerevisiae. Molecular and Cellular Biology *11*, 6317-6327.

Voehringer, D., Liang, H.E., and Locksley, R.M. (2008). Homeostasis and effector function of lymphopenia-induced "memory-like" T cells in constitutively T cell-depleted mice. J Immunol *180*, 4742-4753.

Wagner, E.F., Keller, G., Gilboa, E., Ruther, U., and Stewart, C. (1985). Gene transfer into murine stem cells and mice using retroviral vectors. Cold Spring Harb Symp Quant Biol *50*, 691-700.

Wang, Z.Q., Fung, M.R., Barlow, D.P., and Wagner, E.F. (1994). Regulation of embryonic growth and lysosomal targeting by the imprinted Igf2/Mpr gene. Nature *372*, 464-467.

Wang, Z.Q., Kiefer, F., Urbanek, P., and Wagner, E.F. (1997). Generation of completely embryonic stem cell-derived mutant mice using tetraploid blastocyst injection. Mech Dev *62*, 137-145.

Wilkinson, D.G., Bhatt, S., and Herrmann, B.G. (1990). Expression pattern of the mouse T gene and its role in mesoderm formation. Nature *343*, 657-659.

Wolpert, L. (1998). Principles of development (London ; New York Oxford ; New York, Current Biology ;Oxford University Press).

Wood, S.A., Allen, N.D., Rossant, J., Auerbach, A., and Nagy, A. (1993). Non-injection methods for the production of embryonic stem cell-embryo chimaeras. Nature *365*, 87-89.

Yamamoto, M., Saijoh, Y., Perea-Gomez, A., Shawlot, W., Behringer, R.R., Ang, S.L., Hamada, H., and Meno, C. (2004). Nodal antagonists regulate formation of the anteroposterior axis of the mouse embryo. Nature *428*, 387-392.

Zambrowicz, B.P., Imamoto, A., Fiering, S., Herzenberg, L.A., Kerr, W.G., and Soriano, P. (1997). Disruption of overlapping transcripts in the ROSA beta geo 26 gene trap strain leads to widespread expression of beta-galactosidase in mouse embryos and hematopoietic cells. Proc Natl Acad Sci U S A *94*, 3789-3794.

Zhao, Q., Behringer, R.R., and de Crombrugghe, B. (1996). Prenatal folic acid treatment suppresses acrania and meroanencephaly in mice mutant for the Cart1 homeobox gene. Nat Genet *13*, 275-283.